STANFORD UNIVERSITY
ENGINEERING IN MEDICINE AND BIOLOGY

AN EXPERIMENTAL STUDY OF THE TRANSMISSION CHARACTERISTICS OF PRESSURE WAVES IN THE AORTA

PH. D. DISSERTATION

BY

MICHAEL BENJAMIN HISTAND

BIOMECHANICS LABORATORY

DEPARTMENT OF AERONAUTICS AND ASTRONAUTICS

MARCH 1969

This work was carried out at the Ames Research Center of the NASA under a collaborative research arrangement with Stanford University (NASA Grant NGR 05-020-223) and was supported in part by an NSF Traineeship.
Some of the material from SUDAAR No. 342 has been included here for the sake of completeness.

SUDAAR NO. 369

Department of Aeronautics and Astronautics
Stanford University
Stanford, California

AN EXPERIMENTAL STUDY OF THE TRANSMISSION CHARACTERISTICS OF PRESSURE WAVES IN THE AORTA

Ph. D. Dissertation

by

Michael Benjamin Histand

SUDAAR NO. 369

March 1969

This work was carried out at the Ames Research Center of the NASA under a collaborative research arrangement with Stanford University (NASA Grant NGR 05-020-223) and was supported in part by an NSF Traineeship. Some of the material from SUDAAR No. 342 has been included here for the sake of completeness.

ACKNOWLEDGMENT

I would like to express my sincere appreciation to Dr. Max Anliker who suggested the problem examined in this dissertation and whose guidance and advice were valuable throughout my research program. Dr. I-Dee Chang and Dr. Leo Sapirstein are to be thanked for their reading of the preliminary manuscript and the helpful criticism and suggestions they have contributed.

Jane Fajardo, Teresa Storm, and Mary Goodno have typed the final manuscript.

My work has been supported in part by a National Science Foundation Traineeship and by NASA Grant NGR 05-020-223.

To my wife Dede, I express gratitude for her confidence, patience, and encouragement during the pursuit of these studies.

Finally, I dedicate this dissertation to my parents whose understanding and support made this culmination of my university education possible.

ABSTRACT

A method was developed to determine the elastic behavior of large blood vessels in terms of their transmission characteristics for small sinusoidal pressure signals. The method is new insofar as it utilizes transient signals of the form of finite trains of sine waves that are superimposed on the naturally occurring pressure fluctuations and are generated by an electrically driven impactor or by a pump. Its application to the thoracic aortas of 18 mature mongrel dogs anesthetized with Nembutal has shown that dispersion and attenuation data for frequencies between 40 and 200 cps can be obtained without requiring either Fourier transform computations or resolution of reflection interference. For the frequency range considered, the descending aorta is only mildly dispersive. It exhibits strong attenuation that must be attributed primarily to the viscoelasticity of the vessel wall and not to the viscosity of the blood or conduction of mechanical energy into the surroundings. For all frequencies tested the amplitude ratio of the waves portrays the same exponential decay pattern with distance measured in wavelengths independent of the pressure level. The values of the logarithmic decrement k in the downstream direction ranged between 0.7 and 1.0 at normal blood pressure levels. The wave speed during diastole can have a value between 4 and 6 m/sec.

The analysis of small sinusoidal wave trains generated at different instants of the cardiac cycle show significant variations in wave transmission characteristics due to the effects of pressure and flow. Values for $\partial c/\partial p$, the change in wave speed due to pressure in the absence of a mean flow, ranges

between 3 and 6 $\frac{\text{cm/sec}}{\text{mm Hg}}$. $\partial c/\partial p$ can be considered essentially constant for the natural pulse pressure, but high and low pressure occlusion studies show that $\partial c/\partial p$ gradually changes in magnitude. Simultaneous measurements of wave speed in the upstream and downstream directions in a single aortic segment indicate that pressure waves are convected by the blood flow and have a speed equal to the sum of the mean flow velocity and the wave speed in an undisturbed system. The wave speed difference between downstream and upstream waves yields values for mean flow velocity which compare very favorably with those measured with catheter-tip flowmeters. From wave transmission studies it has been shown that the mean flow velocity increases from approximately 0.1 m/sec during diastole to more than 0.6 m/sec during early systole. These results imply that blood vessels exhibit nonlinear behavior with respect to large pressure fluctuations such as those produced by the heart. A discrepancy in the value of the attenuation for downstream waves ($k = 0.7$ to 1.0) and upstream waves ($k = 1.2$ to 1.6) is attributed to taper of the vessel, and the actual value of the logarithmic decrement due to dissipative mechanisms in the vessel wall would have a magnitude between 1.0 and 1.2 for a vessel with a uniform cross section.

The circumferential Young's moduli E have been calculated by two methods using instantaneous diameter and wave speed data measured simultaneously in a segment of the aorta for small sinusoidal wave trains. The moduli calculated from distensibility data were consistently higher in value. The magnitudes of E calculated by the two methods ranged between 3×10^6 and 12×10^6 dynes/cm^2.

TABLE OF CONTENTS

LIST OF ILLUSTRATIONS

List of Illustrations (Continued)

List of Illustrations (Continued)

List of Illustrations (Continued)

CHAPTER 1

GENERAL INTRODUCTION

The mechanical properties of blood vessels have been a subject of intensive study during the past fifteen years. This interest is in part based on a vigorous drive to develop a better understanding of the causes of cardiovascular diseases, the changes in the circulatory system with age, and the control mechanisms involved in regulating blood flow in normal situations as well as under physical and physiological stresses. The determination of the mechanical properties of living tissue such as blood vessels is considerably more difficult than for inert materials. One of the complications arises from the fact that neural and humoral stimuli can mediate rapid changes in the mechanical behavior of living tissue. The inherent capability of living organisms to adjust their mechanical properties to a changing environment is often germane to their survival. It is, therefore, essential to assure that the measurement of the parameters of interest causes a minimal interference with the naturally occurring phenomena and does not elicit a noticeable response of the system which would alter the results of the measurement.

Medical researchers have known for more than one hundred years that the speed of a pressure pulse propagating in a blood vessel is related to the elasticity of the vessel wall, although this fact has seen only limited application. Expanding on this idea, it is shown here that the physical properties of large arteries and veins can be deduced from the dispersion and attenuation of pressure waves propagating in such vessels. This is accomplished by utilizing recently published theoretical studies of the wave

transmission characteristics of blood vessels[1)2)] which include extensive parametric analyses based on a simple constitutive law for the vessel wall material.[1)2)] While more complex mathematical models have also been postulated for the vessel wall behavior[3)4)] none of the constitutive laws proposed so far could be singled out as the most accurate one, since the experimental evidence required for such a decision has yet to be established. This lack of experimental data is particularly striking when compared with the many significant theoretical contributions made for example by Witzig[5)], Iberall[6)], Morgan and Kiely[7)], Womersley[8)], Hardung[9)], Klip[10)] and many other investigators. For comprehensive reviews of theoretical as well as experimental investigations of wave transmission in blood vessels and hemodynamic problems in general the reader is referred to recent publications by McDonald[11)], Fox and Saibel[12)], Rudinger[13)], Skalak[14)] and Fung[15)].

The experimental work described in this dissertation involves the surgical exposure of blood vessels in dogs to allow for the examination and interpretation of the occurrence of hemodynamic phenomena under well defined conditions. However, the ultimate goal of these efforts is the development of a noninvasive, nontraumatic technique to measure changes in the mechanical properties of the larger vessels in man. Fluctuations in flow and diameter can be sensed in major limb vessels with ultrasonic doppler shift flowmeters located on the surface of the skin. (Measurement of transit times of pressure waves and changes in vessel diameter would allow the determination of the material properties of the vessels using a valid mathematical model for their mechanical behavior.) The transcutaneous measurement of vessel elasticity might be used as a clinical

tool. For example, periodic monitoring of human vessel elasticity could indicate incipient vascular diseases and the stage of the aging process. Also, the effects of weightlessness on the cardiovascular system of astronauts during a prolonged space flight could possibly be assessed in terms of the mechanical properties of their major limb vessels.

CHAPTER 2

DISPERSION AND ATTENUATION OF PRESSURE WAVES IN THE CANINE AORTA

2.1 Instroduction

Experimental data on the mechanical properties of various blood vessels have been obtained by previous investigators using four different approaches:

1) Force-displacement measurements on excised vessels (16, 17, 18)
2) Force-displacement measurements on vessels in situ or in-vivo (3, 19, 20)
3) Determination of the propagation characteristics of individual harmonic components of the natural pulse wave generated by the heart (21, 22)
4) Measurement of transmission characteristics of artificially induced pressure waves (23, 24, 25, 26)

None of these approaches is ideal from all points of view, but it appears that the last one should be given preference for a variety of reasons. The removal of the vessels from their natural surroundings raises a multitude of physiological questions and also introduces some mechanical uncertainties regarding the simulation of the forces and constraints to which the vessels are subjected under natural conditions. Force-displacement measurements on vessels under in-vivo conditions seem to be more meaningful, particularly when the circulation through the vessel of interest does not have to be interrupted; however, the question of the extent to which this measuring technique alters the "normal" mechanical behavior of the vessel still exists. The accuracy of data derived from an analysis of the propagation characteristics of individual harmonic components of the pulse wave generated by the heart is highly debatable. There is increasing evidence

that the transmission of the natural pulse is influenced by nonlinear phenomena that preclude in a strict sense its resolution into harmonic components for the purpose of determining their speeds and attenuation (27, 28). The data presented in this dissertation appear to lend further support to this view.

With the development of extremely sensitive displacement-, pressure- and flow transducers with a high frequency response it has become possible to measure accurately in various large blood vessels the propagation characteristics of artificially induced waves of controlled shape and amplitude. The mechanical properties of these vessels can then be determined by making use of recent theoretical studies of the transmission of small waves in arteries and veins (29, 30, 31). The relevance of the properties obtained in this manner depends on the validity of the mathematical model that was introduced for the mechanical behavior of blood vessels in the theoretical prediction of the wave propagation characteristics. As far as the determination of elastic and viscoelastic properties of the vessel wall are concerned this approach is obviously an indirect one, and, as such, somewhat cumbersome. However, its advantages are that it yields essentially local and instantaneous values. The usefulness of such an approach in assessing changes in the elastic behavior of blood vessels caused by altered physiological conditions or vascular diseases is self-evident. Also, with the help of transcutaneous ultrasound sensors the technique should theoretically be applicable to certain vessels in man without requiring the penetration of the skin.

2.2 Theoretical Considerations

The manner in which a signal is propagated in any medium depends in general on the nature and form of the signal. For example, the propagation characteristics of a pressure pulse of a given shape normally depend on the amplitude if it exceeds a certain range. Large amplitude signals are extremely difficult to analyze mathematically since their behavior is influenced by nonlinear phenomena that are negligible when the amplitude is small. Also, the nonlinear effects do not permit a complex propagating signal to be synthesized from--or resolved into--simple harmonic components whose properties can be readily defined and analyzed. Therefore, in most theoretical studies the amplitude has been assumed to be sufficiently small to allow for linearization.

The propagation characteristics of small signals in a given medium or system are customarily described by the speed and attenuation of infinitely long trains of sine waves (harmonic waves) as a function of the frequency or wavelength (31). Considering the simplest case of such a train of sine waves with a frequency f propagating in a specified direction, say the x-axis, one can express mathematically the variation of the signal p with the coordinate x and the time t by

$$p(x,t) = A(x) \sin \frac{2\pi f}{c} (x - ct)$$

where $A(x)$ is the amplitude of the signal at station x and c the speed. Since c can be determined from the instantaneous phase difference

$$\frac{2\pi f}{c} \Delta x$$

between two points separated by the distance Δx, the speed of an infinite train of harmonic waves is commonly referred to as phase velocity. When the phase velocity varies with frequency, the system is called dispersive (32). As a convenient measure for the attenuation of harmonic waves one can use the ratio $\frac{A(x)}{A(x_o)}$ of the amplitude at a distal station x to that at a proximal station x_o. Henceforth the amplitude at station x will be denoted simply by A and that at station x_o by A_o.

In reality one does not have infinitely long trains of harmonic waves since the media are of finite dimensions. Moreover, it may even be impossible to observe finite trains of appreciable length when reflection sites are in close proximity of the point of observation. Therefore, the dispersion and attenuation of infinitely long trains of harmonic signals can practically only be determined from the propagation properties of signals of finite length. When the signals are of nonsinusoidal shape, this requires the laborious evaluation of the Fourier transform of the propagating signal at various locations within the medium and a careful accounting of the uncertainties that may arise from the occurrence of reflections.

For a mildly dispersive medium, i.e., one in which the phase velocity varies only a few percent whenever the frequency is changed by 10 percent, the need for Fourier transform computations can be circumvented if the transient signal is of the form of a finite train of sine waves. This is demonstrated by Figure 1 which illustrates the Fourier transform of such nonperiodic signals. A nonperiodic function $f(t)$ can be synthesized by an infinite aggregate of harmonic functions whose circular frequencies $\omega = 2\pi f$ may assume all possible values in the continuous range $-\infty \leq \omega \leq \infty$. Mathematically this synthesis assumes the form of an integral which is

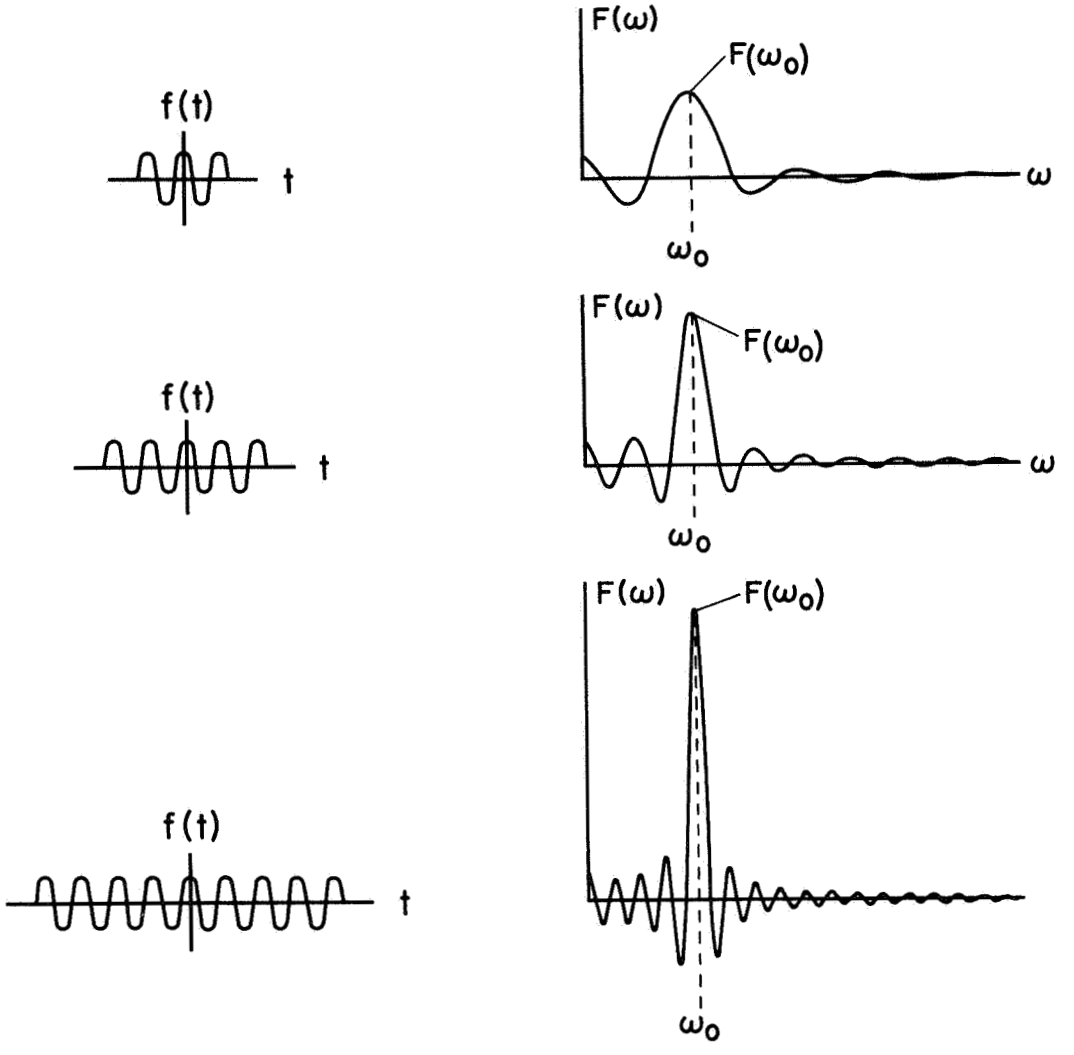

$$f(t) = \frac{1}{2\pi} \int_{-\infty}^{\infty} F(\omega)\, e^{i\omega t}\, d\omega \qquad F(\omega) = \int_{-\infty}^{\infty} f(t)\, e^{-i\omega t}\, dt$$

$$f(t) = \begin{cases} \cos(\omega_0 t), & |t| < \frac{\tau}{2} \\ 0, & (t) > \frac{\tau}{2} \end{cases} \qquad F(\omega) = \frac{\tau}{2} \left[\frac{\sin\left(\frac{\omega-\omega_0}{2}\right)\tau}{\left(\frac{\omega-\omega_0}{2}\right)\tau} + \frac{\sin\left(\frac{\omega+\omega_0}{2}\right)\tau}{\left(\frac{\omega+\omega_0}{2}\right)\tau} \right]$$

Figure 1. Fourier transform of finite trains of sine waves.

called a Fourier integral and which, in complex notation, can be written as given in the Figure. The function $F(\omega)$ is usually referred to as the Fourier transform of $f(t)$ and is in general complex. $F(\omega)$ therefore, can also be expressed as $F(\omega) = |F(\omega)| e^{i\theta(\omega)}$, where $|F(\omega)|$ is the so-called frequency density spectrum and $\theta(\omega)$ the phase density spectrum. $|F(\omega)| d\omega$ specifies the degree in which sine waves with frequencies between ω and $\omega + d\omega$ are represented in the aggregate of harmonics that synthesize the function $f(t)$. When $f(t)$ is an even function $[f(-t) = f(+t)]$ as in the case of the finite trains of sine waves shown on the left side of the Figure, then $F(\omega)$ is real and also an even function; moreover, the phase angle θ is 0^o when $F(\omega) > 0$ and 180^o when $F(\omega) < 0$. In such cases the description of $F(\omega)$ may be restricted to positive values of ω. The uppermost pair of graphs illustrates a train of 2 1/2 sine waves of circular frequency ω_o (left) and the corresponding Fourier transform $F(\omega)$ (right). The pairs of graphs in the center and at the bottom correspond respectively to trains of 4 1/2 and 8 1/2 sine waves of the same circular frequency ω_o. In each case the Fourier transform $F(\omega)$ has a distinct maximum at ω_o. With increasing length of the train $F(\omega)$ peaks more sharply at $\omega = \omega_o$, and $F(\omega_o)$ dominates the spectrum in increasing proportion. In the limiting case of an infinitely long train $F(\omega_o)$ would be infinite at $\omega = \omega_o$ and zero everywhere else. The progressive dominance of $F(\omega_o)$ with increasing length of the sine wave train implies that in a mildly dispersive medium such signals should have a speed of propagation which is a close approximation to the phase velocity corresponding to ω_o. Also, it is possible to avoid the interference of reflections with the transient signal if the signals are of sufficiently short duration or if the medium exhibits strong attenuation.

For sufficiently high frequencies and short trains the waves can be recorded before their reflections arrive at the recording site. In the case of strong attenuation, the reflections of a small wave can be completely damped out before they reach the transducer location.

2.3 Methods

Guided by the preceding theoretical considerations, small pressure perturbations in the form of finite trains of sine waves have been induced in the aortas of eighteen anesthetized dogs. The animals weighed 20-40 kg and were anesthetized with 30 mg/kg sodium pentobarbital (Nembutal) intravenously. They were generally mature mongrels of uncertain age. The dogs were in the supine position throughout the experiment and artificially ventilated with room air at the rate of 9 to 11 liters per minute by means of a Palmer respirator. The blood pressure was continuously monitored with the aid of a Statham P23Dd manometer connected to a radio-opaque catheter inserted through the left carotid artery or the omocervical artery and positioned with an X-ray fluoroscope in the aortic arch.

The basic experimental arrangement is schematically illustrated in Figure 2. The pressure signals were generated either by an electrically driven impactor or by a pump producing sinusoidal pulses of controlled frequency and amplitude. Both the impactor and the pump were designed and constructed in our laboratory. When the pump was used, a polyethylene cannula with an internal diameter of 4 mm was inserted through the left subclavian branch into the descending aorta. When the sinusoidal waves were induced with the aid of the impactor, it was positioned over the aorta in such a manner as to produce small indentations of the vessel wall. The impactor was inserted into the chest through an opening in the left 4th or 5th

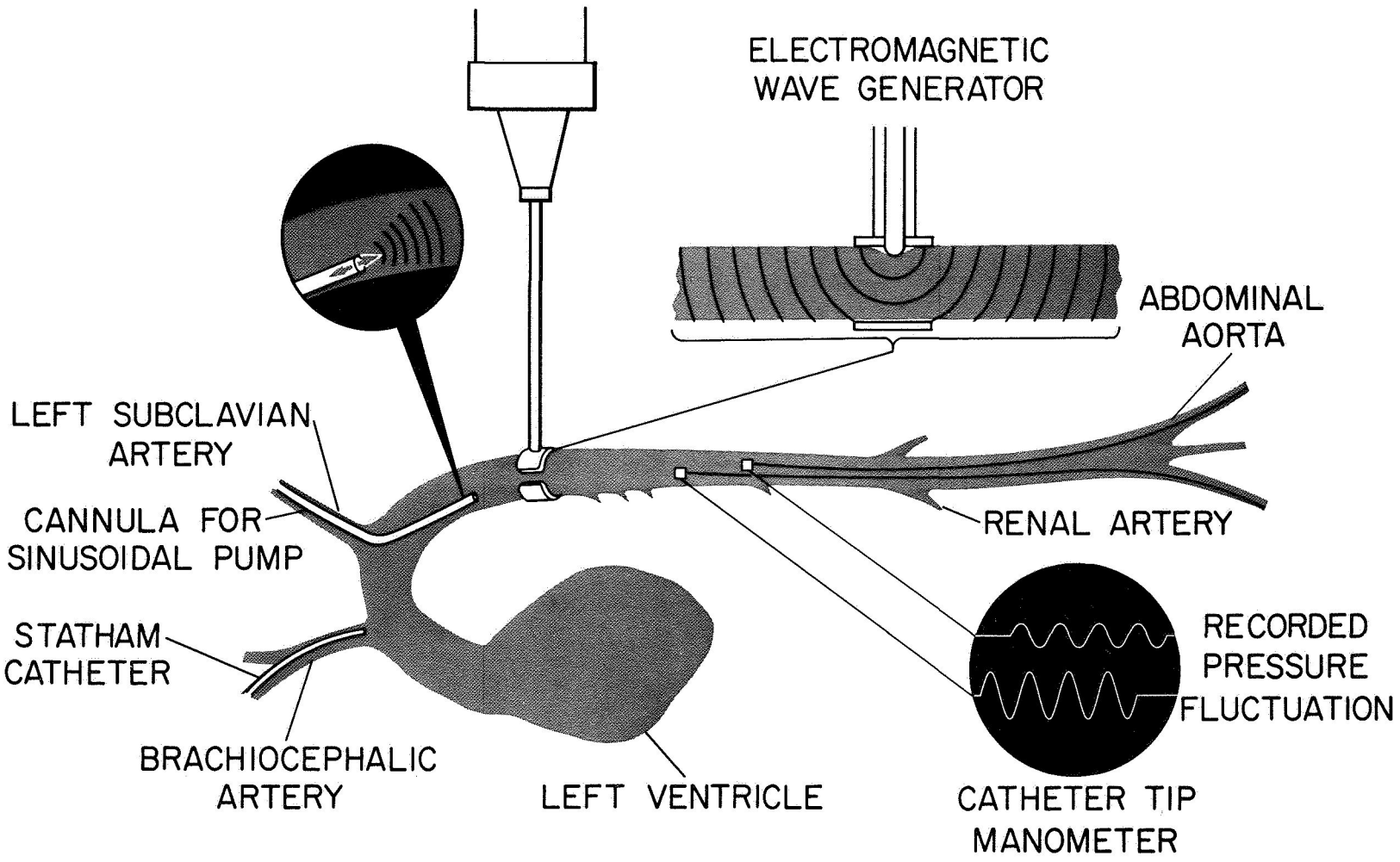

Figure 2. Arrangement of the experimental apparatus for generating and sensing small sinusoidal pressure waves in the aorta of an anesthetized dog. Both methods of inducing the pressure signals are illustrated; however, the wavelengths of the waves indicated in the magnifications of the details showing the cannula and vibrating piston are much shorter than those analyzed in this investigation (2 to 15 cm).

intercostal space or one along the midline. It was usually placed a few cm below the left subclavian branch. In some cases the intercostal branches were ligated and the aorta was freed from its attachment to the thoracic wall. The pressure signals generated by the indentations of the vessel wall or the sinusoidal pump were measured by means of highly sensitive pressure transducers adapted for physiological applications as catheter-tip manometers. Two types of pressure transducers were used for this purpose. Both were originally designed for the measurement of rapid pressure fluctuations in wind tunnel models. One of the transducers is a commercially available Bytrex pressure cell Model HFD-5*) which utilizes silicon semiconductor strain gauges. The other is a capacitance-type pressure cell recently developed at the Ames Research Center (33). Figure 3 shows a photograph of both types of catheter-tip manometers.

The Bytrex pressure cell has a diameter of 3 mm. It is gold-plated to reduce the corrosive effects of body fluids. The shielded leads and the venting tube are protected by a heat-shrinkable plastic tube forming a leakproof flexible catheter. The cell has a sensitivity of $80\mu V/mm\,Hg$ with an excitation of 25 volts. It is linear within 1% from 0 to 300 mm Hg, and has a natural frequency above 60 kc in air. A circuit diagram for the Bytrex pressure cell and temperature compensating module is shown on Figure 3. The output from the bridge circuit is amplified by means of Astrodata amplifiers Model 885.**)

---

*) Schaevitz-Bytrex, Inc.
223 Crescent Street
Waltham, Mass. 02154

**) Astrodata, Inc.
240 E. Palais Rd.
Anaheim, Calif. 92805

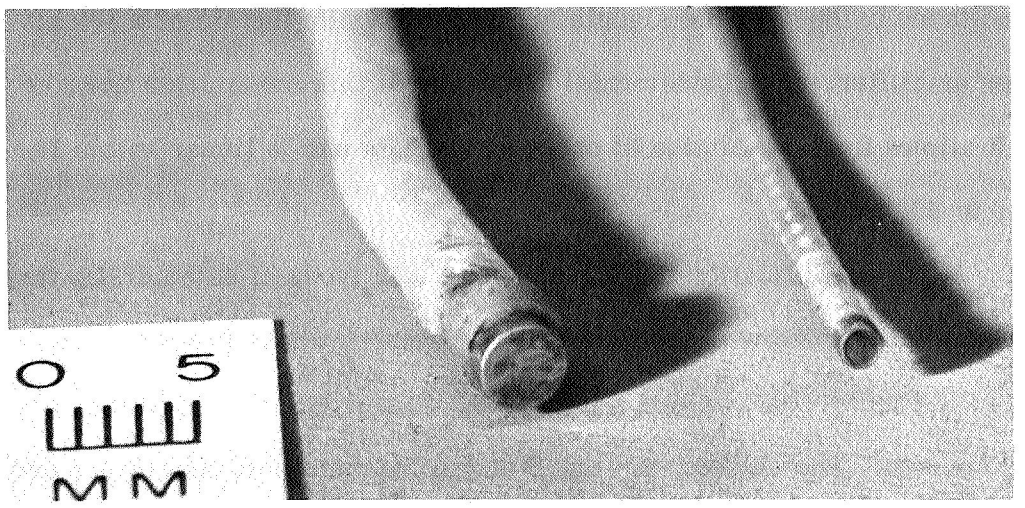

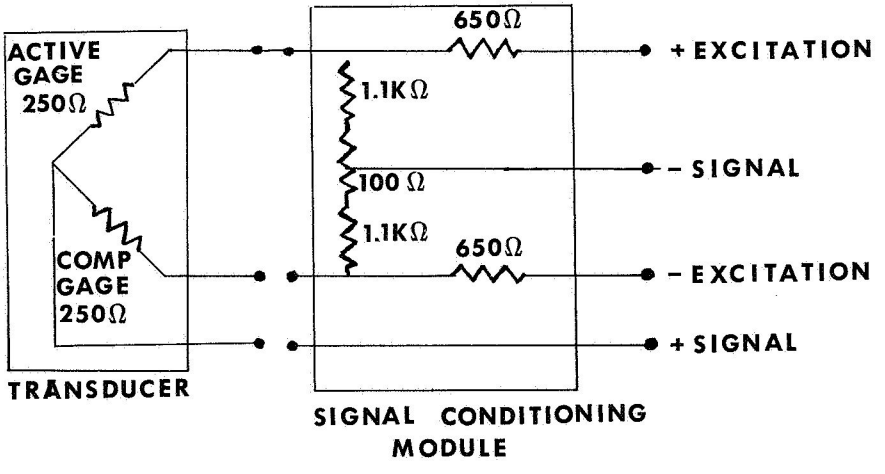

Figure 3. Pressure cells adapted for use as catheter-tip manometers. Top left: Bytrex transducer HFD-5 (strain gauge type). Top right: Coon pressure sensor (capacitance type) developed by NASA. Bottom: Circuit for the Bytrex pressure cell and compensating module.

The capacitance-type pressure cells used in the experiments have a diameter of 1.4 mm or 1.0 mm and are mounted at the tip of a catheter which encloses the electrical leads and the venting tube. The cell forms part of a capacitance bridge and the signals are recorded with the aid of a 100 kc carrier amplifier. The fundamental frequency of this manometer is 82 kc in air. It allows for a resolution of about 0.2 mm Hg and is linear within 1% from 0 to 200 mm Hg.

After amplification the signals from both types of catheter-tip transducers were recorded with the aid of galvanometers whose frequency response is flat up to 3300 cps and a Honeywell Visicorder with a paper speed up to 200 cm/sec. The catheter-tip and Statham manometers, amplifiers and recording equipment were calibrated as a system for each experiment using a mercury manometer as a standard. Also, the catheter-tip transducers were repeatedly checked for drift and changes in sensitivity. This was accomplished by placing the catheter-tip manometers and the tip of the cannula from the Statham gauge at the same location in the aorta. The Bytrex catheter-tip manometers were usually inserted through the left and right femoral arteries; the smaller capacitance transducers were inserted through the left and right saphenous arteries and thus did not cause any major blockage of the circulation through the legs.

The relative positions of the catheter-tip manometers and the impactor or pump cannula could readily be varied and measured to an accuracy of 1 mm through the use of an X-ray image intensifier and a radio-opaque grid with a mesh size of 1 cm. In measuring the distances between the transducers the parallax of the X-ray apparatus was taken into account. Usually the proximal manometer was positioned at a minimal distance of 5 to 6 cm

from the wave generator and the distance between the transducers was systematically varied in increments of 1 or 2 cm. For wave studies in the thoracic aorta the maximum distance between transducers was generally less than 12 cm.

In most of the experiments the trains of sine waves were generated by an electrically driven impactor. One of the electric pistons or impactors used is shown in Figure 4. It consists of a solenoid whose core is connected to a light rod which indents the blood vessel. The rod is protected by a stiff tube which also serves as the support of a hook placed around the vessel. For repetitive generation of sinusoidal signals the size of the hook should be compatible with the size of the artery. A sinusoidal motion of the piston is induced with the aid of an electronic oscillator and a high fidelity amplifier. The number of sine waves and the intervals between the trains are controlled by a tone burst generator.

Since the displacements of the vessel wall caused by the electrically driven impactor have axisymmetric as well as nonaxisymmetric components, the corresponding pressure fluctuations must also be expected to exhibit components of both kinds. Theoretical studies show that the propagation characteristics of nonaxisymmetric waves are vastly different from those of axisymmetric disturbances (1,2). The presence of nonaxisymmetric components may, therefore, make it impossible to observe a single finite train of sine waves, at least within close proximity of the wave generator. Fortunately, these nonaxisymmetric waves are completely attenuated within a distance of about ten vessel radii (5 to 6 cm) from the impactor. This has been verified by comparing the pressure recordings from two transducers positioned at different points of a given lumen cross-section. When the amplitude and

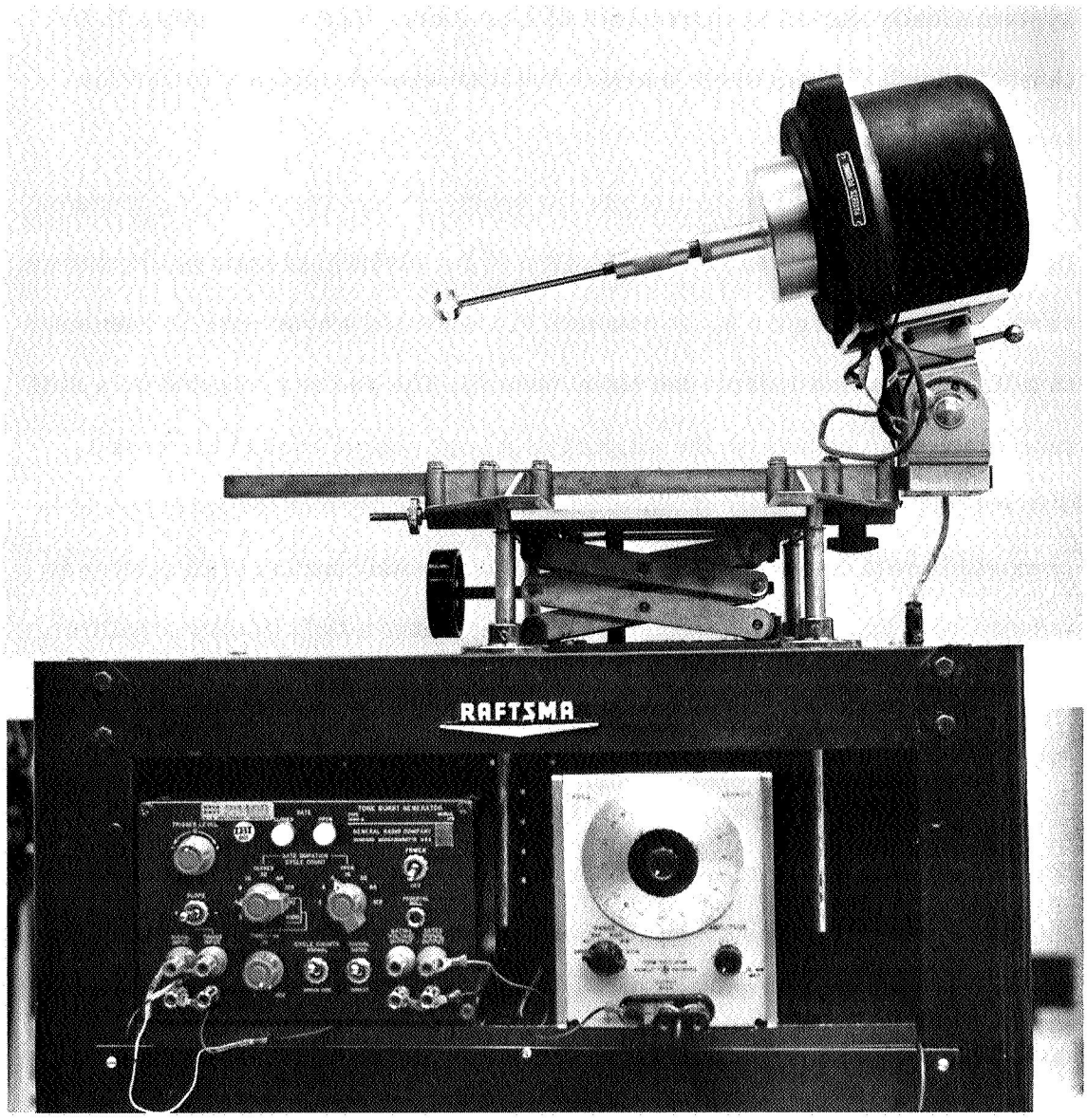

Figure 4. Electromagnetic wave generator with exchangeable hook, electronic oscillator, and tone burst generator. For frequencies between 40 and 80 cps the maximum piston travel in this model is about 5.5 mm while above 80 cps it rapidly diminishes with increasing frequency.

the phase difference between the two pressure signals were negligible for any relative location of the transducers in that cross-section, it was concluded that the signal was axisymmetric.

It is relatively easy to determine the speed of a train of small sinusoidal pressure perturbations by measuring the transmission time of readily identifiable corresponding points of the signal. As illustrated in Figure 5, the intersections of the tangents at successive inflection points were selected as characteristic points. From the time Δt (8 milliseconds) it takes for this point to travel the distance Δx(4 cm) between the transducers the signal speed $\frac{\Delta x}{\Delta t}$ (5 m/sec) can be computed. This signal speed is interpreted as an approximation of the phase velocity corresponding to the frequency of the sine wave which is 70 cps in this particular case. With a recording speed of 100 cm/sec and time lines at 10 millisecond intervals it was in most cases possible to determine time lag Δt with an accuracy of 0.3 milliseconds. The amplitude is defined as indicated in Figure 4 and denoted by A_o at the proximal transducer and by A at the distal transducer. By measuring Δt and A/A_o for the various frequencies and distances Δx between the transducers one obtains the dispersion and attenuation characteristics of these waves for different segments of the aorta.

2.4 Results

Examples of actual recordings of small pressure signals in the form of finite trains of sine waves superimposed on the naturally occurring pressure fluctuations in the aortas of anesthetized dogs are given in Figure 6. Each of the three pairs of pressure records shown was obtained with the aid of two catheter-tip manometers positioned at different points of the

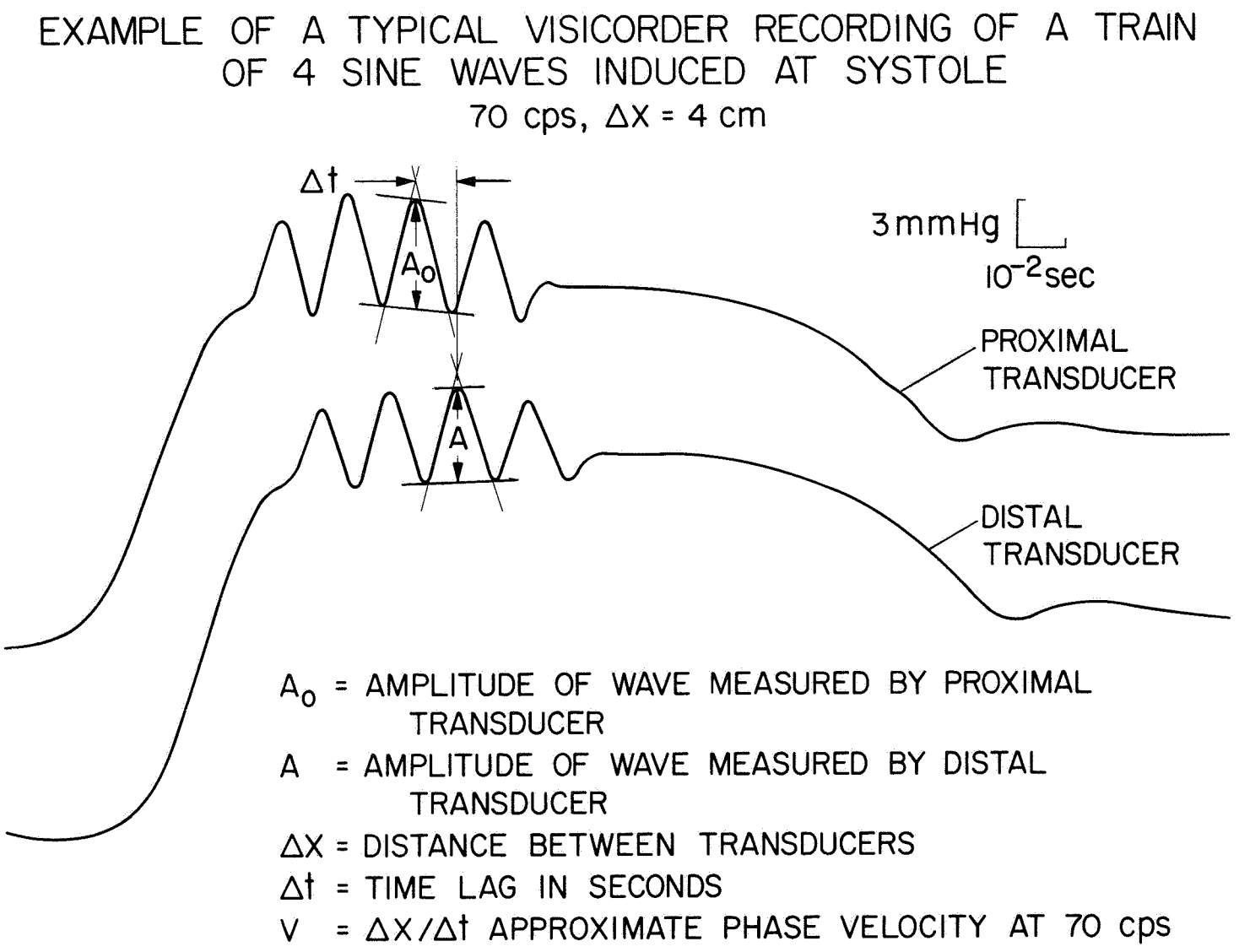

Figure 5. Sample recording of a transient pressure signal with illustration of signal speed and amplitude determination.

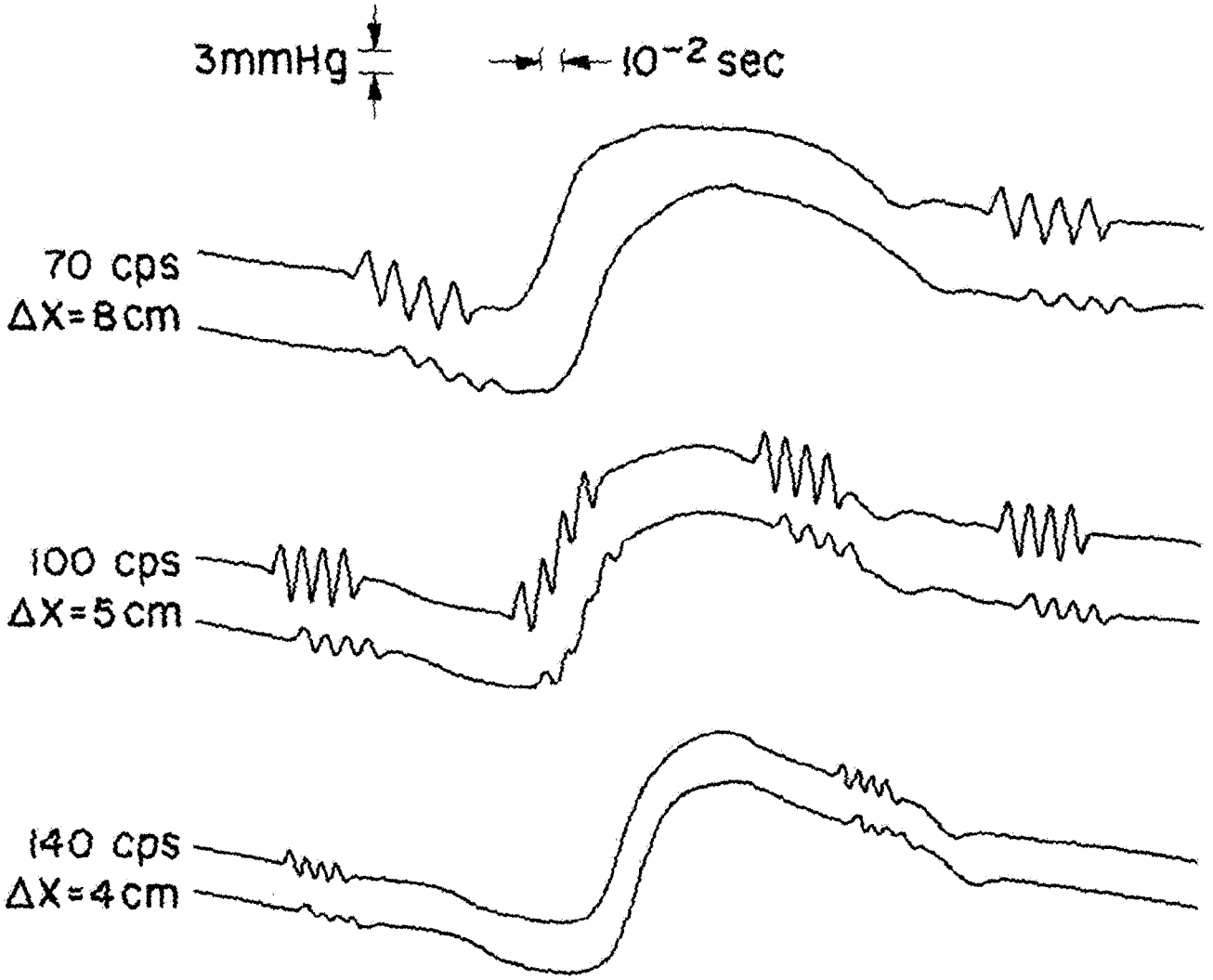

Figure 6. *Representative tracings of recordings of the natural pulse wave in the thoracic aorta of an anesthetized dog, with artificially superimposed trains of sinusoidal waves.* The transient signals can be induced at any time during the cardiac cycle. Note that the sine waves are highly damped but retain their sinusoidal character during propagation.

thoracic aorta. The natural pulse wave and the artificially induced pressure signals can easily be recognized. In these instances the frequencies of the sine waves were 70 cps, 100 cps and 140 cps. The recordings in Figures 5 and 6 are from experiments in which the low frequency impacts were deliberately made larger than normal in order to provide a clear illustration. In the data discussed below, the amplitudes of the sine waves were generally less than 5 mm Hg and their frequencies ranged from 40 to 200 cps. Wave trains with frequencies below 40 cps could be recorded over a distance of more than 20 cm. Most of the results given here are based on wave transmission data obtained from a segment of the thoracic aorta less than 12 cm in length to minimize the effects of taper and branching.

The sinusoidal pressure signals were generated at various times in the cardiac cycle in each dog as illustrated in Figure 6. Though attenuated during their propagation, inspection indicates that they retain their sinusoidal character. The absence of noticeable distortions of the sinusoidal pressure waves suggests that the aorta is not strongly dispersive for pressure waves in the frequency range considered here and that there are no discernible effects of reflections. In a strongly dispersive medium one should observe "forerunners" (34) of the trains of sine waves, especially when the trains are short. However, no "forerunners" of the pressure signals could be discerned in the aorta. For sinusoidal waves recorded during diastole, the time lag Δt did not vary measurably with the selection of a characteristic point within the same train. This can be interpreted as further evidence that the aorta is not strongly dispersive and that the effects of reflections are negligible.

However, for signals produced during systole, Δt was observed

to be noticeably different for different characteristic points within the same train and appeared to vary systematically with the cardiac phase. This implies that the signal speed also varied with the cardiac phase during systole. Theoretical analyses indicate that the wave speed may be affected by both pressure (1, 2, 29) and mean flow (35). Any description of the dispersive nature of the aorta should therefore include a reference to the pressure and the instantaneous mean flow levels at which the wave speeds were determined. The results of a detailed study of the effects of pressure and mean flow on the velocity of various waves are given in Chapter 3. The dispersion curves given here are restricted to waves generated during the diastolic phase during which the mean flow velocities are insignificant compared with the signal speed (11).

A typical dispersion curve is shown in Figure 7. In this particular case the wave speed is approximately 5 m/sec and is nearly independent of frequency between 60 and 200 cps. The attenuation of sinusoidal waves in terms of the amplitude ratio A/A_o as a function of the distance between the transducers in cm is given in Figure 8. It is evident that the low frequency waves are transmitted over a much larger distance than are the high frequency signals. This attenuation can be attributed to the combined effect of three main causes:

1. Dissipation mechanisms in the vessel wall;
2. Radiation of energy into the surrounding tissue or vascular bed;
3. Viscosity of blood.

The radiation of energy into the surrounding medium must play a minor role in the case of the thoracic aorta since the complete surgical exposure of the thoracic aorta segment in which the waves were studied did not cause a

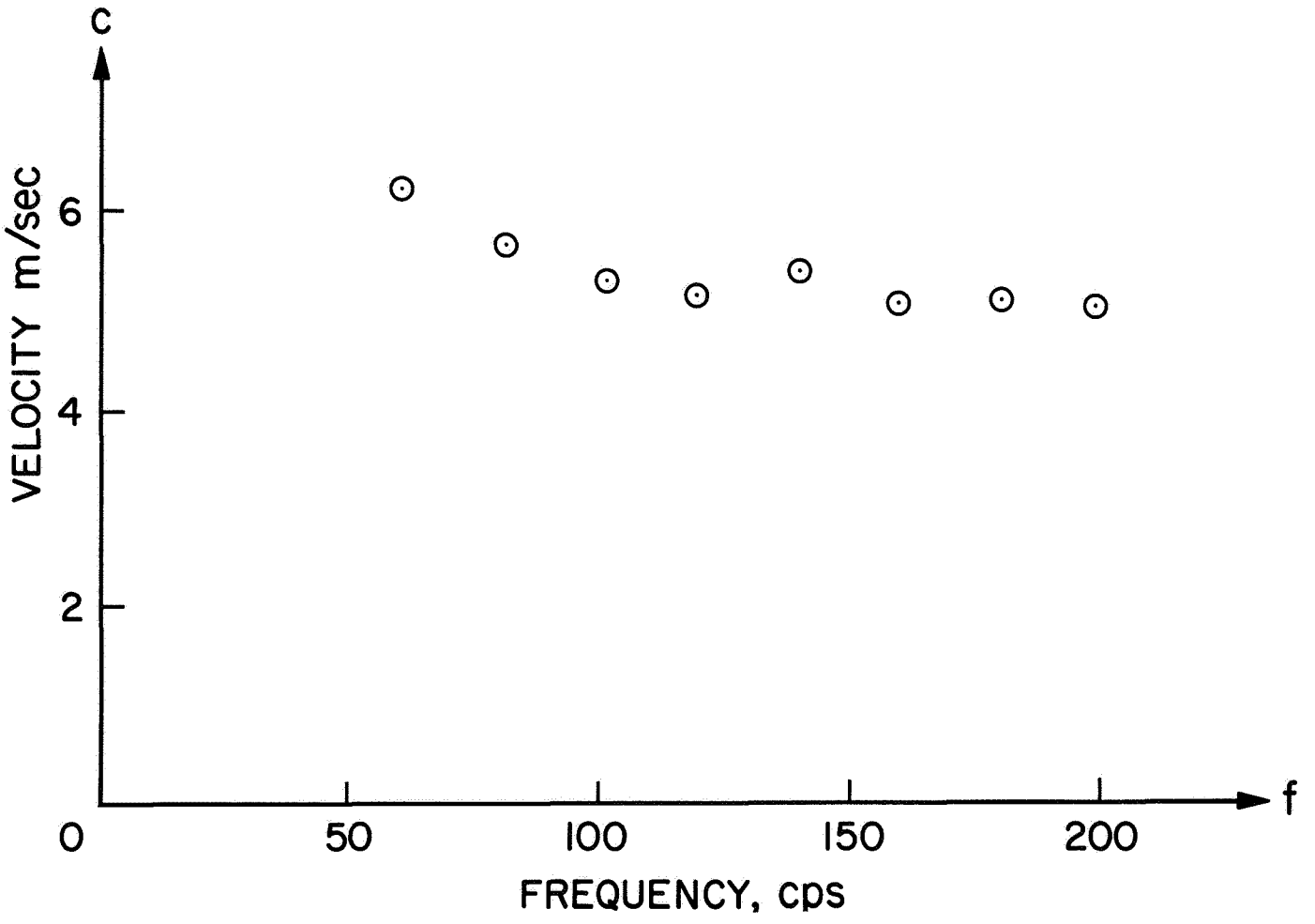

Figure 7. Typical dispersion of waves generated in the thoracic aorta of a dog during diastole. Each point represents an average of 3 to 10 speed measurements of different wave trains at the same pressure levels during diastole.

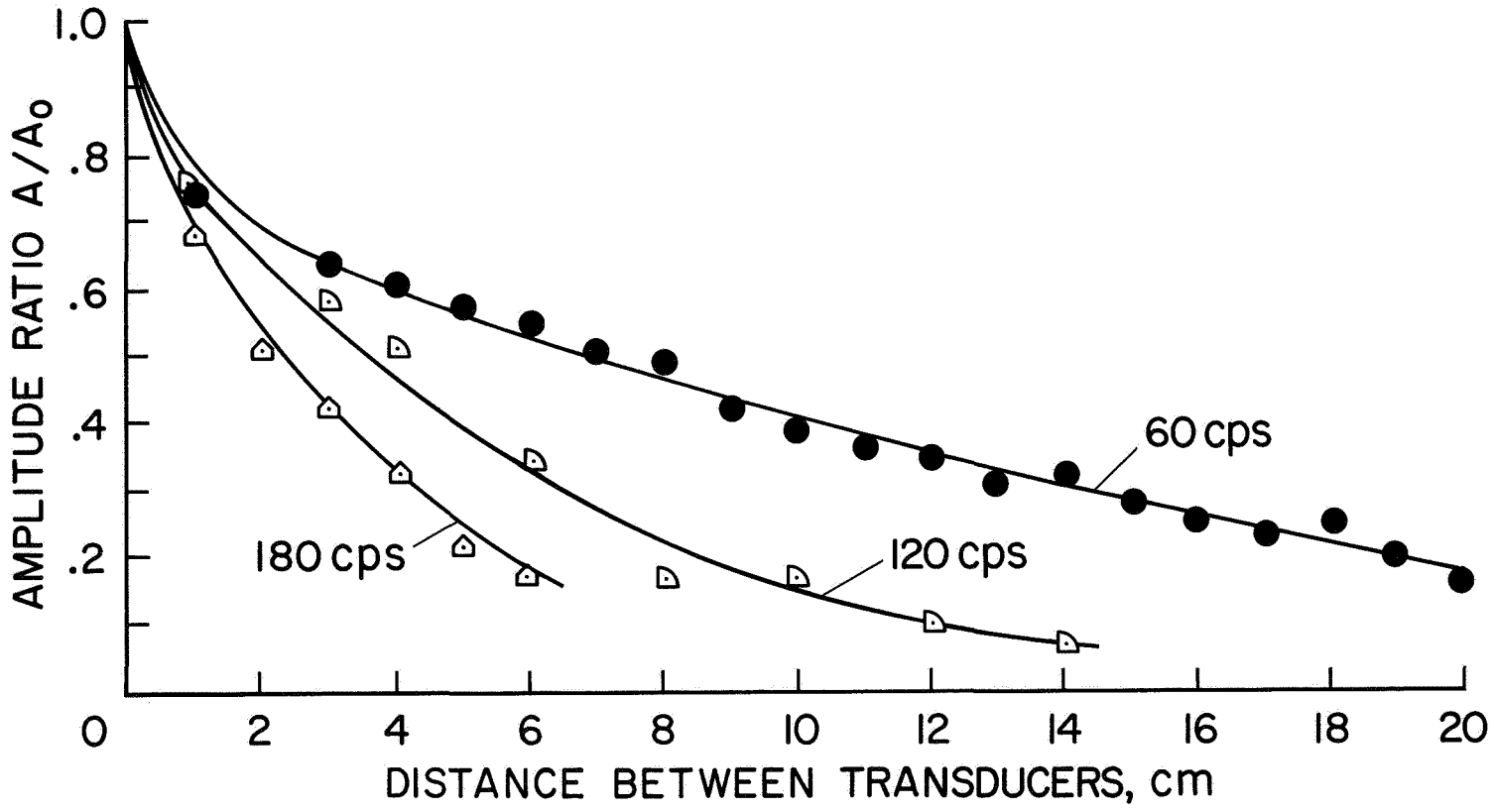

Figure 8. Attenuation of small sinusoidal pressure waves with 3 different frequencies in the aorta of a dog during diastole. The attenuation is given in the form of the amplitude ratio as a function of the distance travelled by the waves measured in cm. Note the rapid dissipation of the signals at higher frequencies.

noticeable change in the dissipation of the waves observed prior to exposure. Moreover, it has been shown theoretically (30) that the viscosity of the blood can only account for a small fraction of the observed attenuation for the frequency range and type of waves considered here. Therefore, the damping of pressure waves can be almost entirely attributed to dissipation mechanisms in the vessel wall.

Knowing the phase velocity c as a function of the frequency one can compute the wavelength $\lambda = \frac{c}{f}$ and represent the attenuation as a function of the nondimensional distance $\frac{\Delta x}{\lambda}$ for all frequencies. Figure 9 gives the attenuation pattern when A/A_o is plotted against $\frac{\Delta x}{\lambda}$. It appears that for all frequencies the amplitude ratio A/A_o decreases in the same exponential fashion with $\frac{\Delta x}{\lambda}$:

$$\frac{A}{A_o} = e^{-k \frac{\Delta x}{\lambda}}$$

where $k = .89$ is the logarithmic decrement. It is therefore convenient to plot A/A_o on a logarithmic scale as illustrated in Figure 10.

Additional dispersion and attenuation curves representative of a total of 17 further experiments are given in Figures 11 to 16. The results of these experiments indicate that at normal blood pressure levels the wave speed in the thoracic aorta during diastole has a value between 4 and 6 m/sec, while the attenuation coefficient k varies between 0.7 and 1.0 for waves propagating in the peripheral direction. The data from all these experiments show a high degree of consistency in contrast to the findings of Faber et al (36) who recorded the speeds of various frequency components of the

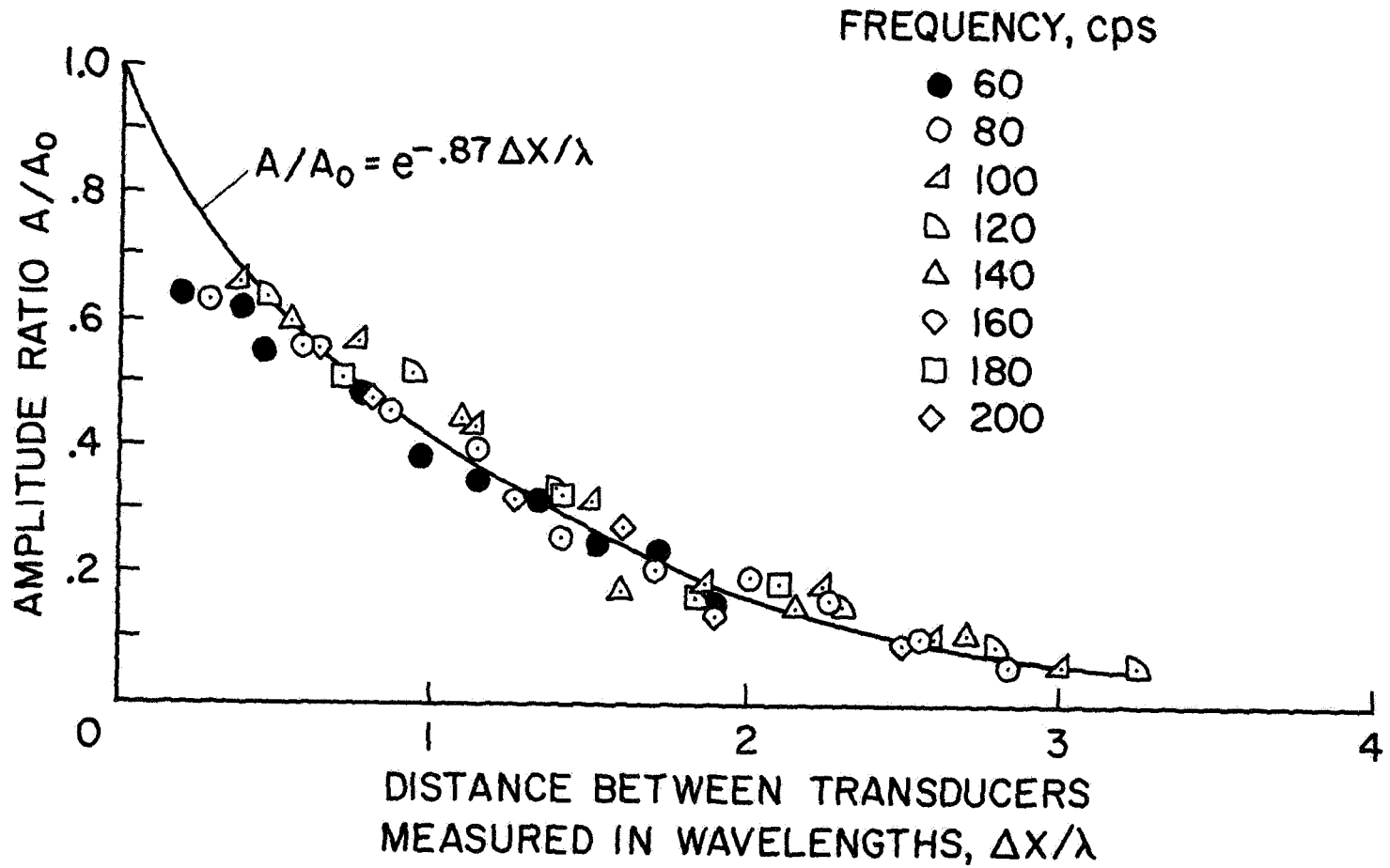

Figure 9. Attenuation of pressure waves in terms of the amplitude ratio as a function of the distance traveled in wavelengths. Some of these data are also shown in Figure 8. Note exponential decay pattern of the wave amplitude independent of frequency.

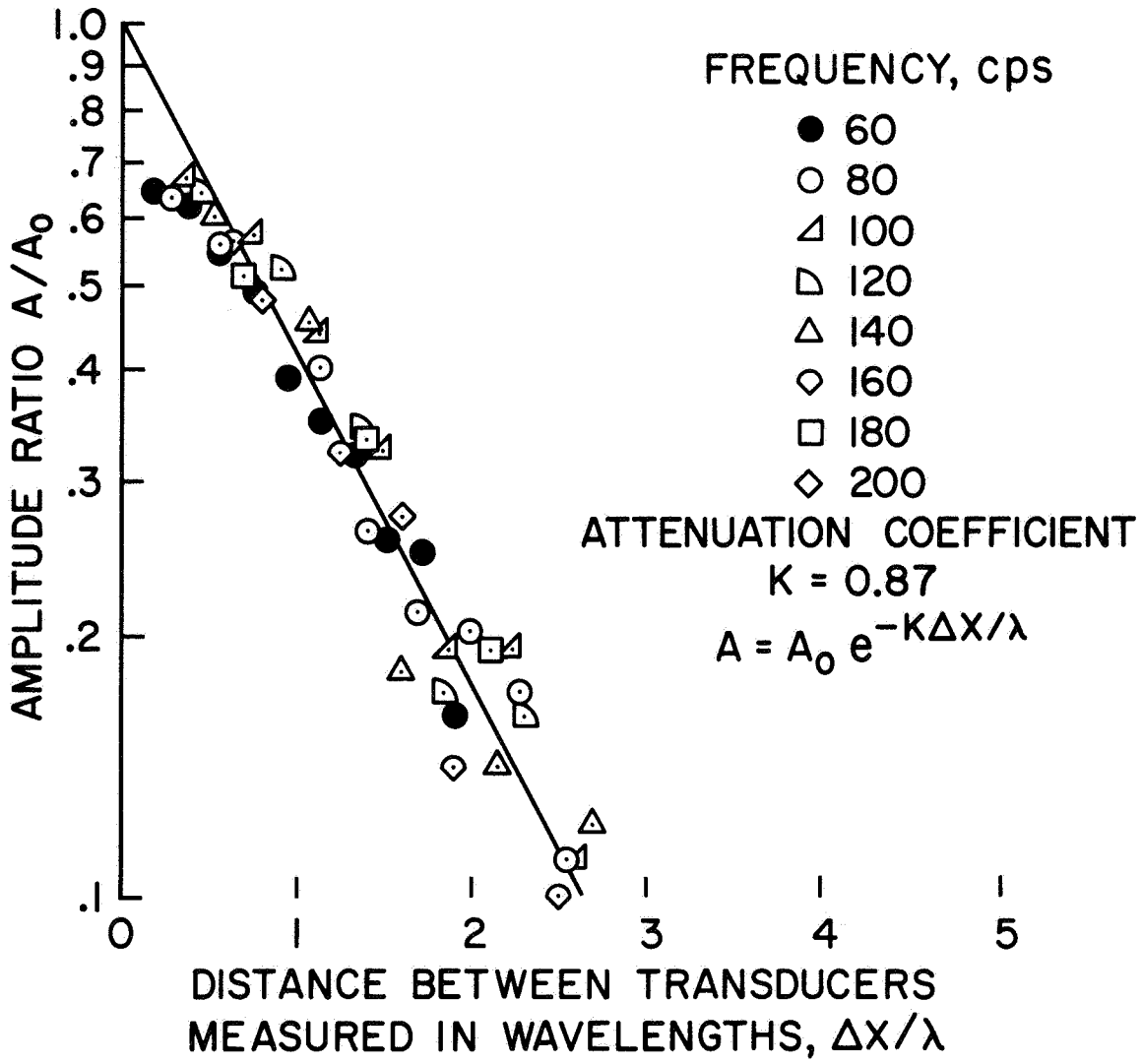

Figure 10. Attenuation data given in Figure 9 with A/A_o plotted on a logarithmic scale. The slope of the line approximating the variation of $\ell n(A/A_o)$ with $\Delta x/\lambda$ defines the attenuation coefficient k, which in this case is .87.

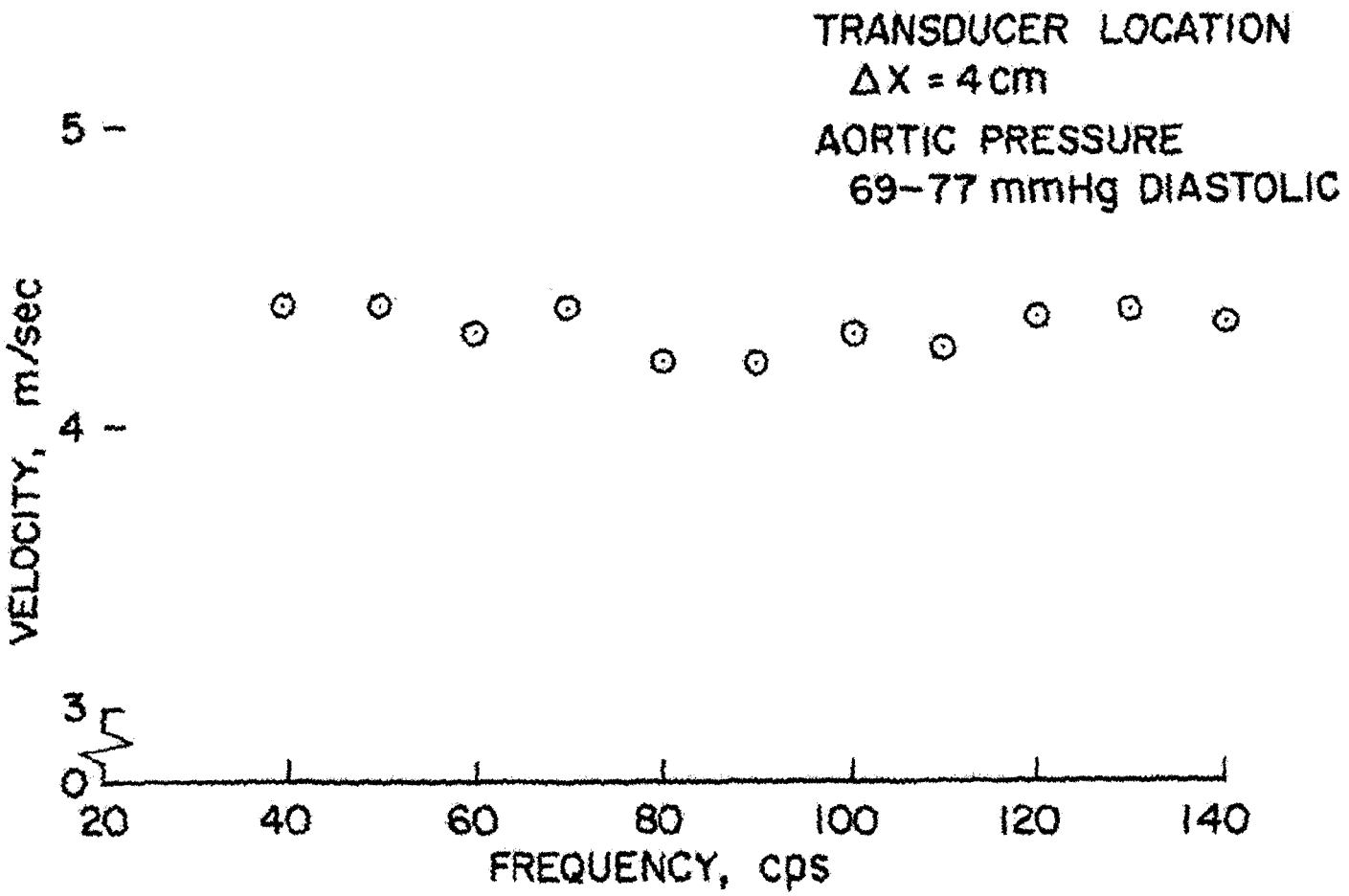

Figure 11. Dispersion curve for waves generated during diastole at a pressure between 69 and 77 mm Hg. Each point represents an average of 3 to 10 speed measurements of different wave trains at the same pressure levels during diastole.

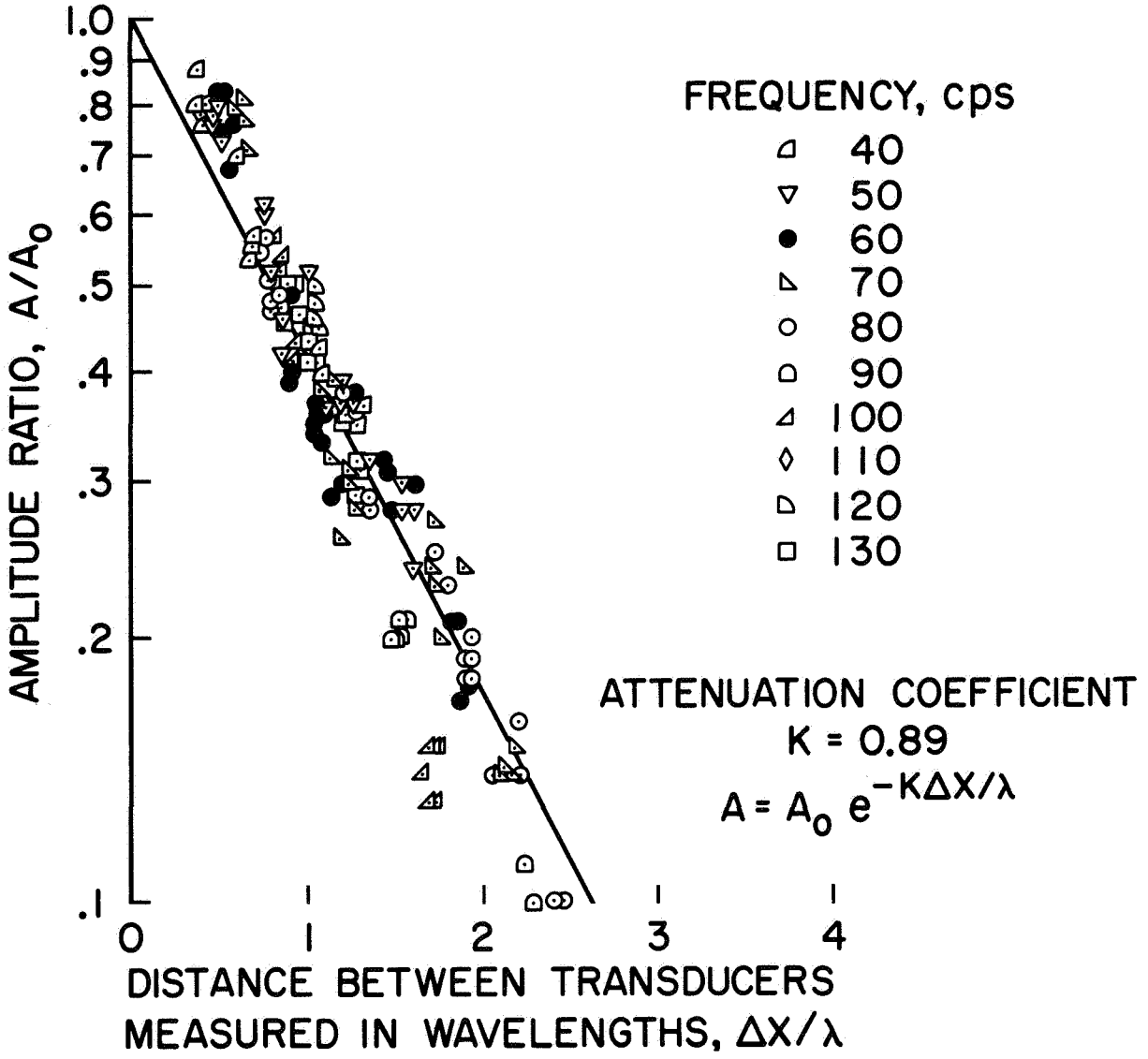

Figure 12. Attenuation of waves corresponding to dispersion data given in Figure 11. k = .89

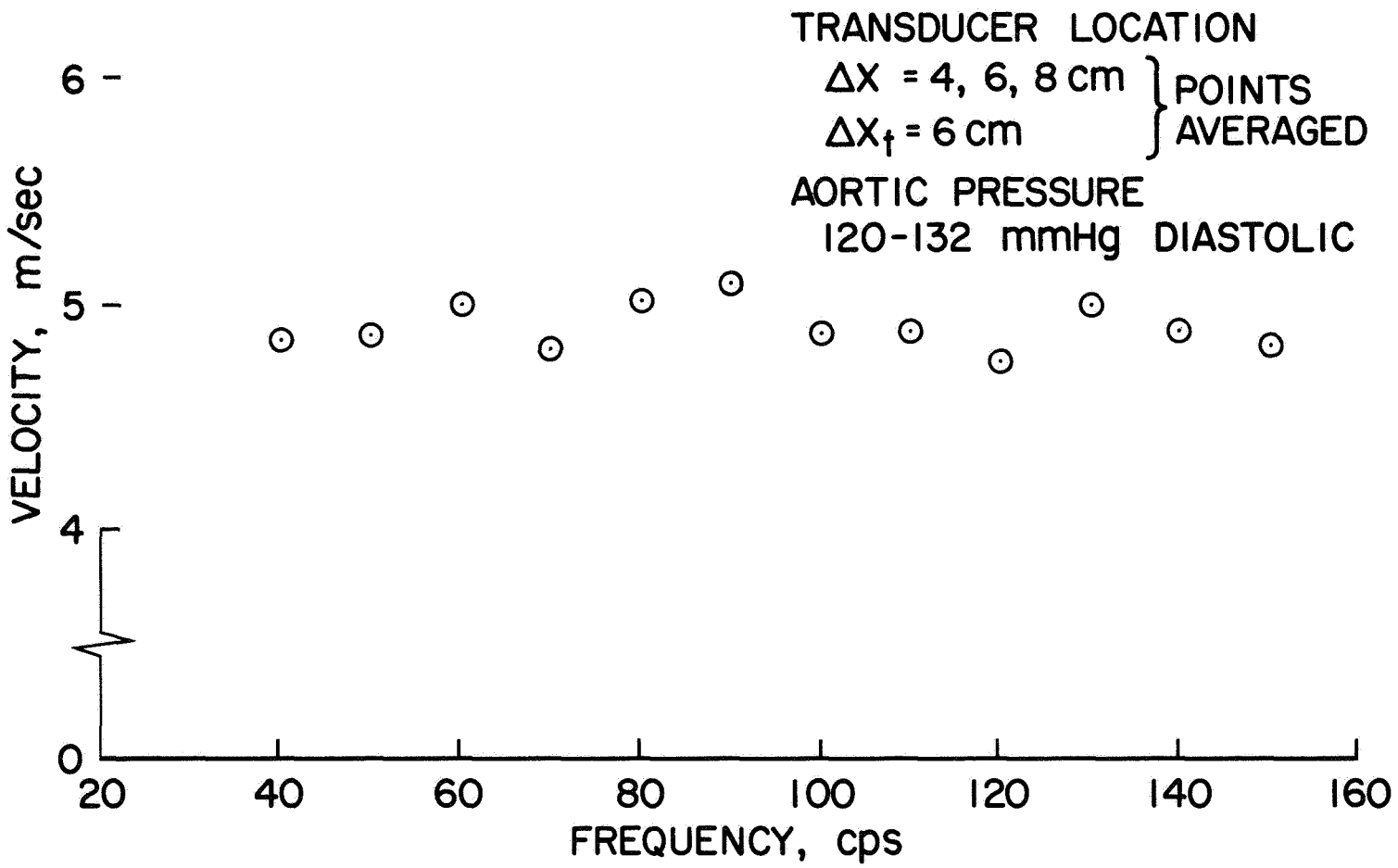

Figure 13. Dispersion curve for waves generated during diastole at a pressure between 120 and 132 mm Hg. Δx_t denotes the distance between the proximal transducer and the wave generator. Each point represents an average of 3 to 10 speed measurements of different wave trains at the same pressure levels during diastole.

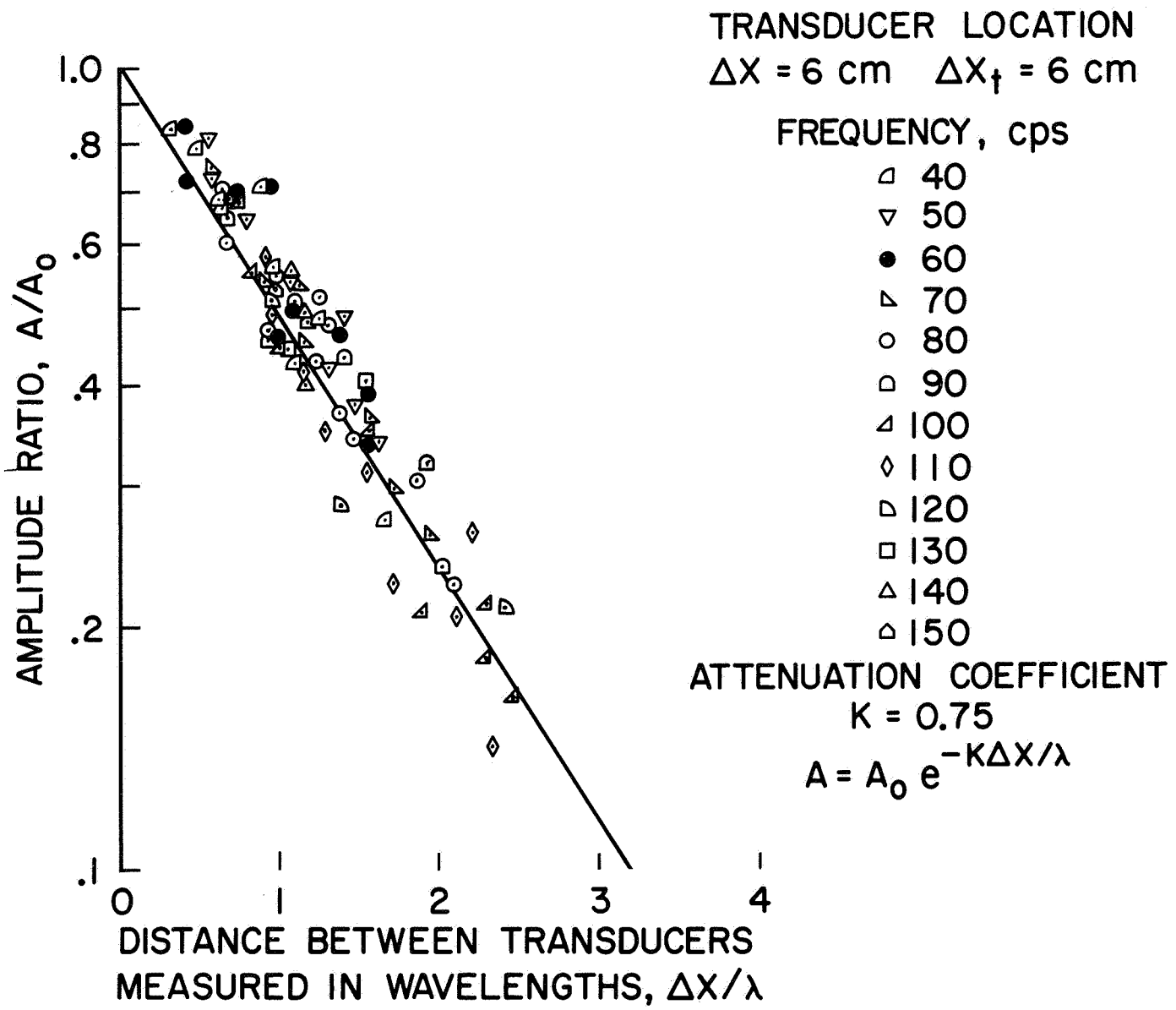

Figure 14. Attenuation of waves corresponding to dispersion data given in Figure 13. k = .75

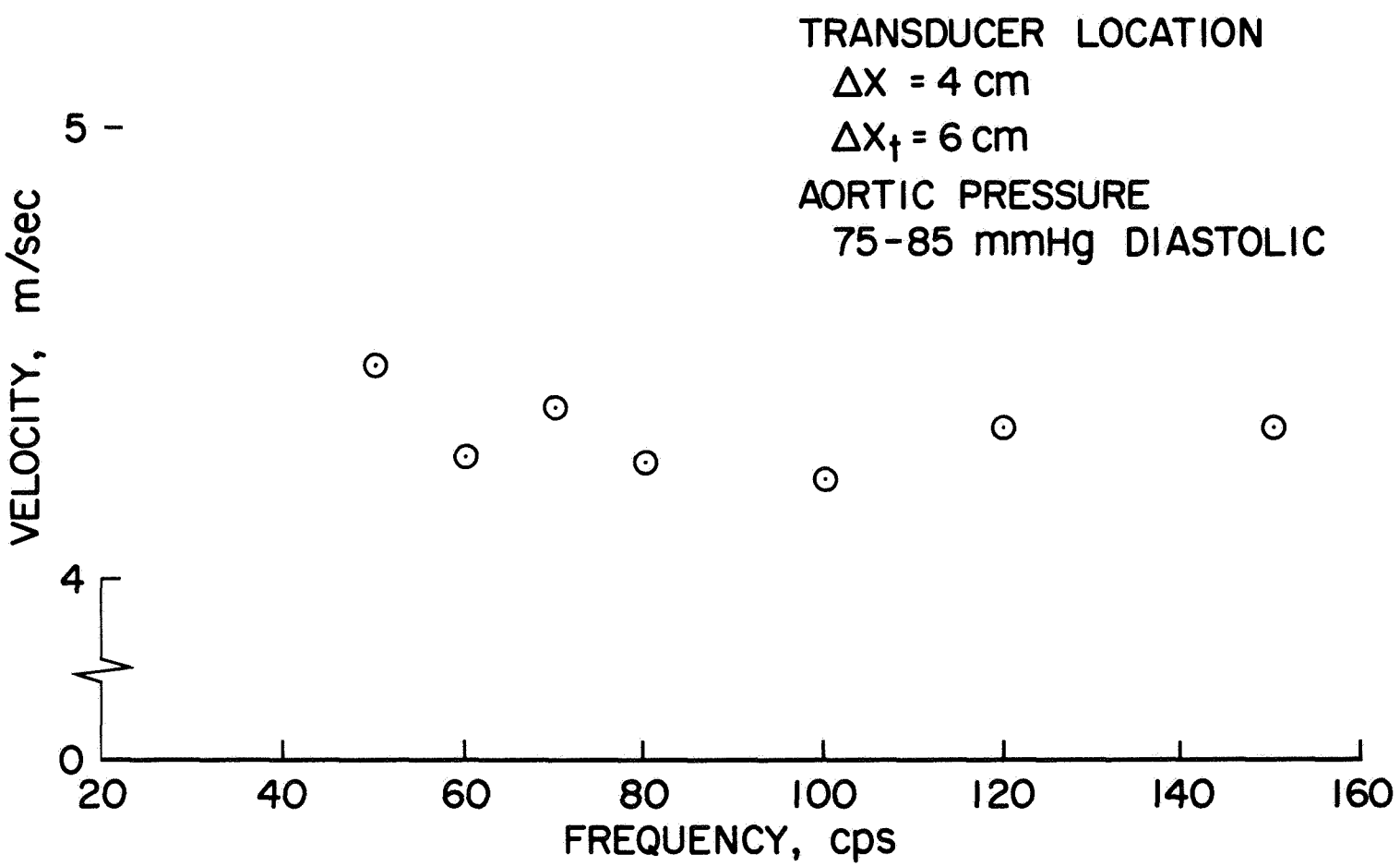

Figure 15. Dispersion curve for waves induced during diastole at a pressure between 75 and 85 mm Hg. Each point represents an average of 3 to 10 speed measurements of different wave trains at the same pressure levels during diastole.

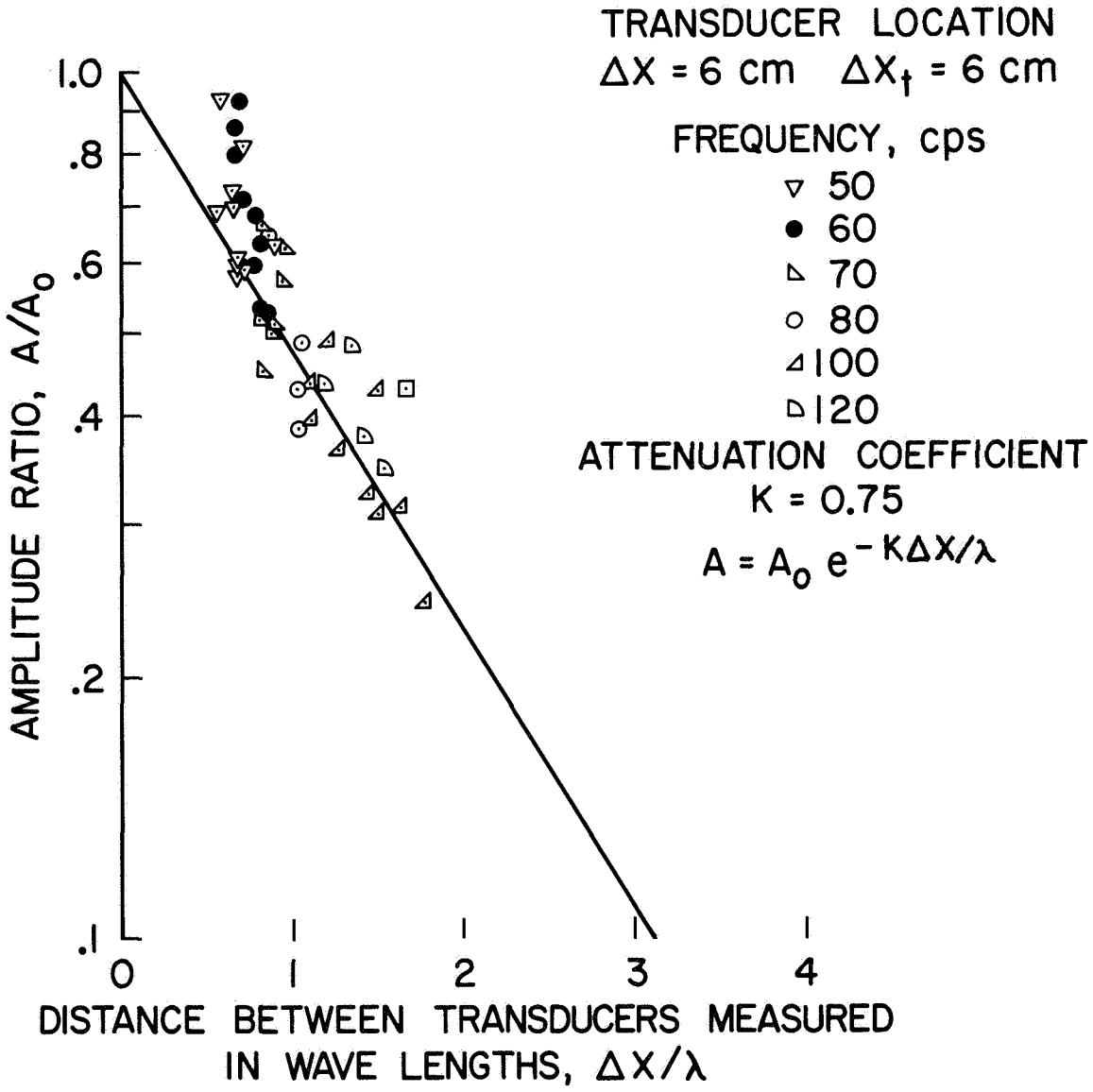

Figure 16. Attenuation of waves corresponding to dispersion data given in Figure 14. k = .75

second heart sounds in the upper thoracic aortas of anesthetized dogs. For frequencies below 40 cps the waves induced by the impactor generally no longer had the form of pure sine waves and the data from such waves usually showed a somewhat larger scatter and were therefore not used. Even so, between 20 and 40 cps the waves were sufficiently close facsimiles of pure harmonics to warrant noting that their transmission properties were essentially the same as those for waves with frequencies higher than 40 cps.

2.5 Discussion

The wave transmission data derived from eighteen experiments consistently portrays a very weak dispersion for pressure waves generated during diastole and exhibits in all cases the same exponential decay pattern for the amplitude of a propagating sinusoidal pressure wave. The attenuation per wavelength is nearly independent of frequency between 40 and 200 cps and the attenuation coefficient $-k$ ranges from 0.7 to 1.0. Therefore, during propagation over a distance of one wavelength (2 to 15 cm) the amplitude of a sine wave will diminish to about 50% to 30% of its initial value. This loss of energy must be attributed primarily to dissipative mechanisms in the vessel wall since the viscosity of the blood and the radiation of energy into the surroundings of the aorta can only account for a relatively small fraction of the attenuation in the frequency range considered.

The absence of any significant dispersion and reflection interference was indicated by the facts that for small amplitudes the sine waves retained their sinusoidal form during propagation and that the signal speed was independent of the choice of a characteristic point. Under such conditions one can justify interpreting the signal speed as an approximation of the

phase velocity corresponding to the frequency of the sine wave and thus avoid the laborious Fourier transform computations.

The frequency and amplitude of the sinusoidal pressure waves could be accurately controlled irrespective of whether they were generated by the pump or by the electrically driven impactor. However, the number of sine waves contained in each train and the interval between the trains were most accurately regulated when the impactor was used. Therefore, in most of the experiments conducted the waves were generated by a controlled tapping of the aorta. To minimize any possible manifestations of nonlinear effects associated with large pressure fluctuations, the amplitudes of the sine waves were generally chosen no larger than necessary for a precise determination of the signal speed. For wave amplitudes less than 5 mm Hg no evidence of reflections or nonlinear behavior was discernible for frequencies above 40 cps. For frequencies between 20 and 40 cps there were also no obvious manifestations of nonlinear propagation characteristics, but it should be noted that such waves in general exhibited minor distortions, even with small amplitudes. However, these waves were so close to being pure harmonics that their speeds and attenuation may be interpreted as meaningful data with some qualification. For frequencies below 40 cps it was possible to generate waves with amplitudes up to 20 mm Hg. Such waves clearly altered their shape during propagation, but no attempt was made to interpret these changes as the result of reflections or specific nonlinear properties of the aorta.

The dispersion and attenuation properties of the aorta for a given pressure level and axial stretch can be utilized in the determination of a valid mathematical model for the mechanical behavior of the aorta and specifically in establishing the constitutive laws of the vessel wall. The insignificant

dispersion of pressure waves within the frequency range covered by the experiments has been predicted by several theoretical studies (1, 2, 29, 31). In these and other analytical investigations it was shown that there are three different kinds of waves that can be transmitted by a vessel of the shape of a circular cylinder. The waves can be distinguished by the corresponding displacement pattern of the vessel defined by the motion of an arbitrary point of the wall in the axial, circumferential and radial directions. The propagation characteristics of the wave will depend strongly on which of the three displacement components dominates. For example, a wave in which the radial motion of the wall dominates is transmitted at a relatively low speed and exhibits a strong intraluminal pressure fluctuation. Such a wave is generally referred to as a pressure wave. Waves with dominant axial or circumferential wall motion by contrast produce extremely small pressure perturbations but travel at a considerably higher speed than do pressure waves. In references (1) and (2) the three types of waves have been predicted on the basis of a mathematical model in which the elastic and viscoelastic properties of the wall material are free parameters that can be evaluated for example by measuring the propagation characteristics of one type of wave. With this information one can then predict the transmission properties of the other types of waves and by comparing them with those measured in experiments the validity of the model can be conveniently tested.

A quantitative evaluation of changes in the elastic properties of blood vessels on the basis of altered propagation characteristics of waves is only meaningful after a mathematical model has been established which predicts the dispersion and attenuation of the various waves with reasonable accuracy. After such a model has been arrived at, it should be possible to apply the

method described here in a systematic study of the control mechanisms that may govern active changes in the elastic properties of blood vessels.

CHAPTER 3

THE EFFECTS OF PRESSURE AND FLOW ON PROPAGATING PRESSURE WAVES IN THE AORTA

3.1 Introduction

A thorough knowledge of the factors affecting the magnitude of the wave speed in either an artery or a vein, and the manner in which these factors may alter the wave speed is essential when describing changes in the distensibility of large blood vessels in terms of wave speed changes. Morgan and Ferrante (35) have considered the theoretical problem of wave propagation in elastic tubes containing a streaming fluid. For an average steady state flow velocity $\bar{U}$, small compared to the wave speed c, the observed wave speed c_o is approximately equal to $c + \bar{U}$, the sum of the phase velocity for the system at rest and the average steady stream velocity. Muller (37) has conducted wave speed measurements on rubber tubes containing a streaming fluid. He found a wave speed which is slightly less than $c + \bar{U}$ for waves propagating in the direction of flow, while for waves traveling against the flow he measured wave speeds that were somewhat greater than $c-\bar{U}$. The deviation in each case was approximately 17 percent, but no explanation for this was given.

As mentioned in Chapter 2 the speeds of artificially induced pressure waves in the aortas of anesthetized dogs also seem to depend on the mean flow velocity as well as pressure. This was concluded from a systematic variation of the wave speed with cardiac phase. Since the method developed for these experiments permits the generation of transient signals at any instant of the cardiac cycle (Figure 6), it should therefore allow for a study

of the combined effects of the naturally occurring pressure- and flow-fluctuations on the transmission characteristics of pressure signals. Also, by occluding the ascending aorta for a few seconds or by stopping the heart through vagal stimulation and therefore interrupting the flow, the effect of pressure alone on the speed of the sine waves can be determined. The pressure dependence of the phase velocities can then be used as a measure of the change of the elastic properties of the aorta wall with stress.

3.2 Downstream Waves

The initial investigation of the effects of pressure and flow on the wave transmission characteristics was conducted with the experimental arrangement illustrated in Figure 2 used for the study of pressure waves propagating in the downstream direction of the aorta. If the trains of sine waves were superimposed at random on the natural pulse wave, their speeds should reflect the variations in pressure and flow associated with the cardiac cycle. The mean pressure level of a train and its location on the natural pulse wave, i.e., whether it occurred during early systole, systole, or diastole could easily be ascertained.

Early in the experiments described in Chapter 2 it was noted that the wave speed increases with aortic pressure and from diastole to systole. Therefore, the wave speed data was grouped with respect to cardiac phase and aortic pressure. Figure 17 illustrates typical results obtained with such a grouping of the data. In this figure the solid symbols represent the speeds of signals induced during late diastole and an instantaneous aortic pressure within the interval 77-87 mm Hg. The open symbols correspond to signals induced at late systole and an instantaneous aortic pressure

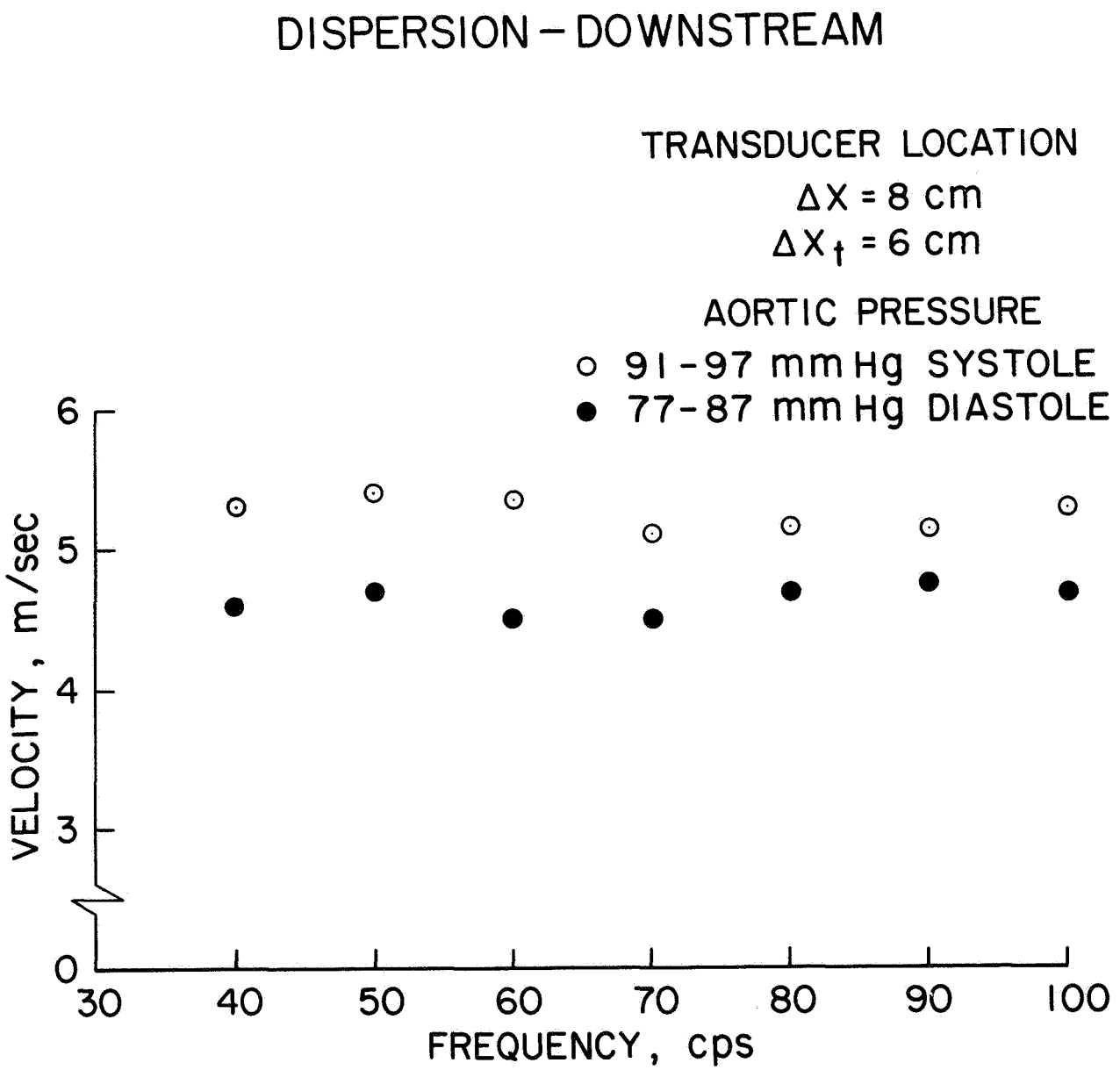

Figure 17. Dispersion data obtained from signals induced late in systole and late in diastole and within a given interval of the aortic pressure pulse.

within the interval 91-97 mm Hg. The systolic data shows a consistent increase in speed of 0.5 to 1.0 m/sec which can be attributed to a stiffening of the aortic wall with pressure and in part to the mean flow present at late systole in the thoracic aorta. For either group of data the dispersion appears to be negligible which confirms the findings given in Chapter 2.

During systole and diastole the speed of the sine trains was consistently evaluated by measuring the time lag Δt of a characteristic point in the middle of the trains. By plotting the speed of randomly induced signals as a function of the instantaneous aortic pressure one obtains as typical data those shown in Figures 18 and 19. The points representing the speeds of waves of different frequencies have been identified by the symbols listed in the left-hand corner of the graphs. Figure 18 demonstrates that with a blood pressure of 100/65 mm Hg the wave speed may increase from approximately 4 m/sec at diastole to about 6 m/sec at systole. This result is independent of frequency in the range from 40 to 120 cps. In other words: with a pulse pressure of 35 mm Hg the phase velocity can increase by as much as 50 percent from diastole to systole. The relatively large scatter of the data points for systolic pressures may be due to the rapid changes in mean flow that occur during the systolic phase of the cardiac cycle.

The increase in wave speed with pressure $\partial c/\partial p$ at negligible flow rates can be determined for limited pressure ranges by intermittently occluding the ascending aorta or by producing cardiac arrest through vagal stimulation. Wave speed-pressure data obtained by both of these maneuvers are shown in Figure 18 and 19. The results of five additional experiments show that $\partial c/\partial p$ may have values between 3 and 6 $\frac{\text{cm/sec.}}{\text{mm hg}}$ Studies (38) designed to determine the functional relationship between pressure and

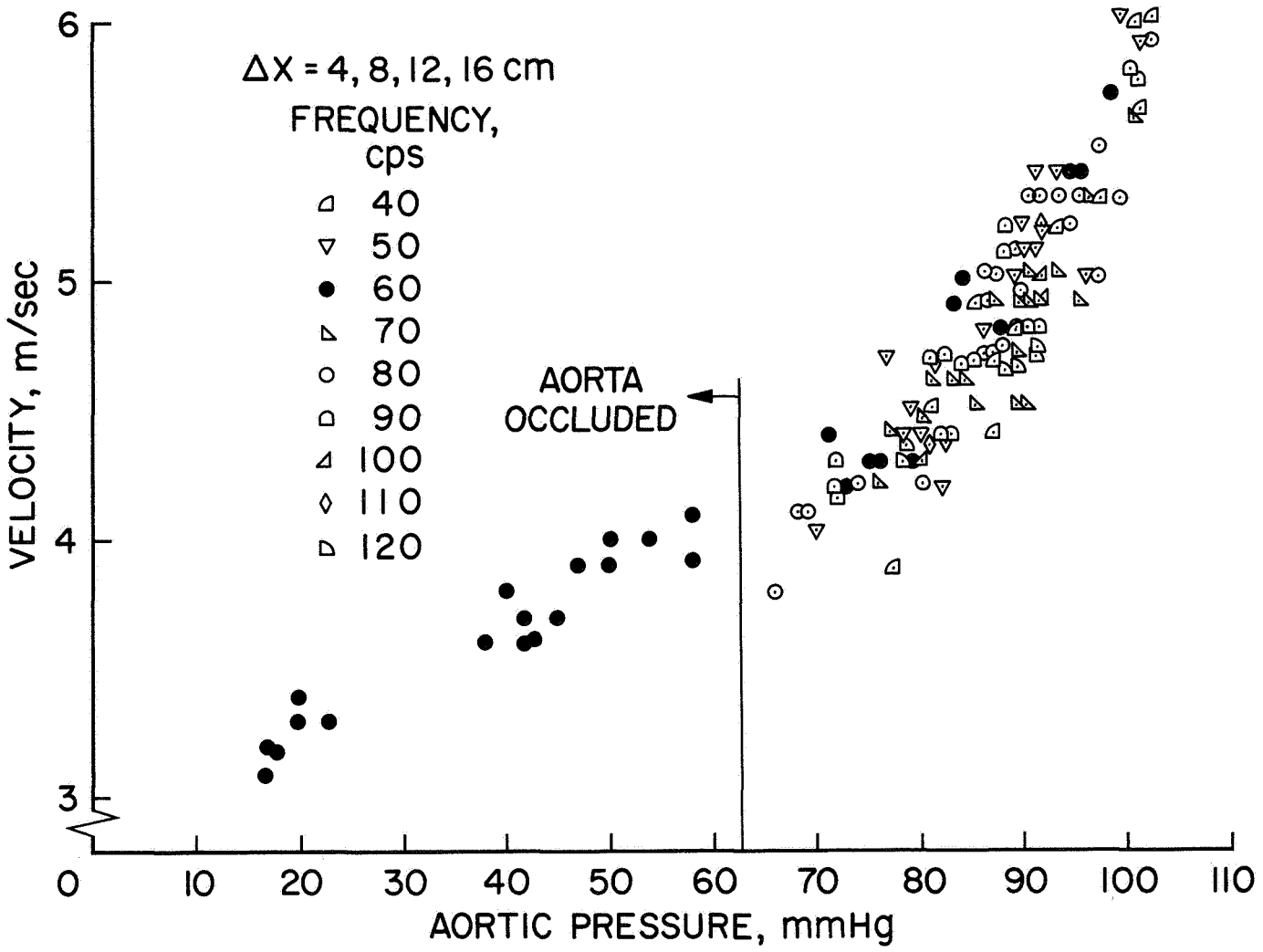

Figure 18. Speeds of sinusoidal pressure waves of various frequencies shown as a function of the instantaneous aortic pressure.

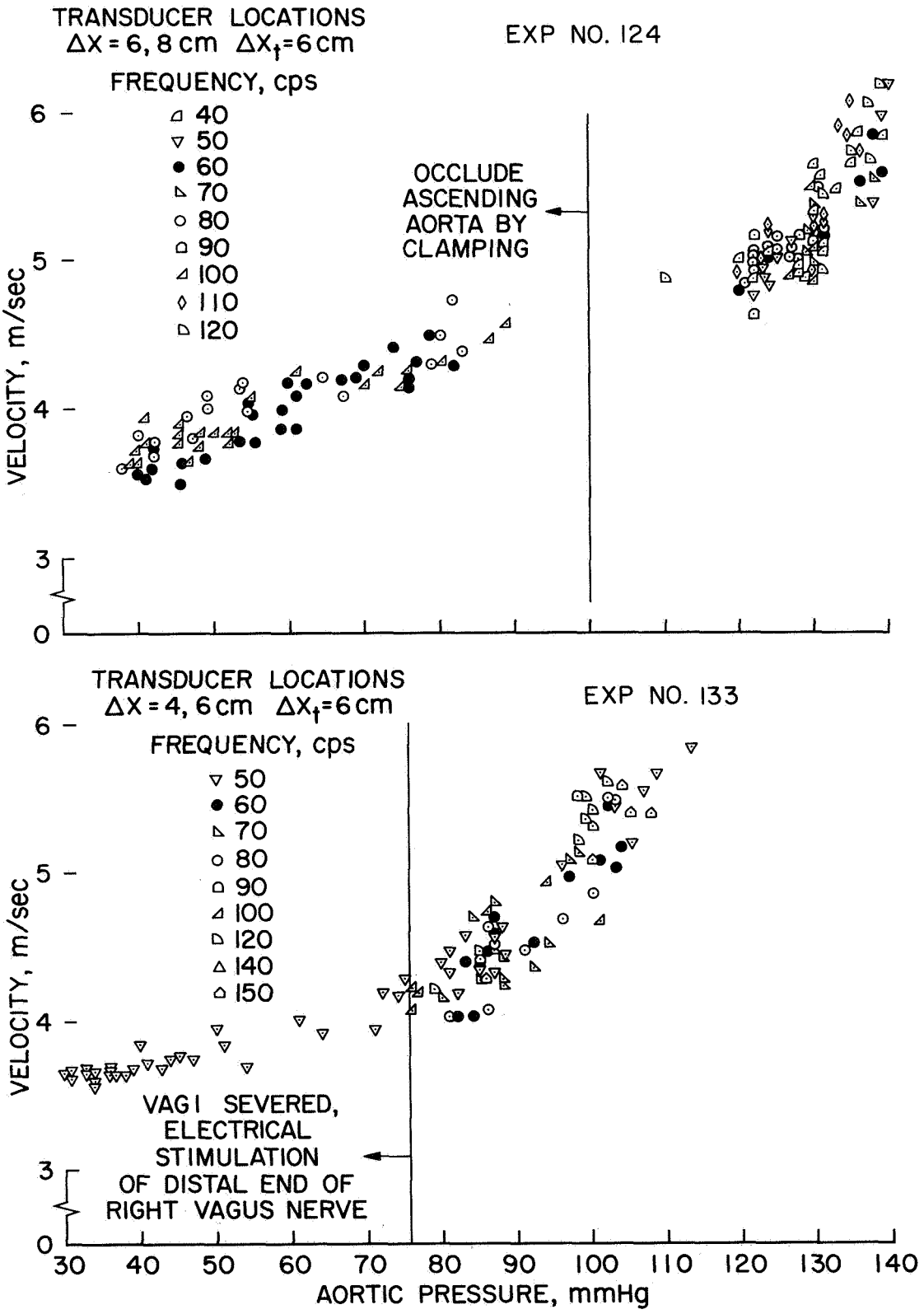

Figure 19. Wave speed variation with instantaneous aortic pressure. The data given here portray essentially the same pattern as those in Figure 18. x_t denotes the distance between the wave generator and the nearest pressure transducer. Data points were obtained for pressures below the diastolic by occlusion and vagal stimulation.

wave speed in the abdominal vena cava yield values for $\partial c/\partial p$ ranging from 1-3 $\frac{cm/sec.}{mm\ H_2O}$ These values are approximately ten times greater than those measured in the thoracic aorta. The disparity could be attributed to differences in geometry and wall properties.

The data from the experiments discussed in this section indicate that the wave speed in blood vessels increases with increasing pressure. This effect is probably due to the combination of the gradual stiffening of the vessel wall as the pressure rises and the convection of the wave by the mean flow in the vessel. The stiffening of the vessel wall implies a change in its elastic properties. The sharp elevation in the wave speed during the early part of systole is most likely caused by the rapid flow of blood.

The attenuation of pressure waves in the thoracic aorta measured in terms of wavelengths appears to be independent of pressure and frequency. Figure 20 shows the attenuation obtained for waves induced at different pressure levels.

3.3 Upstream Waves

The waves generated by the electromagnetic impactor travel in both the downstream and upstream directions as shown schematically in the upper right hand corner of Figure 21. However, so far only the waves propagating in the downstream direction have been discussed. If the observed wave speed increase from diastole to systole is caused by a rise in pressure and flow, then the wave transmission characteristics of the upstream waves will be different than those for downstream waves. To demonstrate this a series of experiments have been conducted in which the impactor was positioned on the thoracic aorta 2 to 4 cm above the diaphragm and the upstream waves were

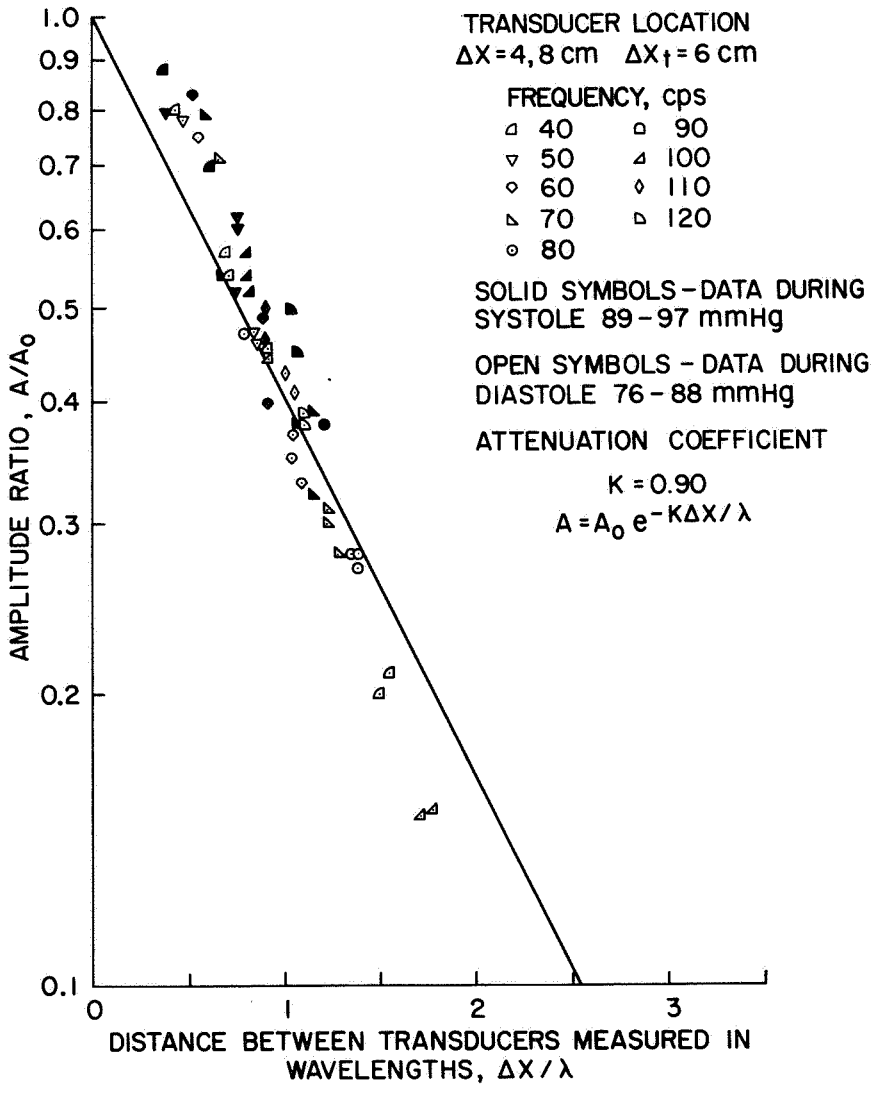

Figure 20. Attenuation of sinusoidal pressure waves propagating in the downstream direction and induced at different aortic pressures.

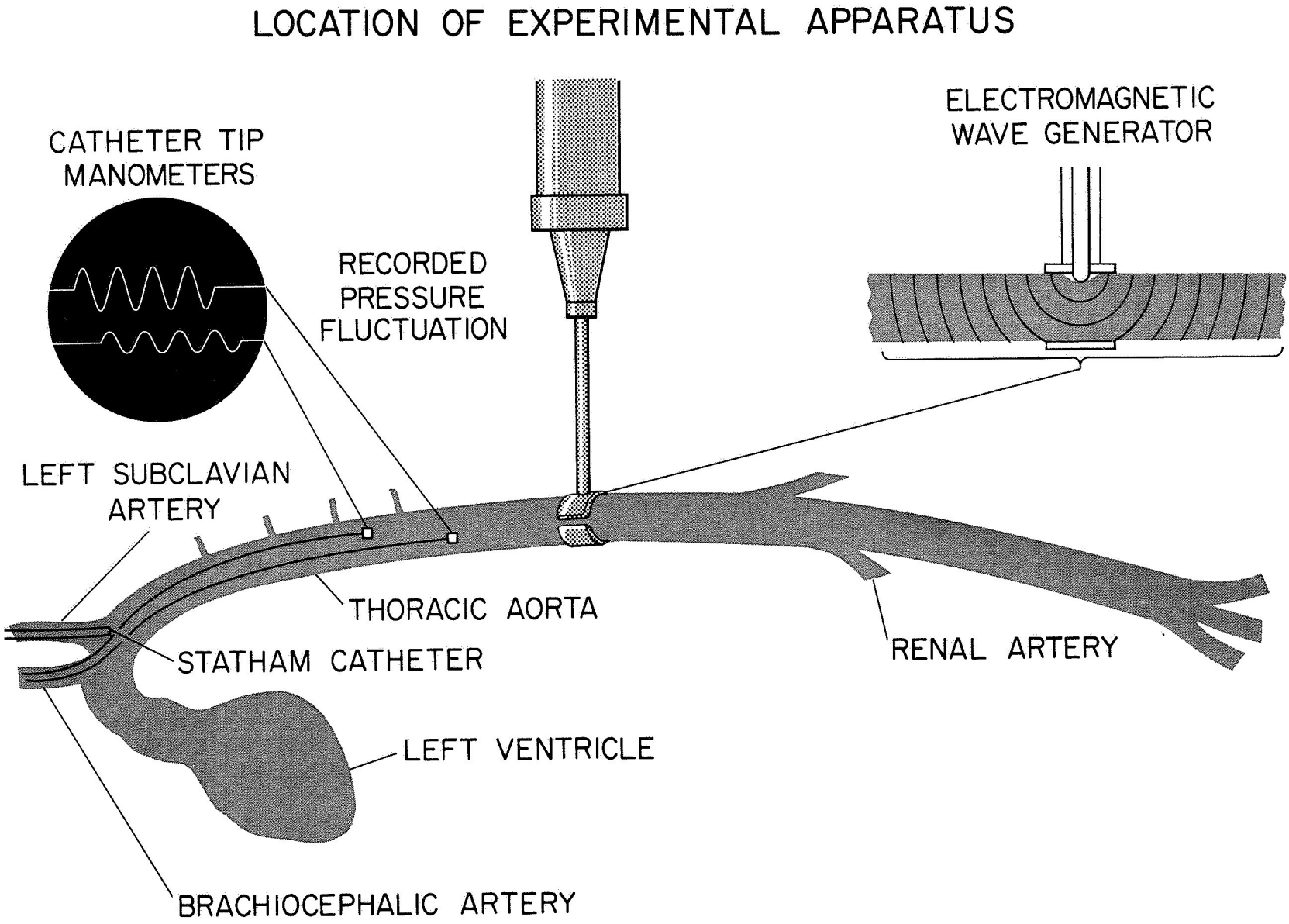

Figure 21. Arrangement of the experimental apparatus used for the upstream wave studies. Only the waves propagating upstream against the flow are recorded.

recorded with catheter tip manometers as shown in Figure 21. Compare this arrangement with the one shown in Figure 2 used for the study of downstream waves. A segment of the aorta was exposed by a 4 cm incision along the 8th or 9th intercostal space and the ribs were retracted. The internal thoracic tissue connecting the aorta to the chest wall was removed from a short segment of the thoracic aorta between two intercostal branches and the stainless steel hook was snugly fitted around the aorta at this position. The manometers were inserted through the left and right carotid arteries and placed 5 cm above the impactor. Usually a rapid rise in mean blood pressure occurred upon ligation of both carotid arteries due to the baroreceptor reflex, but the mean blood pressure returned to normal levels within a few minutes possibly because pressure receptors elsewhere in the circulatory system assumed control. The catheter from the Statham manometer was inserted through the omocervical artery and located in the aortic arch to record instantaneous pressure levels to which the Bytrex manometers could be referenced.

Recordings were made of sinusoidal pressure waves in the frequency range 40 to 160 cps at different instants of the cardiac cycle and representative data are shown in Figure 22. The data shown in this figure do not include those from signals induced during the early part of systole which is characterized by high flow rates. The data from these experiments differ significantly from those obtained for downstream waves shown in Figures 18 and 19. The speed no longer increases significantly with instantaneous pressure from diastole to systole. This implies that the increase in speed due to a stiffening of the aorta with pressure is more or less offset by the decrease in speed due to mean flow. To separate the effects of pressure and flow on wave speed it is necessary to measure the speeds of upstream and downstream

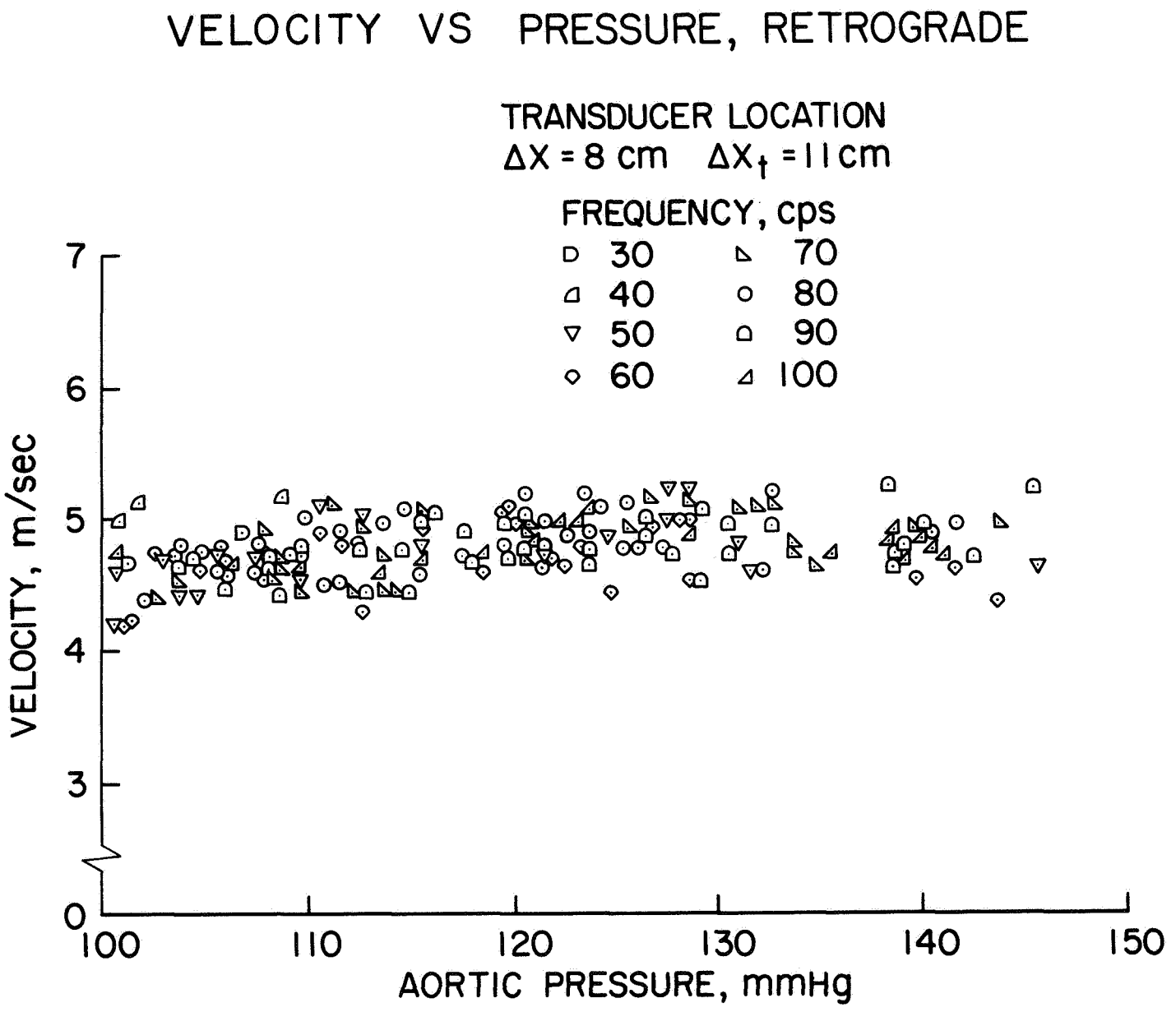

Figure 22. Variations of the wave speed with aortic pressure for upstream waves. Each point represents the speed of a single wave train. Note that data points from trains induced at early systole are excluded.

waves simultaneously.

Typical attenuation observed for upstream waves in the thoracic aorta is shown in Figure 23. The logarithmic decrement for upstream waves was approximately two times that measured for downstream waves and was found to be independent of the pressure level. The value of k calculated from the attenuation data observed in seven additional upstream wave experiments ranged from 1.2 to 1.6. The disparity in the values of k for upstream waves (k = 1.2 to 1.6) and downstream waves (k = 0.7 to 1.0) may be due to taper of the aorta. In the absence of dissipation, the amplitude of a pressure wave increases during propagation in a converging tube and decreases in a diverging tube. However, in the aorta the dissipative mechanisms in the vessel wall exert a salient influence. The combined effects of dissipation and vessel taper on the attenuation for upstream waves moving in a diverging vessel is approximately two times as great as for downstream waves. Therefore, the actual value of the logarithmic decrement due to the dissipative mechanisms in the vessel wall alone would lie between the minimum and maximum for the two directions and hence, would have a value between 1.0 and 1.2.

3.4 Downstream and Upstream Waves

To establish further evidence supporting the conclusion that the wave speed increases with pressure and flow the propagation characteristics of induced pressure signals were recorded simultaneously in the upstream and downstream directions for two segments of the aorta. The arrangement of the experimental apparatus for conducting these studies is shown in Figure 24. The electromagnetic impactor was positioned on the thoracic aorta through the 8th or 9th intercostal space. Bytrex pressure manometers

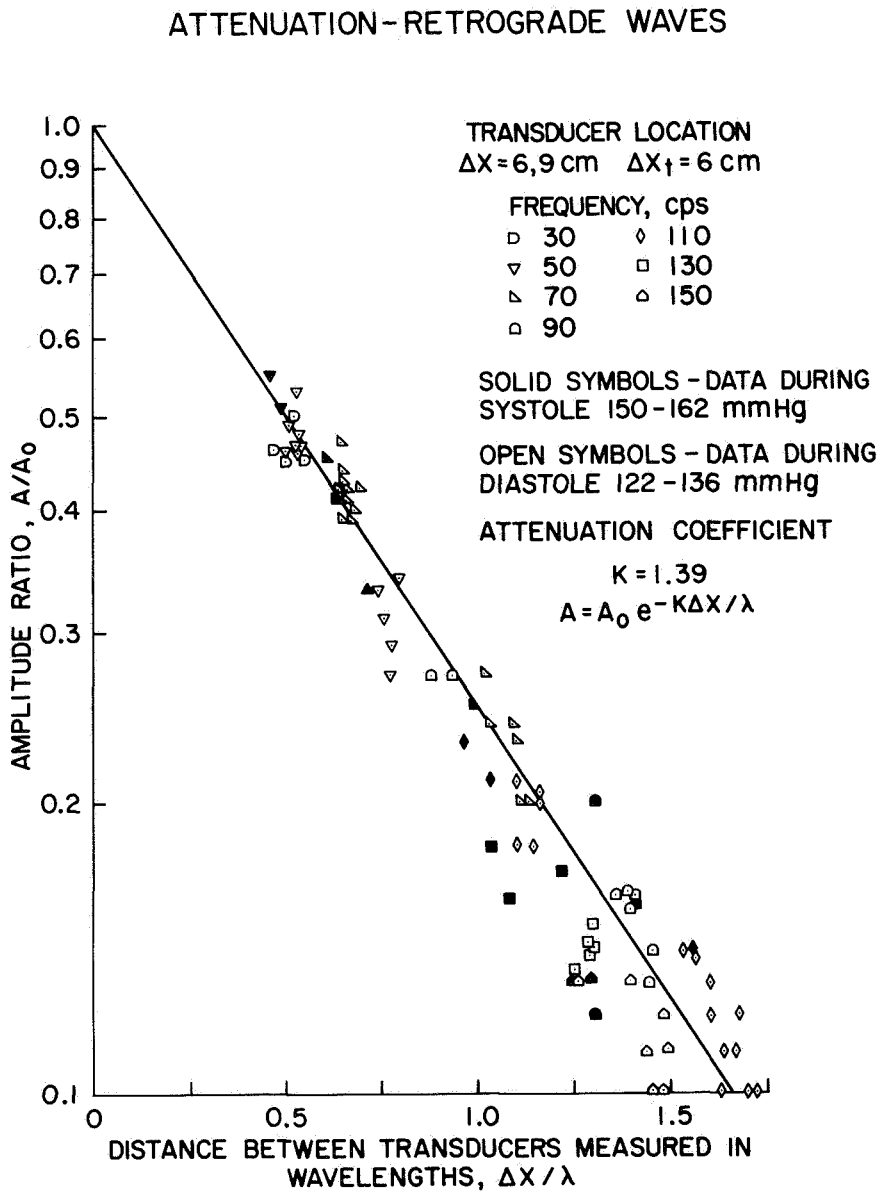

Figure 23. Attenuation of upstream waves for two different pressure levels. Note the higher attenuation for upstream waves (k = 1.39) in comparison with downstream waves for which k = 0.9. See Figure 20.

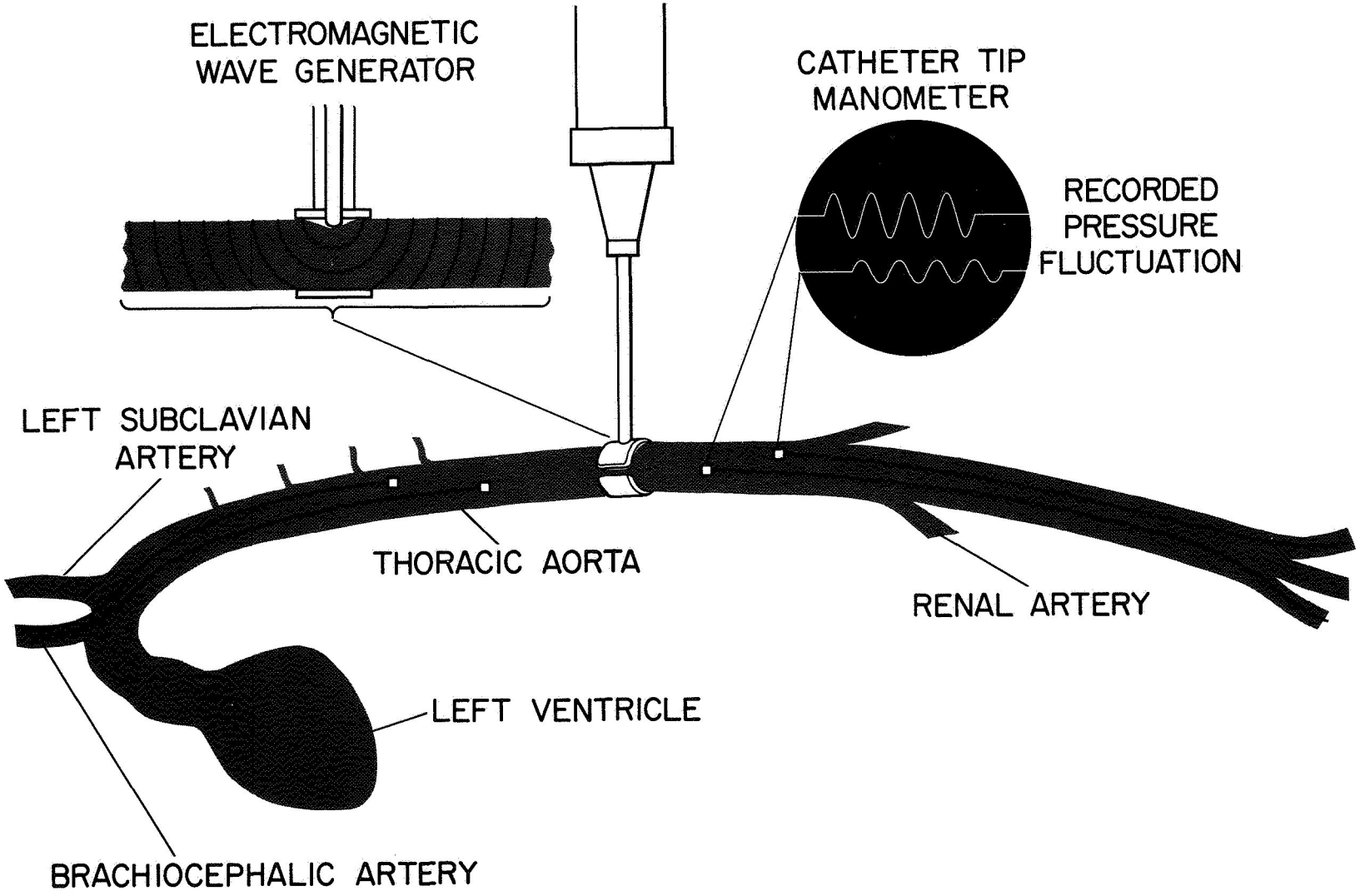

Figure 24. Arrangement of the experimental apparatus for the study of pressure waves propagating upstream and downstream in the aorta.

were inserted into the right and left carotid arteries and were advanced down into the thoracic aorta where they were positioned by means of the X-ray fluoroscope approximately 5 cm apart and at least 5 cm above the impactor. Two of the 1mm diameter capacitance manometers were advanced into the abdominal aorta from the right saphenous and femoral arteries. The capacitance manometers were placed approximately 5 cm apart and at least 7 cm below the impactor. The pressure in the aortic arch was monitored with a Statham pressure gauge.

The dispersion data obtained within narrow pressure ranges for the two segments are shown in Figures 25 and 26. The wave speed is significantly higher in the abdominal aorta than in the thoracic aorta. This result reconfirms the fact that the pulse wave velocity increases with increasing distance from the heart. For the frequency range studied the dispersion was found to be mild in all segments of the aorta. As shown in Figure 27 the attenuation for waves propagating upstream is again approximately twice as large as the downstream attenuation.

The results given in Figure 28 corroborate earlier findings described in sections 3.2 and 3.3. The wave speed downstream increases about 2 m/sec from diastole to systole while the speed of upstream waves increased by less than 1 m/sec. The increase in wave speed with pressure alone, $\partial c/\partial p$, can be measured by vagal stimulation or occlusion techniques which essentially eliminate the flow effects. Results obtained in this fashion are shown in Figure 29.

Since upstream and downstream waves have been recorded for vessel segments with different mechanical properties it is in a strict sense not possible to determine accurately the effects of pressure and flow on the

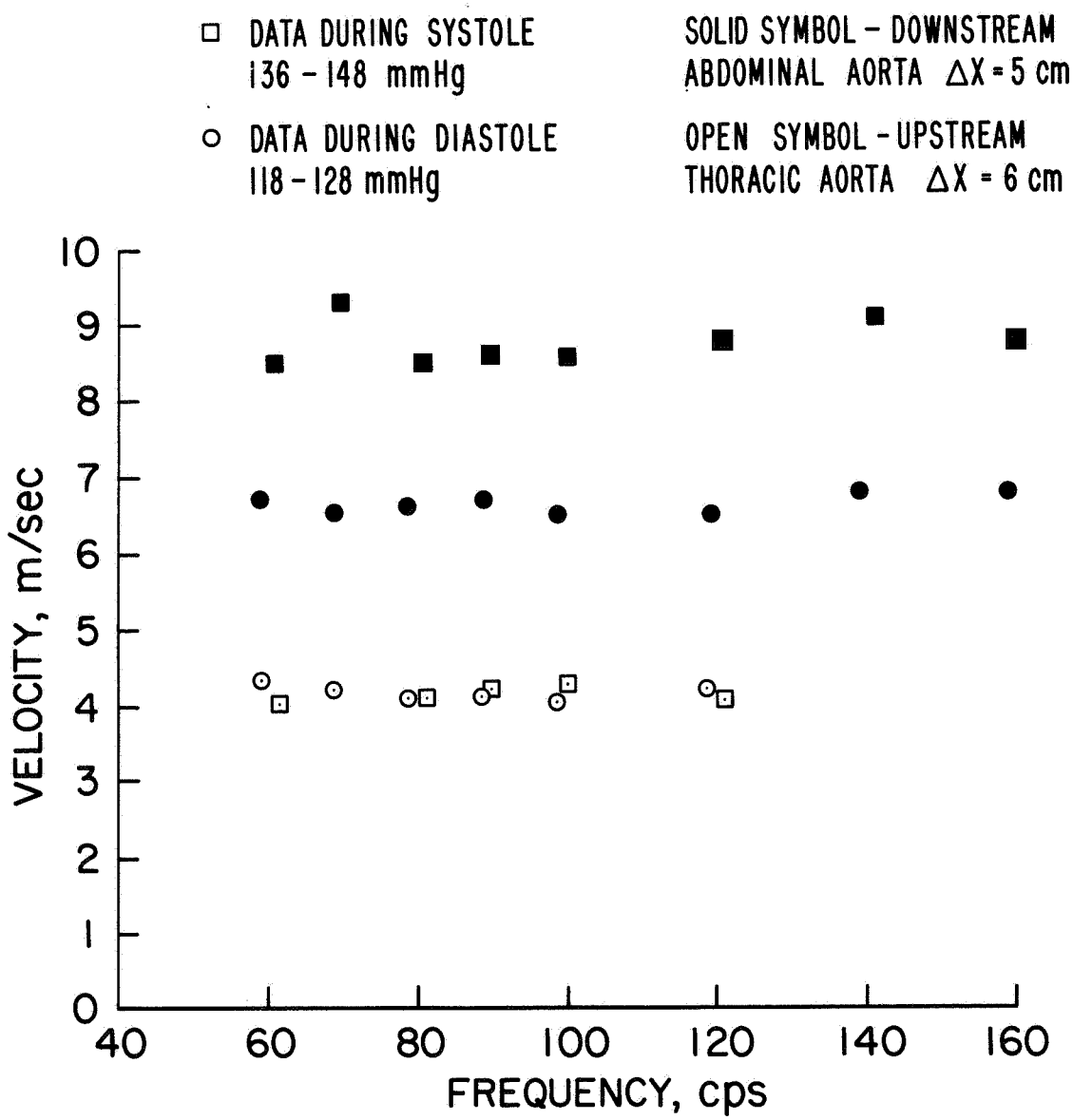

Figure 25. Dispersion data for upstream and downstream waves. Note that data points from trains induced at early systole are excluded.

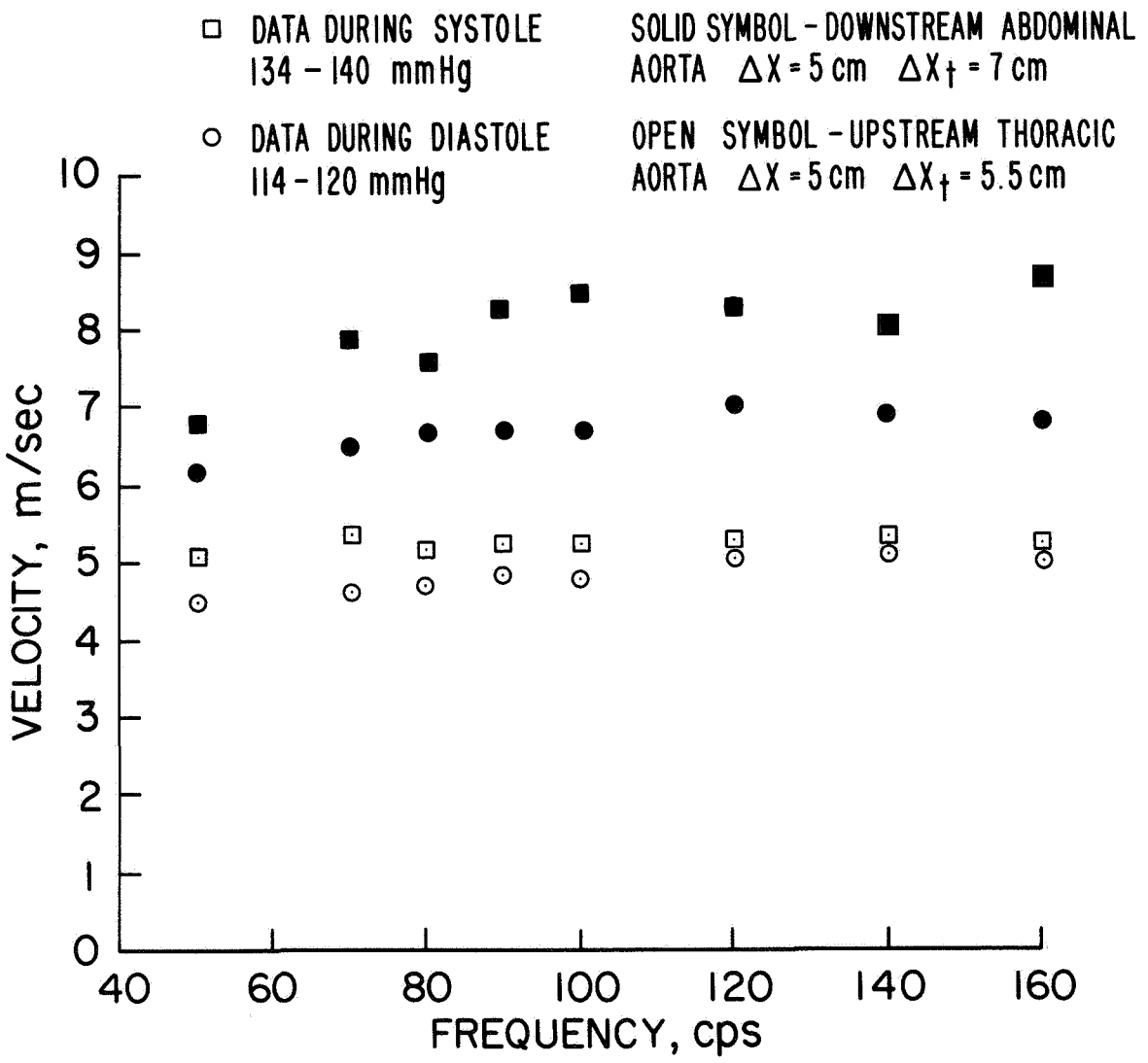

Figure 26. Additional dispersion data for upstream and downstream waves. Note that data points from trains induced at early systole are excluded.

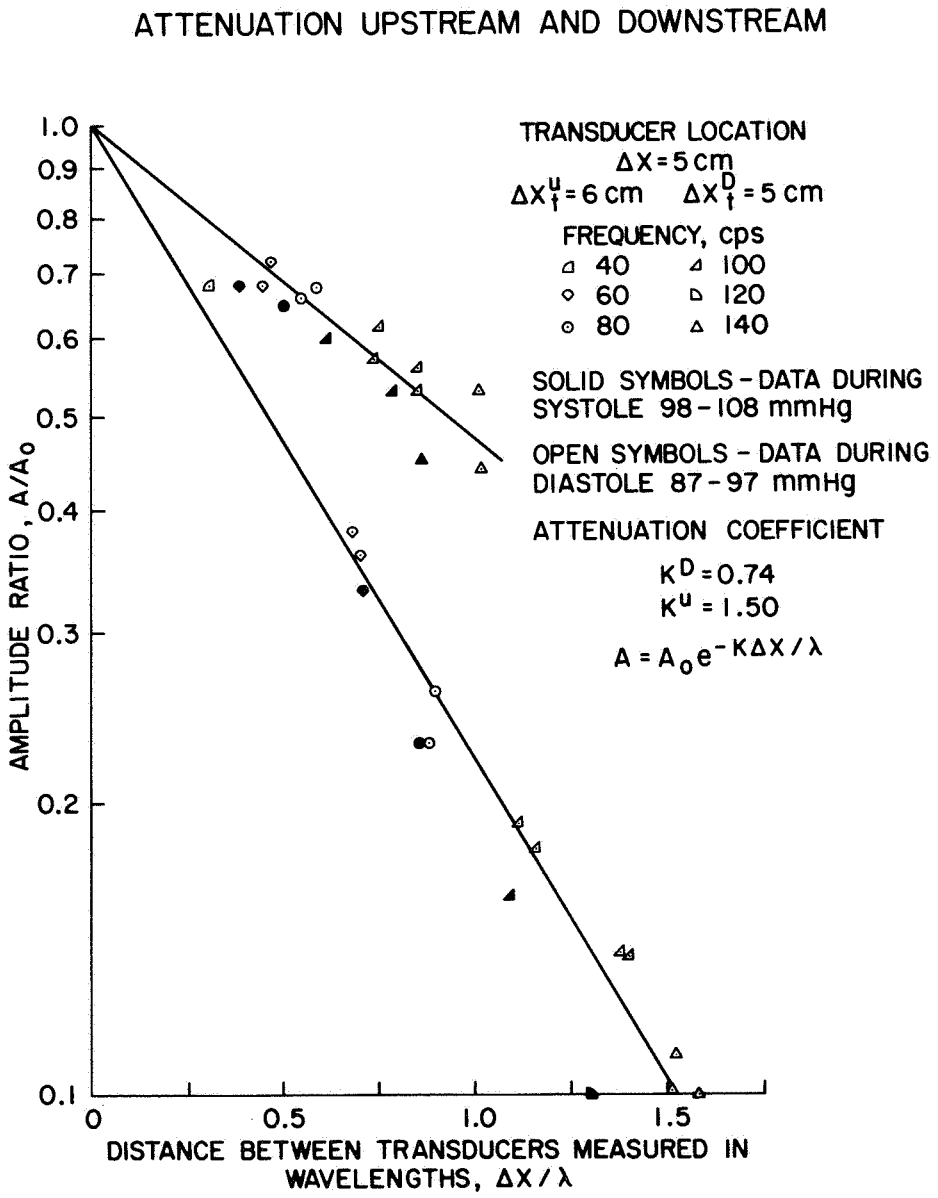

Figure 27. Attenuation for upstream and downstream waves. The attenuation coefficient for the downstream waves $k^D = 0.74$ is approximately half that for the upstream waves $k^U = 1.50$.

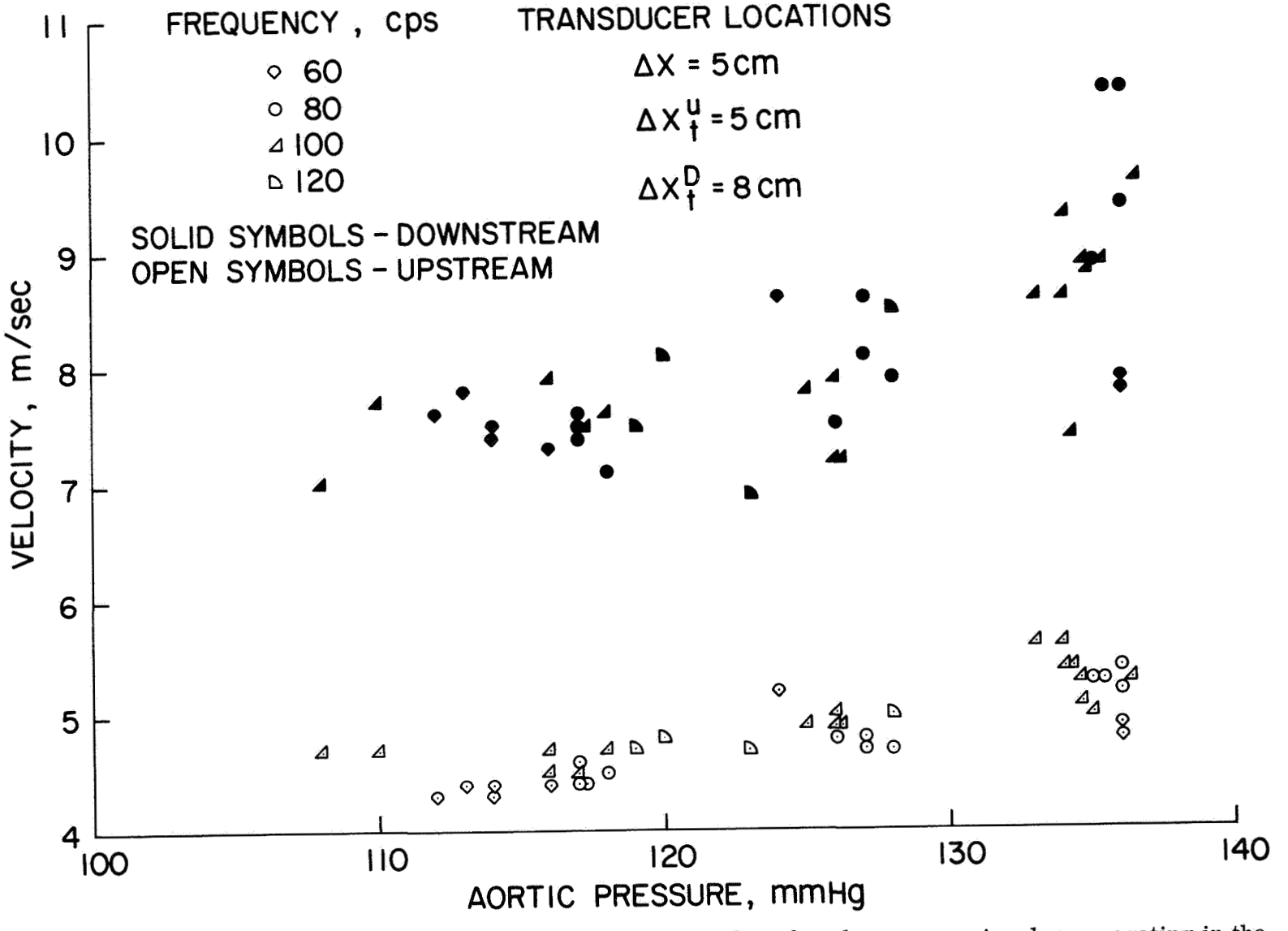

Figure 28. Pressure dependence of wave speed for randomly induced pressure signals propagating in the downstream and upstream directions in two different segments of the aorta. Note the marked increase in speed with aortic pressure for downstream waves.

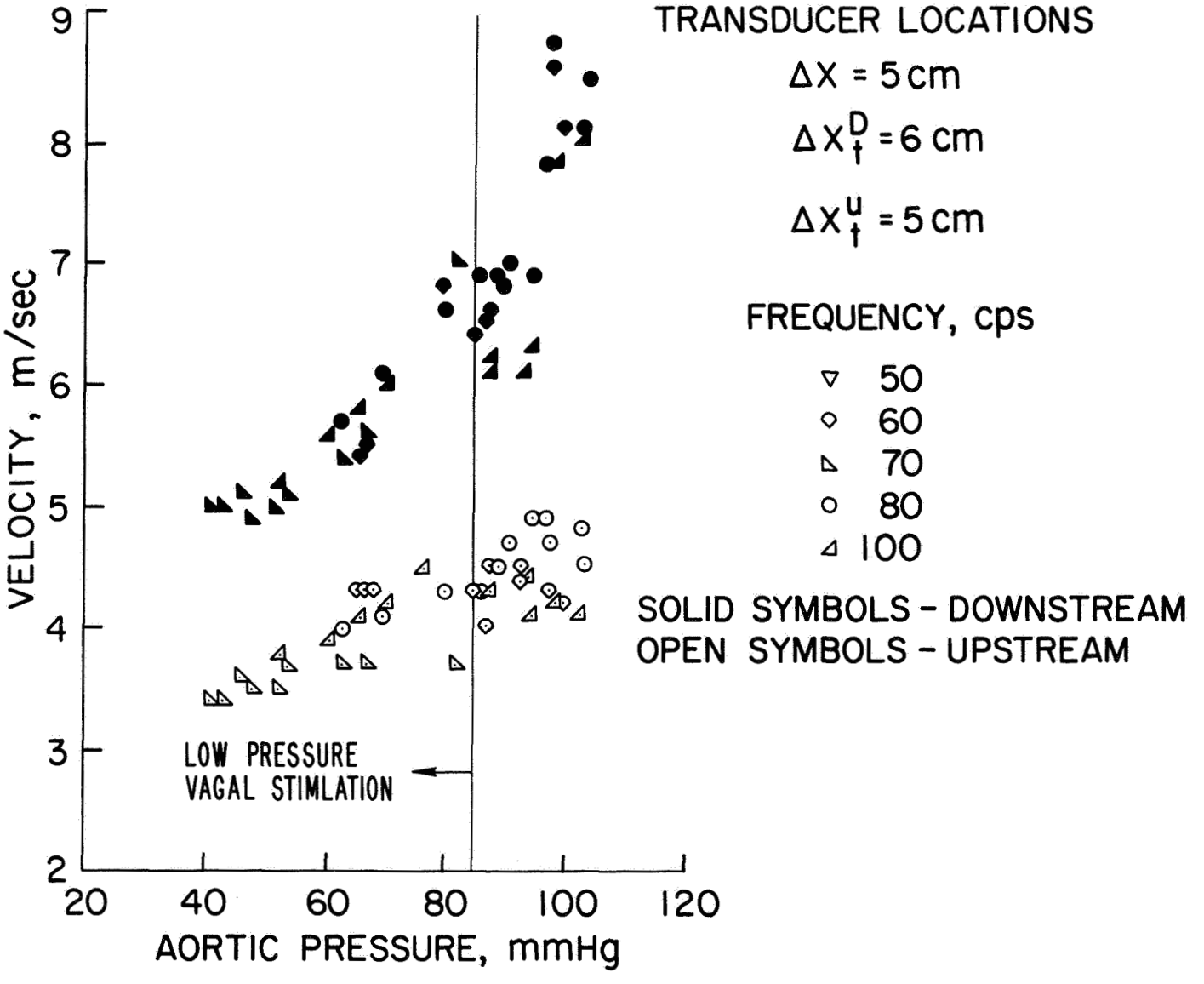

Figure 29. Further data indicating pressure dependence of wave speed for randomly induced pressure signals. Data points below diastolic pressures were obtained by cardiac arrest.

the wave speed for either segment. To obtain data which may be interpreted quantitatively the wave speed must be measured simultaneously for the upstream and downstream directions in the same aortic segment.

3.5 Dual Impactor Experiments

While the results of the experiments described in sections 3.2 to 3.4 indicate that 1) the wave speed is a function of pressure; 2) the wave is convected by the flowing blood; and 3) the propagation of large amplitude pressure signals must be affected by nonlinear phenomena, they do not allow for an accurate evaluation of the various effects. Only when the transmission properties of upstream and downstream waves can be determined for the same instant of the cardiac cycle and for the same aortic segment is it possible to eliminate the uncertainties due to the variations in geometry and flow from segment to segment which affect the results of the earlier experiments.

By placing electromagnetic impactors at the ends of an aortic segment of interest it is possible to create the situation where pressure waves are propagating both upstream and downstream in this segment at the same time. The corresponding arrangement of the experimental apparatus is schematically illustrated in Figure 30. The proximal impactor was inserted into the chest through an opening in the left fourth intercostal space and positioned on the aorta a few centimeters below the left subclavian branch. The distal impactor was inserted into the thoracic cavity through an opening in the left 8th or 9th intercostal space and placed on the aorta a few centimeters above the diaphragm. To record the pressure waves two catheter tip pressure manometers, either Bytrex Model HFD-5 or the capacitance cells shown in Figure 3 were introduced through a femoral artery and

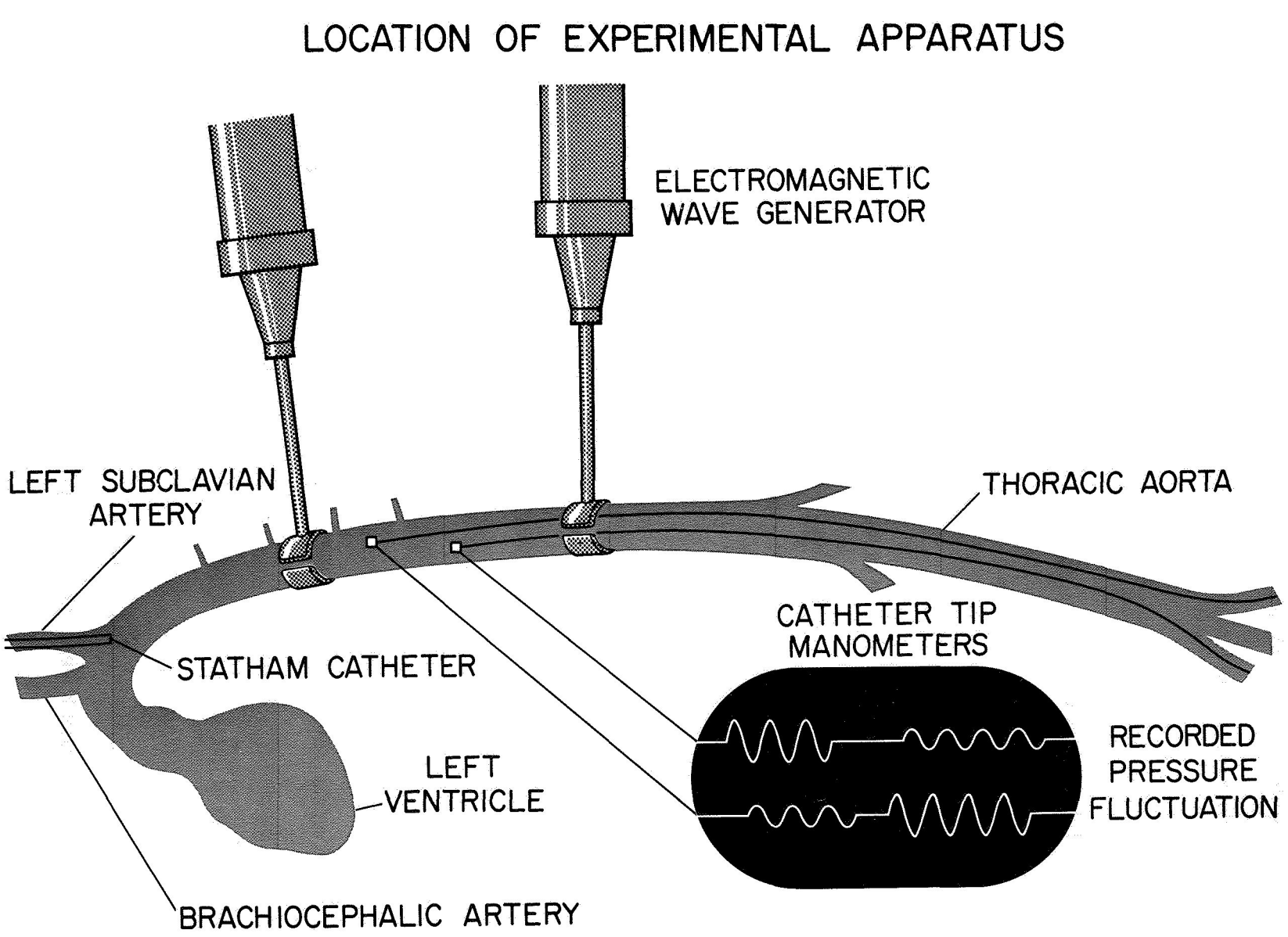

Figure 30. Arrangement of the experimental apparatus used in dual impactor experiments. Two electromagnetic impactors produced upstream and downstream waves in a single aortic segment. The number of sine waves in each train is different for upstream and downstream waves.

located 5 cm apart in an aortic segment equidistant from the two impactors. Usually the distance between manometers and impactors was 5-6 cm. The amplified signals were recorded with the same instrumentation described in the earlier experiments.

Typical oscillograph recordings from the two pressure manometers are shown in Figures 31 and 32. Trains of three sine waves were produced by the proximal impactor and were recorded traveling downstream with the flow. Trains of 4 sine waves were generated by the distal impactor and were recorded traveling against the flow in the aortic segment. By selecting different train lengths the identification of waves traveling upstream and downstream was facilitated.

By plotting the phase velocity as a function of the instantaneous aortic pressure, one obtains as data representative of six experiments of this type those shown in Figures 33, 34, 35, 36, and 37. The points representing the speeds of waves of different frequencies have been identified by the symbols listed in the left hand corner of the graphs.

During diastole the mean flow in the thoracic aorta is quite small although not zero. This has been demonstrated by recordings with a Pieper flowmeter (39). Therefore, the wave speeds upstream and downstream should be nearly the same during diastole and primarily dependent on the instantaneous pressure level. All experimental data corroborate this conclusion. The difference in speed between upstream and downstream waves increases with increasing flow. Regression lines for the upstream and downstream waves have been calculated assuming a linear increase in wave speed with pressure and excluding data points corresponding to high flow velocities. The slope of the resulting average regression line is an approximation for the value of

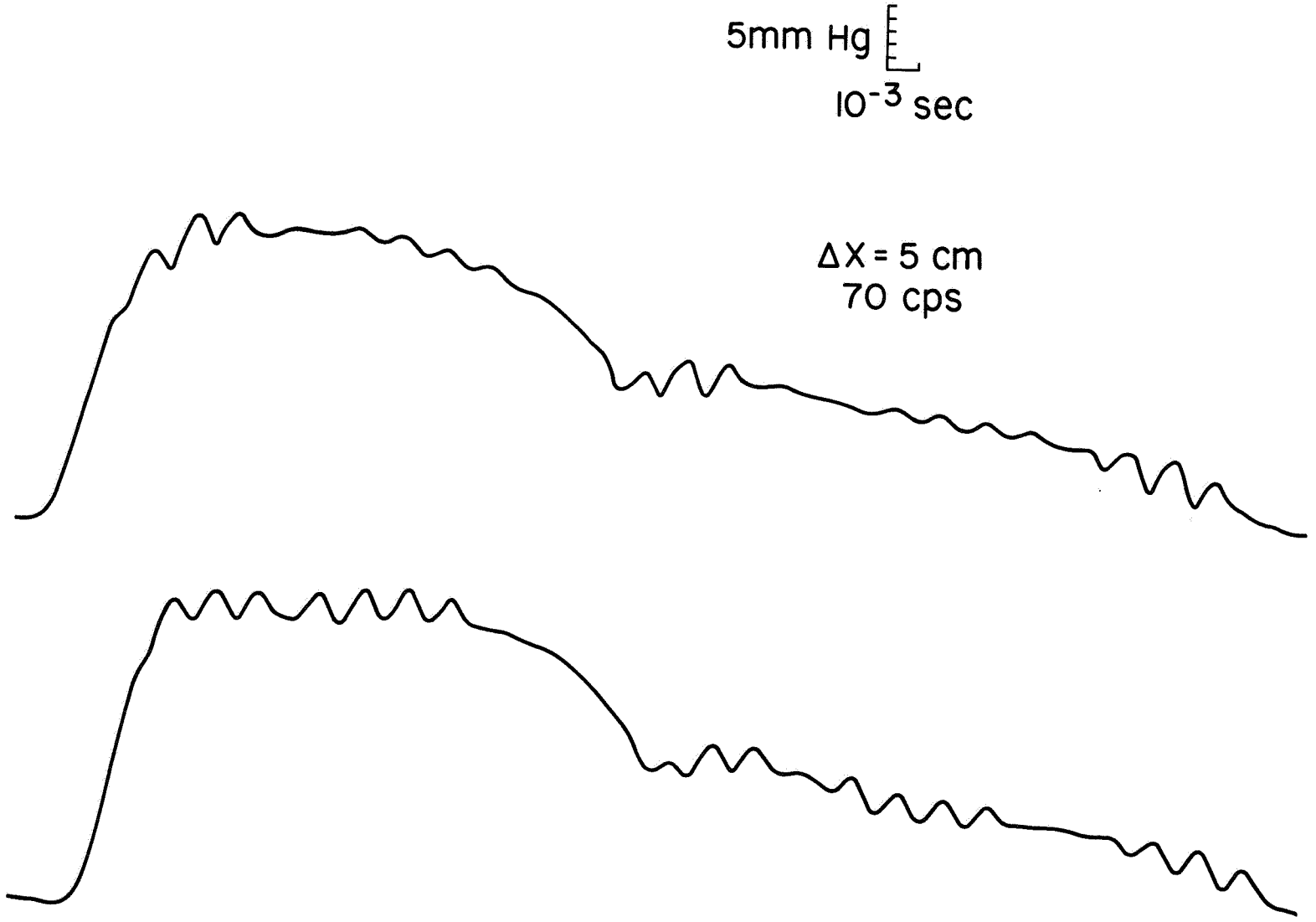

Figure 31. Typical recordings from the two pressure manometers between the two impactors. Trains of 4 sine waves are propagating upstream and trains of 3 sine waves are travelling downstream.

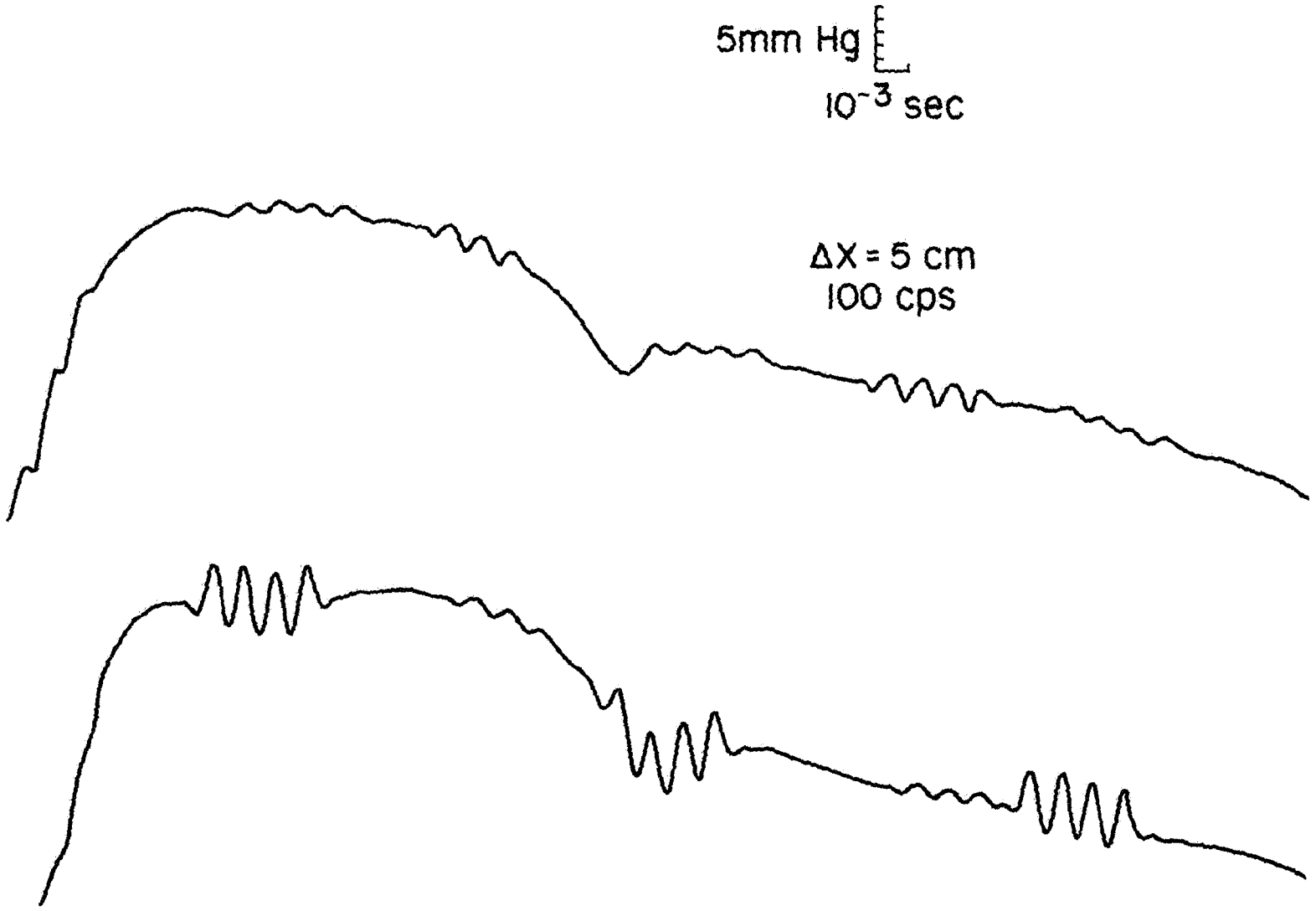

Figure 32. Typical recordings of trains of sine waves with a frequency of 100 cps travelling upstream and downstream.

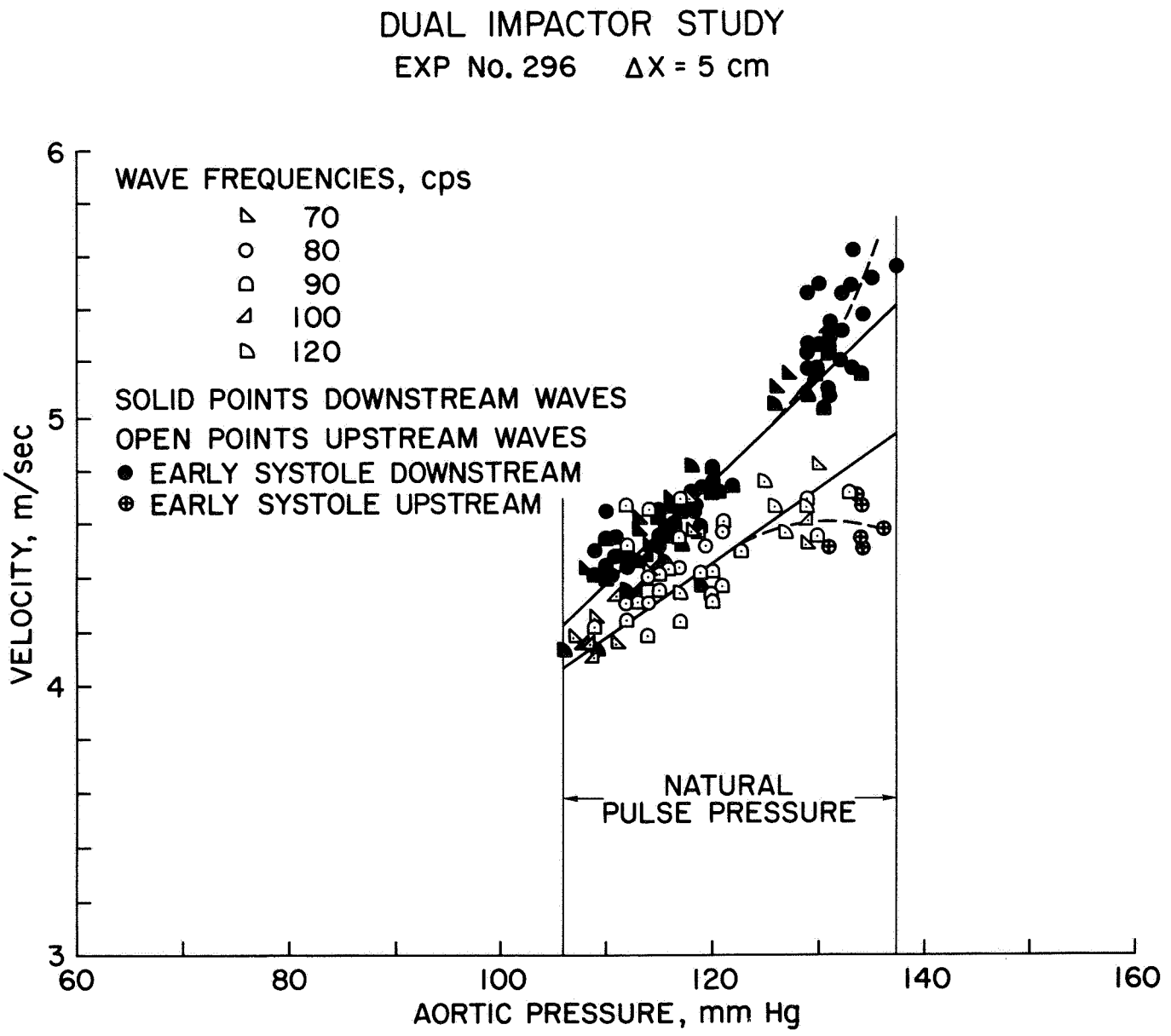

Figure 33. Wave speed-pressure data for upstream waves (open symbols) and downstream waves (solid symbols) showing the increase in speed with pressure and flow. Note the sharp increase in speed differences for signals recorded during early systole when flow levels are large.

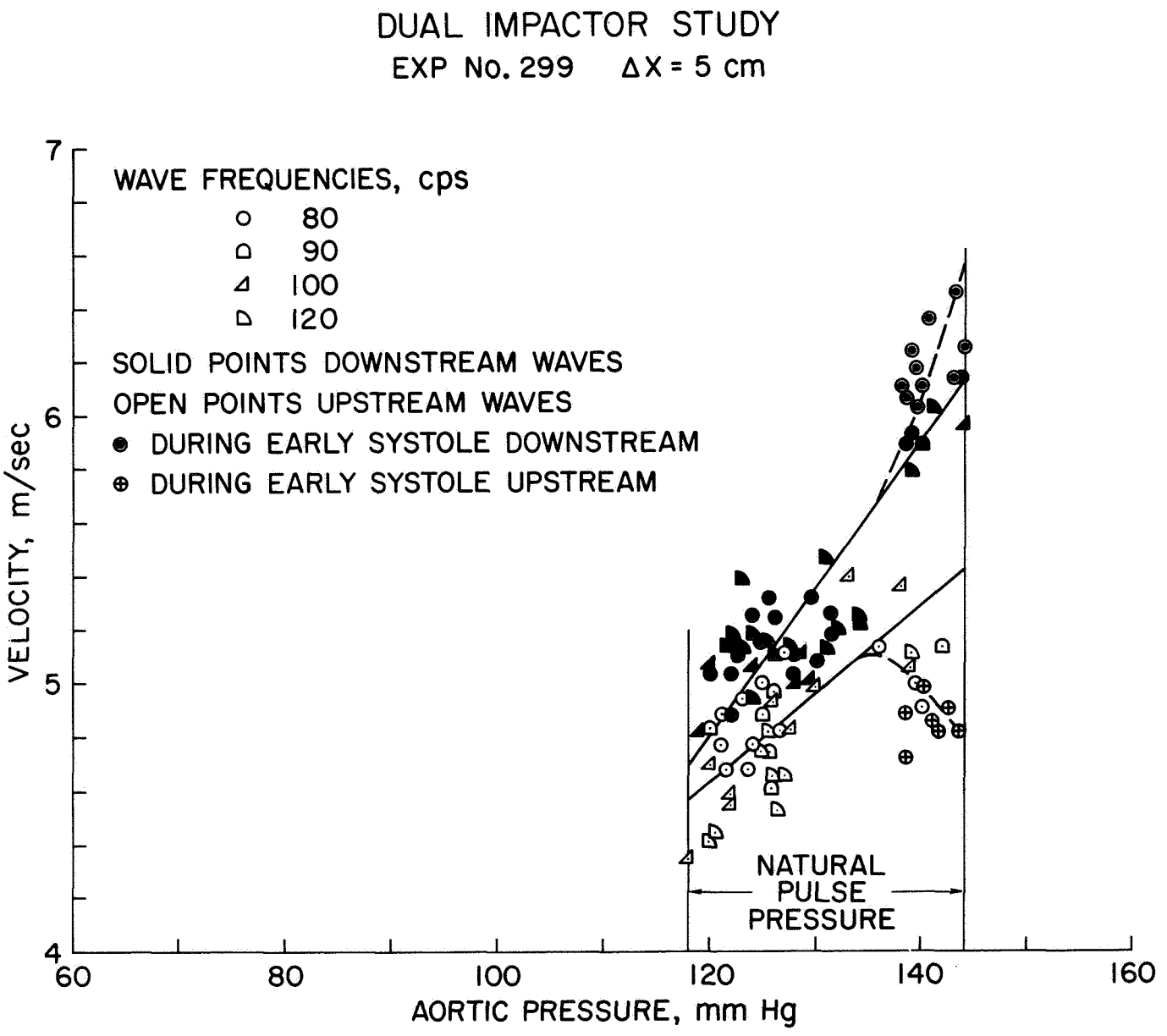

Figure 34. Wave speed - pressure data for upstream and downstream waves.

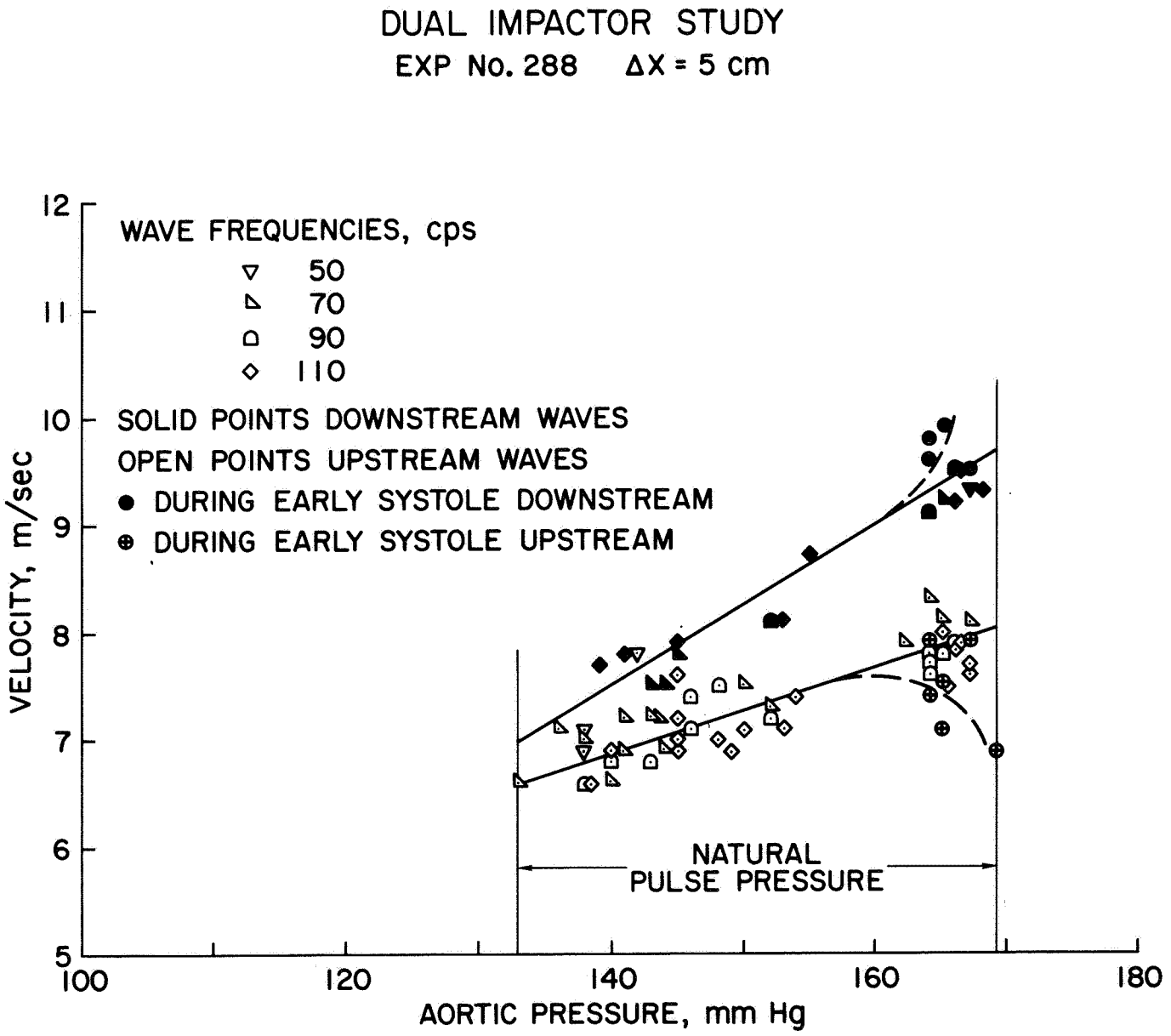

Figure 35. Wave speed - pressure data for upstream and downstream waves.

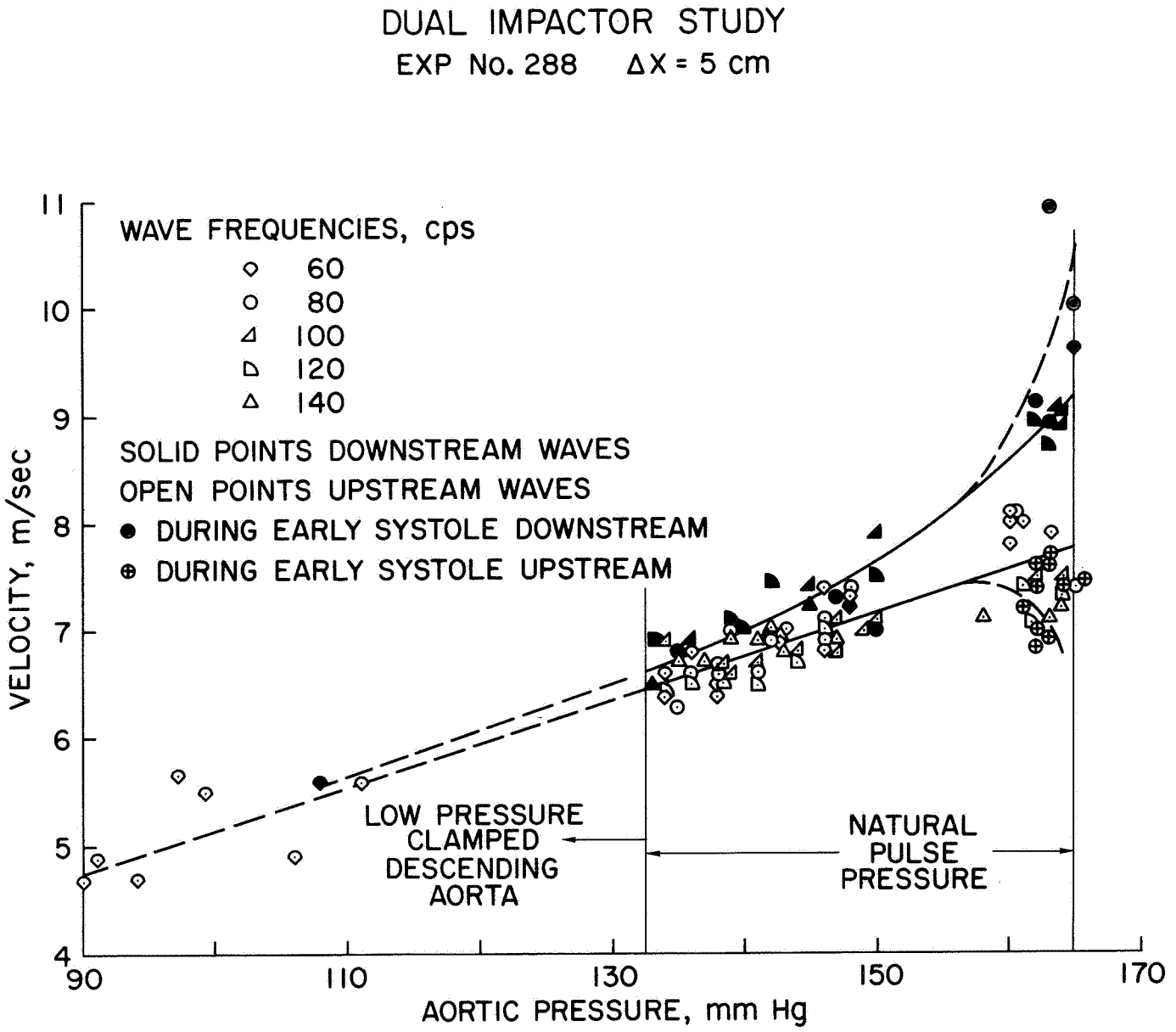

Figure 36. Wave speed - pressure data for upstream and downstream waves. In addition data points corresponding to aortic pressures below the diastolic were obtained by clamping the descending aorta intermittently for a period of 5 seconds.

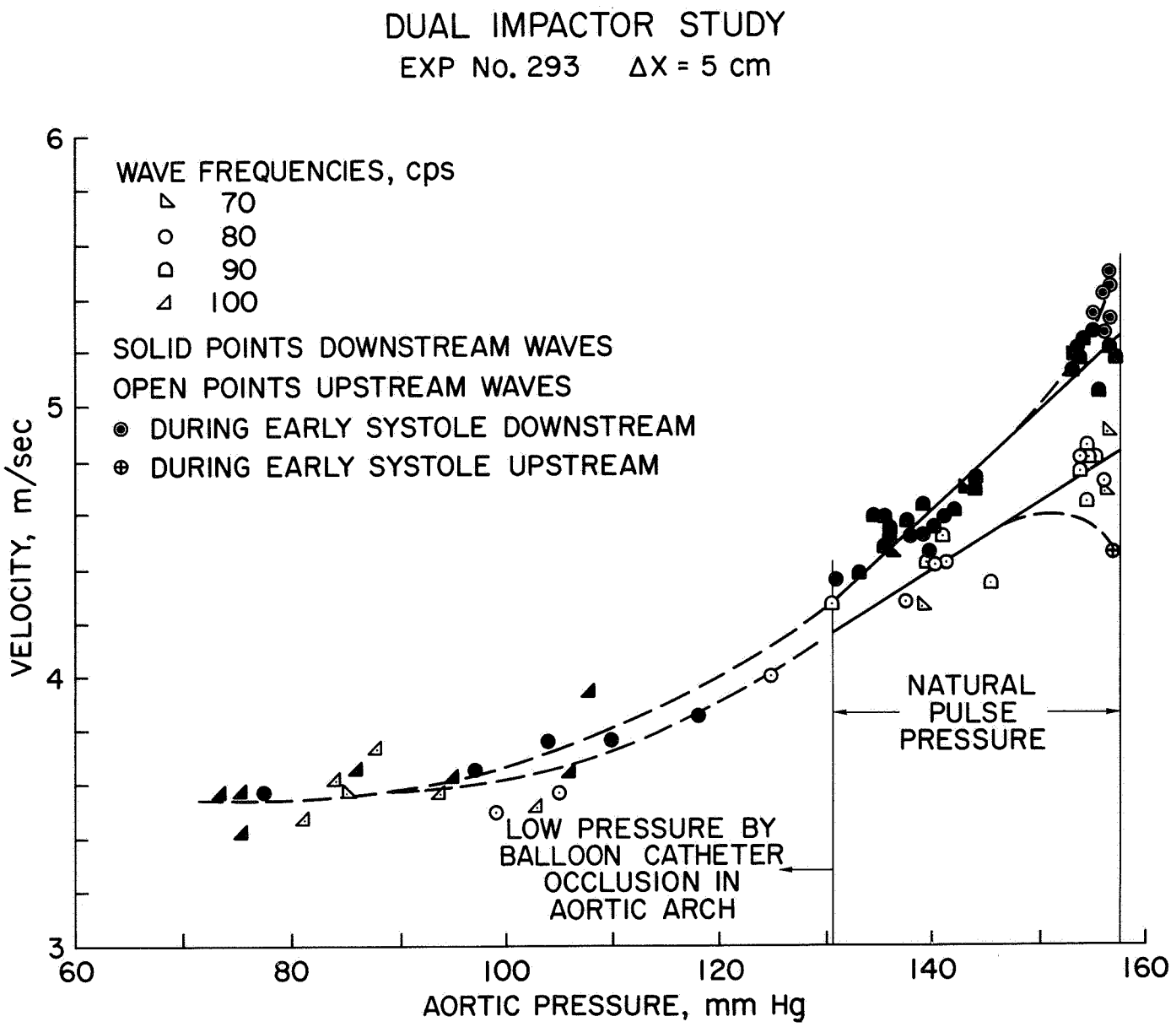

Figure 37. Wave speed - pressure data for upstream and downstream waves. Data points corresponding to aortic pressures below the diastolic were obtained by inflating a balloon catheter in the aortic arch for a period of 3-5 seconds.

$\partial c/\partial p$, the increase in wave speed with pressure alone. Values of $\partial c/\partial p$ for the thoracic aorta are shown in Table I where geometrical measurements and pressure levels are also indicated.

CHANGES IN WAVE SPEED WITH PRESSURE OBTAINED FROM DUAL IMPACTOR EXPERIMENTS

EXPERIMENT NUMBER	$\partial c/\partial p$ $\frac{\text{cm/sec}}{\text{mm Hg}}$	Natural Pulse Pressure mm Hg	h/a	AXIAL STRETCH $\frac{X-X_o}{X_o}$
274	5.1	120-155	—	—
288	5.4	132-168	0.17	0.9/4.5
293	3.2	130-157	0.14	1.6/4.2
296	3.3	105-135	0.18	1.8/5.2

X = naturally stretched length of the aorta
X_o = unstretched length of the aorta
h = wall thickness
a = radius

DATA OBTAINED BY OCCLUDING THE AORTA

EXPERIMENT	$\partial c/\partial p$	PRESSURE RANGE	
288	4.3	140 - 100	occlusion of descending aorta
288	3.5	140 - 100	"
	5.0	140 - 180	occlusion of thoracic aorta
	5.5	180 - 220	below distal impactor
296	3.9	130 - 100	occlusion of descending aorta

During the early systolic and mid-systolic portions of the cardiac cycle the increased pressure and the large blood flow due to cardiac ejection will cause substantial elevations in the wave speed. Figure 38 aids in the explanation of the variation of wave speed in the upstream and downstream directions of the thoracic aorta at different instants of the cardiac cycle. The wave speed measured at (1) on the natural pulse wave is plotted on the pressure-wave speed graph as datum ◇1◇ for a downstream wave and datum [1] for an upstream wave. The wave speed from (2) on the natural pulse wave results in datum ◇2◇ for downstream waves and [2] for upstream waves. The effect of the elevated flow during early systole manifests itself by significant increases in speed for downstream waves and marked decreases in speed for upstream waves. Speeds measured at (3) and (4) during late systole are shown as data ◇3◇ and ◇4◇ for downstream waves and [3] and [4] for upstream waves and indicate that the mean flow at late systole has fallen to lower levels. Finally, a wave speed measured during diastole (5) is shown as datum ◇5◇ for downstream waves and [5] for upstream waves. The solid regression lines represent increases in wave speed due to pressure at moderate flow levels, while the dotted lines indicate the change in wave speed with pressure at relatively high flow rates. The difference in speed in the two directions in diastole suggests that there is a slight mean flow even during diastole. It will be shown that the difference in wave speed for the downstream and upstream directions at a chosen pressure is a measure of the mean blood flow velocity in the region between the two manometers.

Even more convincing evidence for the effect of pressure and flow can be presented when very long trains of small sinusoidal waves with a frequency above 70 cps are superimposed upon the natural pulse wave. The

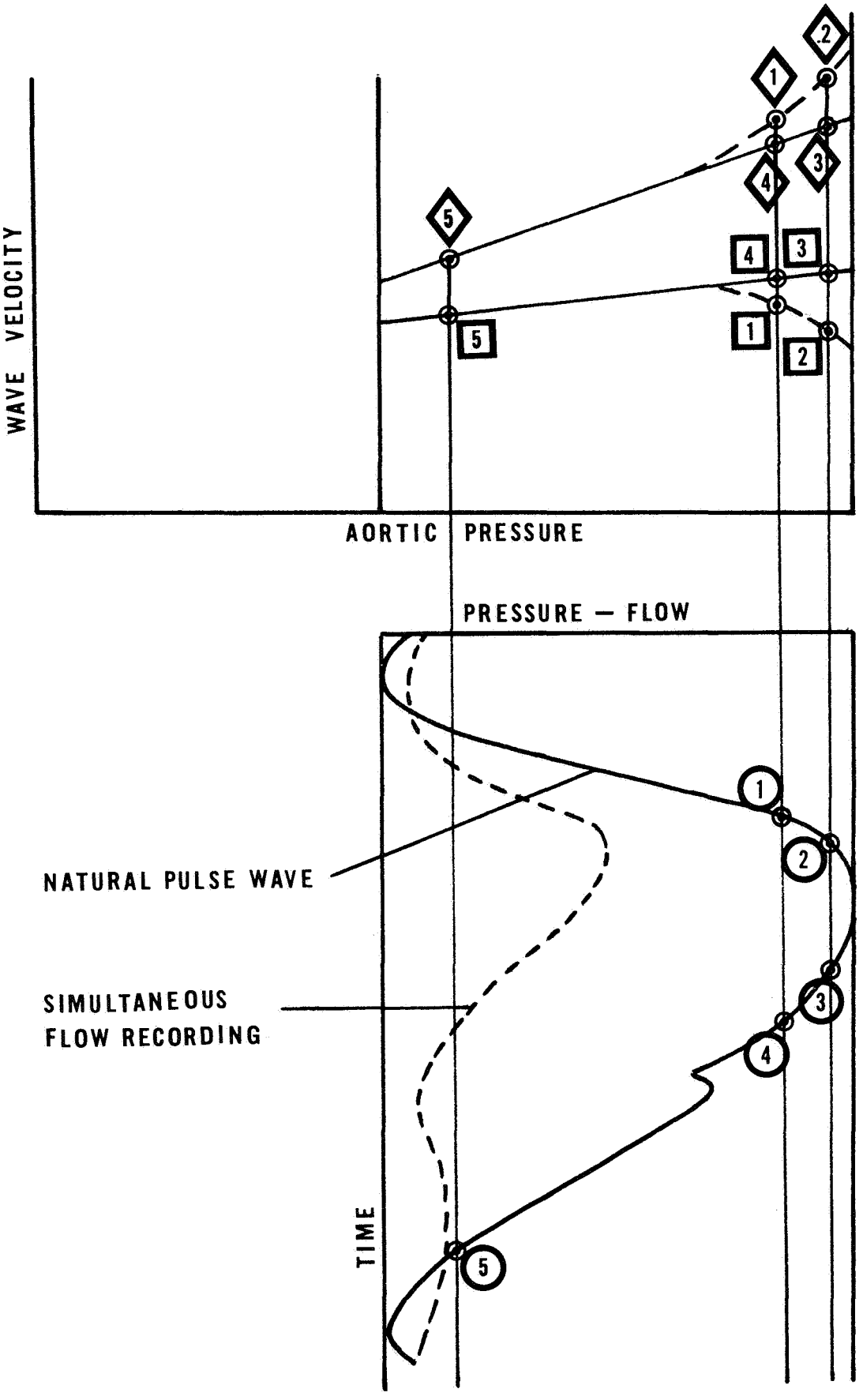

Figure 38. An explanation of the effects of pressure and flow on the wave speed.

variation in speed of individual sine waves within such trains can be determined for upstream and downstream waves as shown in the middle graph of Figure 39. The difference in the speeds of the downstream and upstream waves is a direct measure of the flow. To explain the underlying reasoning it is convenient to introduce the following parameters:

$c^U(p)$ - upstream wave speed at pressure p.

$c^D(p)$ - downstream wave speed at pressure p.

$\partial c/\partial p$ - incremental change in wave speed with incremental change in pressure. This derivative will in general be a function of pressure but for the pressure range between diastole and systole it is here assumed to be constant.

$\Delta p = p - p_o$ = difference between instantaneous pressure p and diastolic pressure p_o.

$\bar{U}(p)$ - mean flow velocity at the instantaneous pressure p.

With this notation the wave speeds in the upstream and downstream directions can now be expressed in terms of the wave speed at the diastolic pressure and zero mean flow and the increments in speed due to pressure and flow. Then:

$$c^U(p) = c^U(p_o) + (\partial c/\partial p)\,\Delta p - \bar{U}$$

and,

$$c^D(p) = c^D(p_o) + (\partial c/\partial p)\,\Delta p + \bar{U}$$

If the diastolic wave speed is the same in both directions, a reasonable approximation since diastolic flows are almost zero, then, $c^U(p_o) = c^D(p_o)$ and,

$$c^D(p) - c^U(p) = 2\bar{U}\ .$$

Thus the difference in speed of waves traveling downstream and upstream is twice the flow velocity. The variation of the flow with cardiac cycle

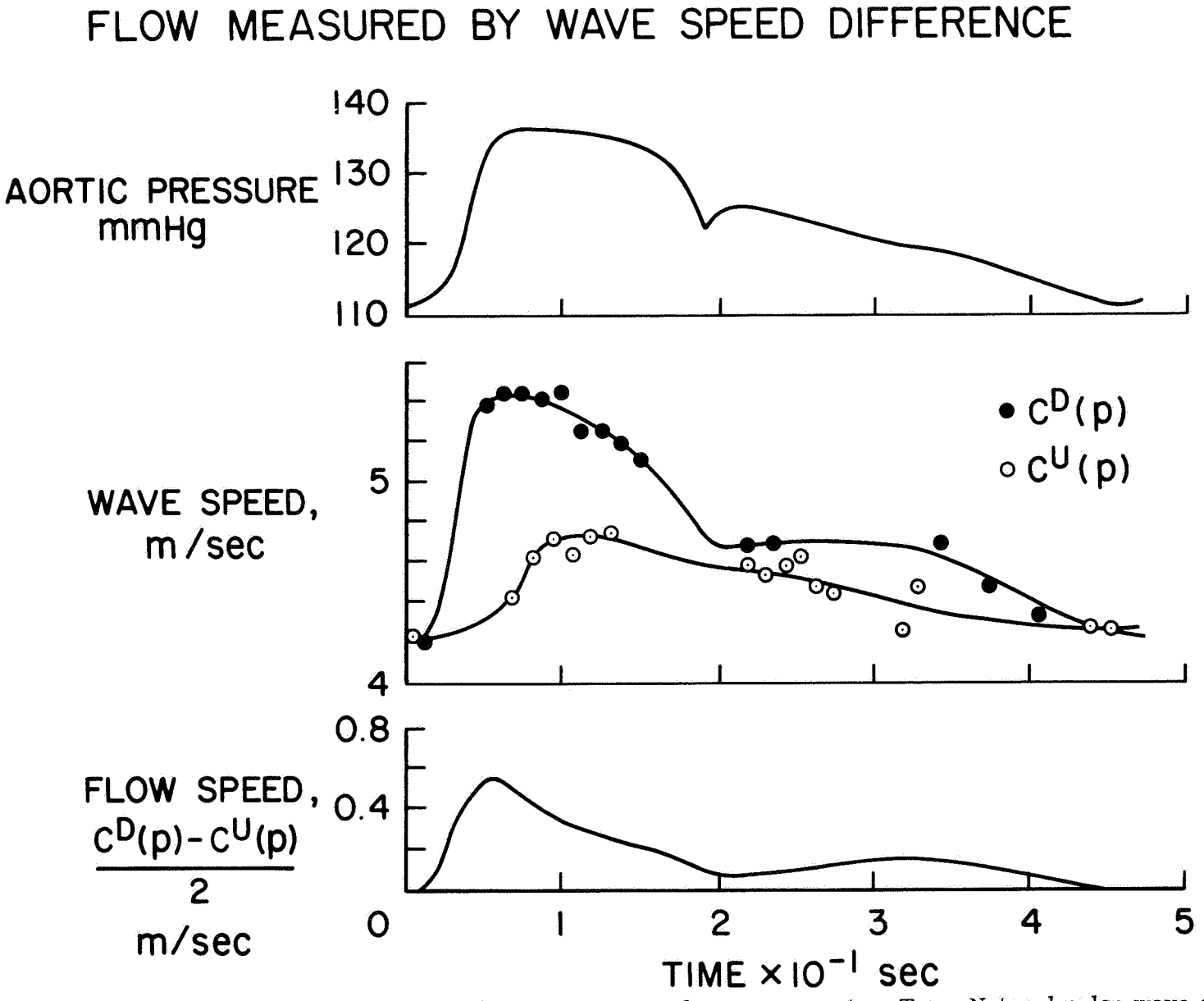

Figure 39. Flow pattern determined from wave speed measurements. Top: Natural pulse wave defining cardiac phase at which the data shown in lower two graphs were obtained. Middle: Upstream wave speeds (open symbols) and downstream wave speeds (solid symbols) measured at different instants of the cardiac cycle. The upstream and downstream data correspond to two heart beats a few seconds apart but with matching pressure patterns. Bottom: Mean flow velocity $\overline{U}$.

obtained with this approximation from wave speed measurements is shown in Figure 39. The close resemblance of this velocity pattern with that measured by a Pieper catheter tip flowmeter (39) and illustrated in Figure 40 corroborates in part the feasibility of the approach described in this investigation. The values for the peak mean flow velocities at systole measured by this method in a number of experiments are shown in Table 2.

TABLE 2 FLOW VELOCITY

EXPERIMENT	$\bar{U}_{max}$, cm/sec	WAVE SPEED, m/sec Systole - Downstream
288	100	8.2
288	120	8.7
293	50	5.0
296	50	5.0

Variations in $\bar{U}$ can be attributed to actual fluctuations in the mean flow due to changes in cardiac output and peripheral resistence.

Maneuvers were again introduced to extend pressure-wave speed studies beyond the normal pressure range. A balloon catheter was inserted through the right carotid artery and advanced to the root of the brachiocephalic artery. Inflation of the balloon for 3 - 5 seconds blocked the flow into the descending aorta, and thoracic aortic pressure rapidly fell below the diastolic level. Pressures above the systolic range were obtained in the test region by occluding the aorta a few centimeters above the diaphragm. Figures 36, 37, 41, and 42 illustrate pressure-wave speed data for aortic pressures below the diastolic level, while Figure 42 shows wave speed data for high as well as low pressures. It is noteworthy that $\partial c/\partial p$ is not constant but varies with the pressure level. At very low pressures

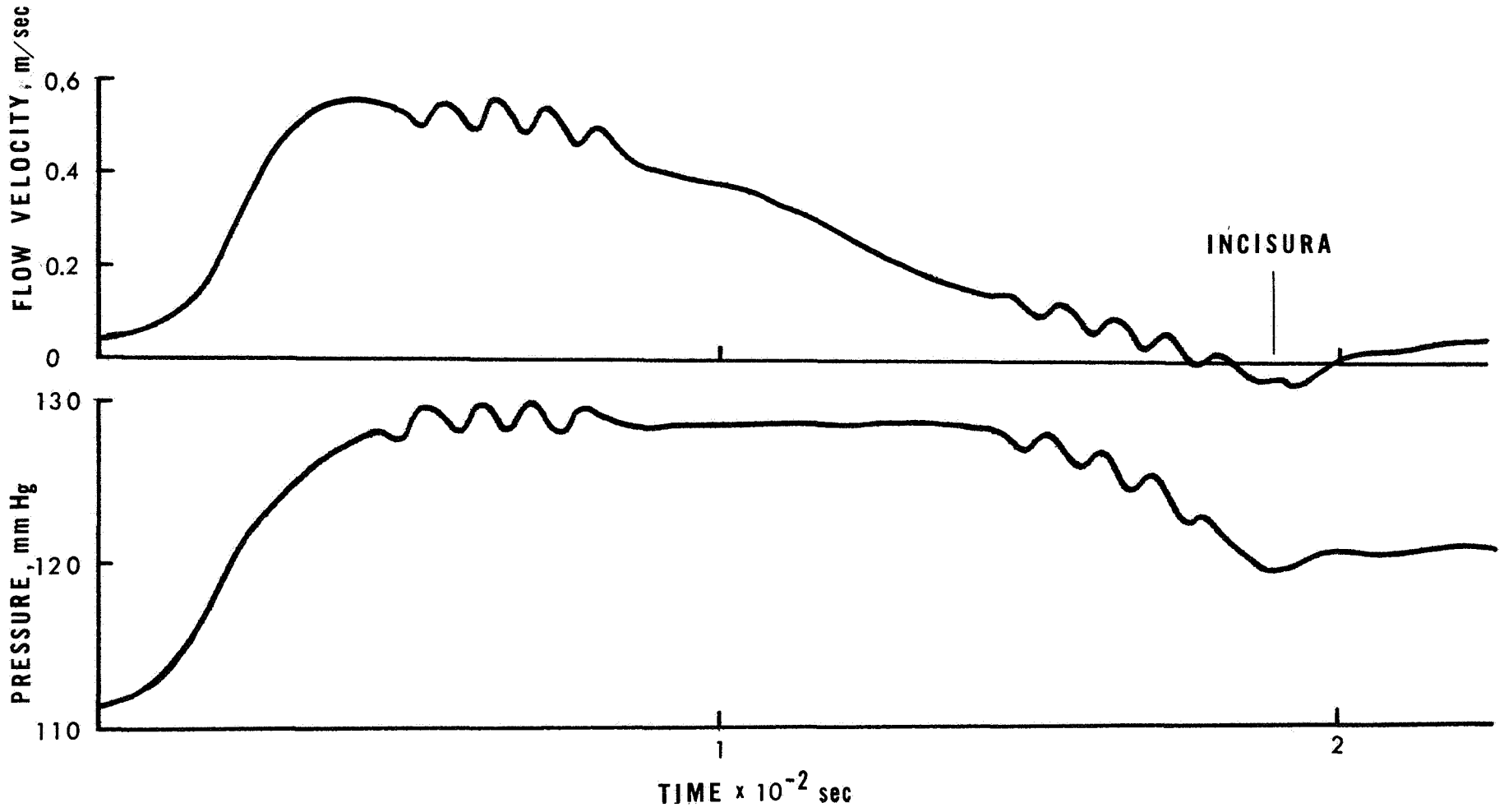

Figure 40. Pressure and flow patterns in the thoracic aorta recorded with Pieper catheter tip flowmeter and capacitance cell. Compare the recorded flow pattern with that obtained from wave speed measurements and illustrated in Figure 39.

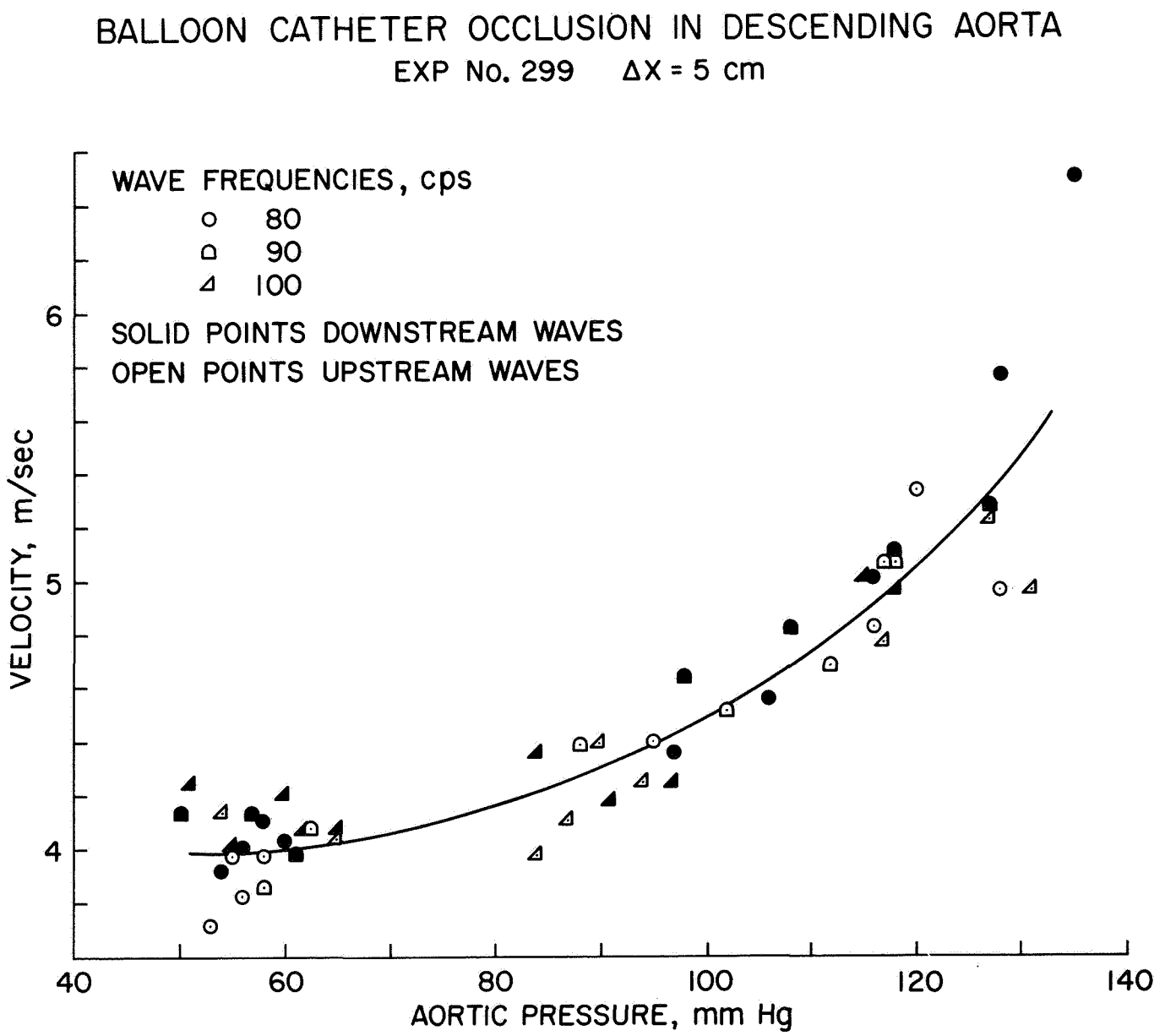

Figure 41. Wave speed - pressure data obtained during aortic occlusion with a balloon catheter in the aortic arch.

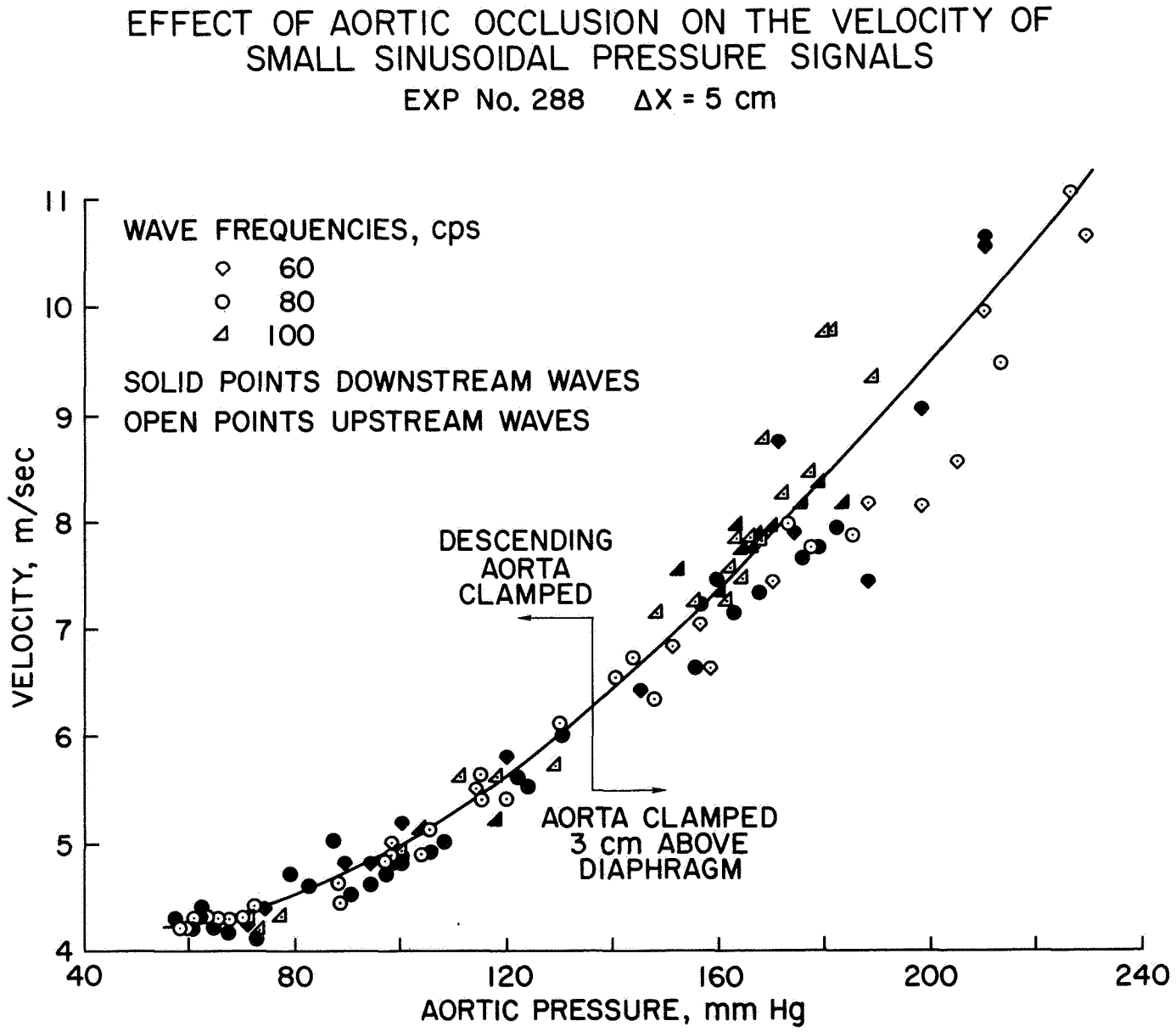

Figure 42. Wave speed - pressure data obtained by aortic occlusion above and below the aortic segment studied. Each point represents the average speed of a peak and successive valley of a sine wave.

the change in speed with pressure is quite small, but at pressures above 180 mm Hg it rises sharply indicating a marked change in the elastic properties of the blood vessel wall. The mean flow is obviously small since the wave speeds are the same in both directions.

The data from six experiments indicates a consistent pattern for the effects of pressure and flow on propagating pressure waves. Of particular significance here is the result that a large increase in wave speed occurs between diastole and systole. This is a strong indication that the aortas of anesthetized dogs exhibit nonlinear behavior with respect to large amplitude pressure waves such as those generated by the heart. Caution should therefore be exercised in applying linear theories in the modeling of hemodynamic phenomena when the pressure fluctuations are of the same order as those produced by the heart. It is of interest to note that Remington (40) discussed the possibility of a wave speed variation with cardiac phase, but he could not substantiate it conclusively from apparent speed measurements of the incisura and the foot of the natural pulse wave. Landowne (24) has shown an increase in the speed of impact waves in the brachial artery between diastole and systole. The actual causes of such large rises in the speed with pressure from his experiments are yet to be explained.

CHAPTER 4

A PRELIMINARY STUDY OF THE DISTENSIBILITY OF THE AORTA

4.1 Introduction

Wave propagation in blood vessels, especially arteries, is not yet fully understood. The elastic properties of the wall undoubtedly play a role in this propagation. Since wall properties may change, in disease, in aging, or in prolonged weightlessness, the relationship between wall properties and the speed of wave propagation should be elucidated.

The present experiments were designed to clarify the relationship. To this end the elastic parameters of the aorta are determined from its wave transmission characteristics and also from independent distensibility measurements. The distensibility of a vessel is defined as dV/dp, the incremental increase in volume of the vessel produced by an incremental increase in the transmural pressure. For small deformations a simple mathematical relationship between the effective circumferential Young's modulus E of the vessel wall and the distensibility can be derived. In addition a convenient formula for E in terms of the wave speed c and the geometry of the vessel is given by the Moens-Kortweg equation. Hence, E can be evaluated from direct distensibility measurements in the form of pressure diameter recordings and from the speed of a propagating pressure-wave. A close agreement in the magnitudes of E obtained by the two methods would support the physical reasoning underlying the method of approach.

The results to be presented here show that the Young's modulus of the aorta varies with pressure. The system is not a linear one.

Learoyd and Taylor (39) calculated changes in Young's modulus from measurements on excised human vessels and observed increases in E as the distending pressure rose. A nonlinear relationship existed between the pressure and diameter for all types of arteries. Roach and Burton (40) have indicated that the nonlinearity most likely was due to the progressive transfer of the circumferential wall stress from the readily stretched elastin fibers to the very inextensible collagen fibers as the pressure and consequently the diameter increased. They feel that E is determined by elastin for small distension and collagen for large distension.

Though there are at hand methods for determining wave speed in man by noninvasive techniques, it will be necessary to define a more adequate mathematical model before these measurements can be used diagnostically.

4.2 Theoretical Relations Between Wave Speed, Distensibility, and Elasticity

It is essential to establish a mathematical relationship between wave speed, distensibility, and elasticity if the characteristics of propagating waves are to be used to deduce the elastic properties of the vessel wall. The Moens-Kortweg equation predicts the speed of a pressure wave in a fluid filled, circular cylindrical vessel in terms of the circumferential Young's modulus of its wall material, its wall thickness to radius ratio and the density of the fluid contained in it. It is only applicable to low frequency waves of small amplitude and can be written as:

$$E = \frac{2 c^2 \rho a}{h} \qquad (1)$$

where c = wave speed, h = wall thickness, ρ = fluid density, a = vessel radius, E = effective circumferential Young's modulus.

For an incompressible wall material and thin walls the product ha is a constant ($ha = K$) and Equation (1) can also be given in the form

$$E = \frac{c^2 \rho D^2}{2K} \tag{2}$$

where $D = 2a$ is the vessel diameter and K can be evaluated at some known geometrical configuration $h_o a_o = K$.

The distensibility of thin walled vessels can be given in terms of the effective circumferential Young's modulus and the vessel geometry by:

$$E = \frac{2a}{h} V \frac{dp}{dV} \tag{3}$$

where V denotes the volume/ unit length, and p the transmural pressure. In this equation the volume/ unit length can be expressed by the diameter D which leads to:

$$E = \frac{D^2}{2h} \frac{dp}{dD} \tag{4}$$

Finally with the incompressibility assumption for the vessel wall material ($ha = K$) one obtains:

$$E = \frac{D^3}{4K} \frac{dp}{dD} \tag{5}$$

For dynamic conditions the inertia forces may be important and would have to be included in Equation (5) which was derived assuming quasi-static changes in pressure. In the dynamic case the force balance at the vessel wall may be written approximately:

$$\begin{aligned} p &= \text{elastic force} + \text{inertia force} \\ p &= \frac{Eh\beta}{a^2} + h\rho_o \frac{\partial^2 \beta}{\partial t^2} \end{aligned} \tag{6}$$

where the additional parameters are:

$\beta = \beta_o \sin \sigma t$ - the small sinusoidal perturbation produced in the wall by the impactor, i.e. $a = a_o + \beta$

$\rho_o h$ - the mass of the wall per unit area

Typical values for the parameters in 6 for the thoracic aorta observed in the experiments conducted as part of this study are:

$$E = 5 \times 10^6 \text{ dynes/cm}^2$$

$$\beta_o = 0.002 \text{ cm}$$

$$h = 0.1 \text{ cm}$$

$$a = 0.6 \text{ cm}$$

$$\rho_o h = 0.1 \text{ gm/cm}^2$$

$$\sigma = 2\pi f = 2\pi 60 \text{ for } f = 60 \text{ cps}$$

therefore,

$$p = 2.8 \times 10^3 \frac{\text{dynes}}{\text{cm}^2} - 7.2 \times 10^{-2} \frac{\text{dynes}}{\text{cm}^2}$$

Elastic Force — Inertia Force

This result indicates that for frequencies less than 60 cps the elastic force is approximately 4 to 5 orders of magnitude greater than the inertia force.

4.3 Methods

Small sinusoidal pressure waves have been induced in the canine thoracic aorta with peak to peak amplitudes which are an order of magnitude smaller than the pulse pressure. In these experiments the pressure perturbations are 2 to 3 mm Hg in magnitude, and corresponding changes in diameter are of the order 0.005 cm with a frequency range of 50 to 120 cps.

dV is significantly smaller than the volume of the vessel per unit length, or the change in volume of the vessel associated with the pulse pressure. Consequently a good approximation to the instantaneous incremental distensibility dV/dp may be obtained from measurements of the diameter variations associated with such small waves.

Distensibility experiments have been conducted on the aortas of six anesthetized mature mongrel dogs. The medication and presurgical preparation of the dogs was the same as described in Chapter 2. A schematic illustration of the experimental arrangement is shown in Figure 43. The pressure signals were generated by the electrically driven impactor which was inserted into the thoracic cavity through an opening along the left fourth intercostal space and placed on the thoracic aorta a few centimeters below the left subclavian branch. A Pieper pressure-diameter gauge was introduced through the left femoral artery and located in the thoracic aorta. The design and operation of the transducer has been described in detail by Pieper and Paul (39). After a series of measurements had been completed the Pieper gauge was removed and calibrated statically in a 37^{o} C bath in which it was withdrawn through a Plexiglas tube whose inside bore varied in increments of 0.05 cm from 1.05 to 1.40 cm, which was the usual range of the inside diameter of the thoracic aorta of the dogs studied. The calibration curve of the diameter gauge is linear within 5 percent and the gauge exhibited very little drift or sensitivity change.

After locating the Pieper gauge, a Bytrex catheter tip manometer was inserted through the right femoral artery and positioned with the aid of

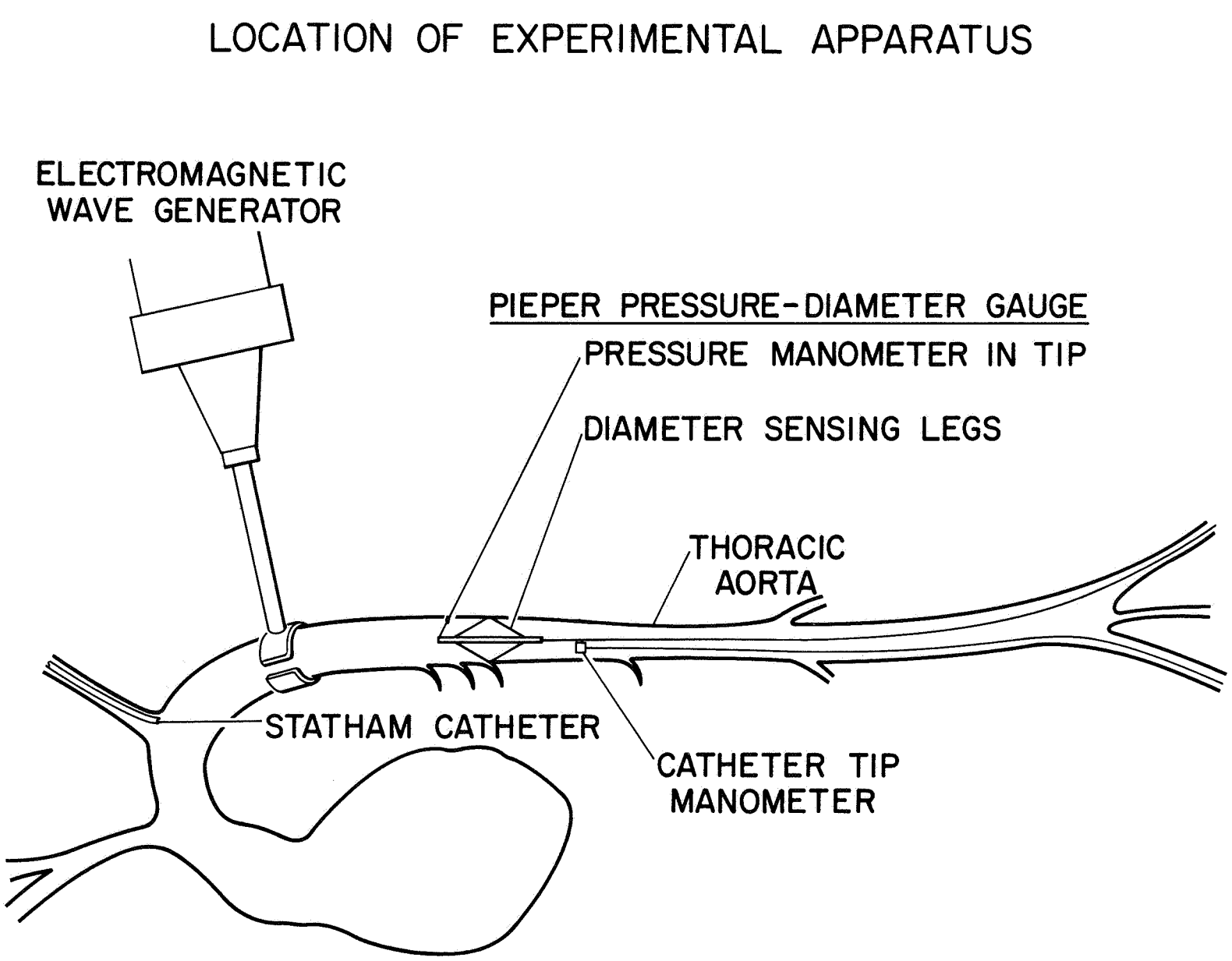

Figure 43. The arrangement of the experimental apparatus is shown for the distensibility studies during which the Pieper gauge measured changes in diameter of the aorta as a function of the pressure. The pressure waves are simultaneously recorded with the aid of two manometers.

the fluoroscope 5 cm behind the front end of the Pieper gauge. The amplified signals from the Pieper gauge and Bytrex manometers were recorded with galvanometers whose frequency response is flat up to 3300 cps, and a Honeywell Visicorder with a paper speed up to 200 cm/sec. The pressure manometers, diameter transducer, amplifiers, and recording equipment were calibrated as a system for each experiment.

4.4 Results

Aortic distensibility measurements were performed on six dogs. Figure 44 shows a typical example of the oscillograph recording of signals from the pressure and diameter transducers. The contour of the diameter recording closely resembles that of the aortic pressure including the small wave trains superimposed on the natural pulse wave. These pressure perturbations are 2-3 mm Hg in amplitude and associated diameter changes are approximately 0.005 cm. The ratio of the diameter and pressure changes measured for the trains of waves yields dV/dp, the distensibility. Since dV and dp are small compared to changes associated with the natural pulse wave, it appears justifiable to treat them as infinitesimal quantities.

The results given in Figures 45 and 46 are pressure-diameter data obtained during the natural pressure fluctuations and during aortic occlusion. The shape of the pressure-diameter curve for pressures ranging from 50 to 120 mm Hg indicates that the wall properties vary with stress. The pressure-volume data calculated from the diameter variation with pressure are also shown on Figures 45 and 46. They are of similar shape as those obtained by other investigators using excised arteries (17, 40).

The most significant results, however, are the Young's moduli for

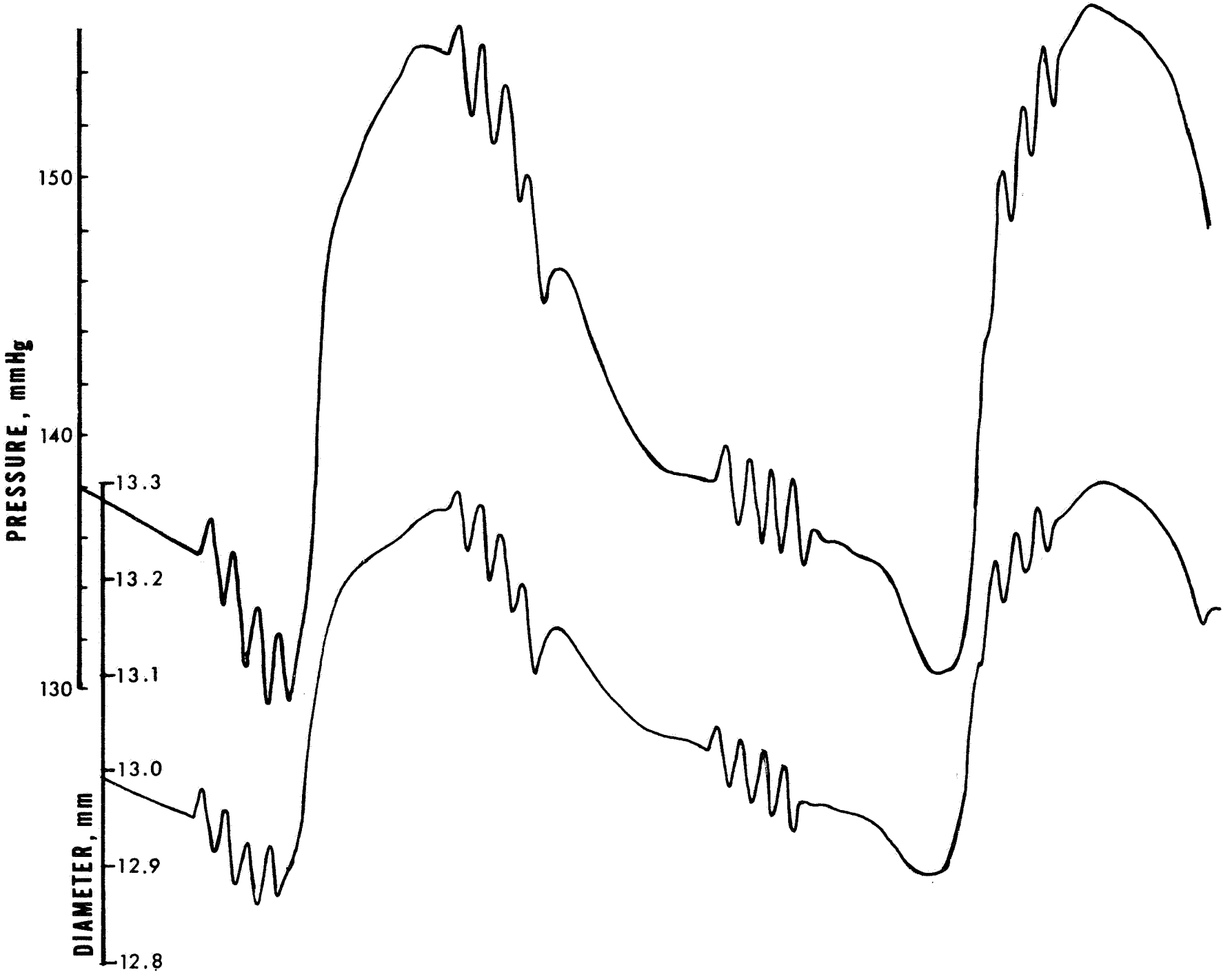

Figure 44. Pressure (top) and diameter (bottom) recordings in the thoracic aorta.

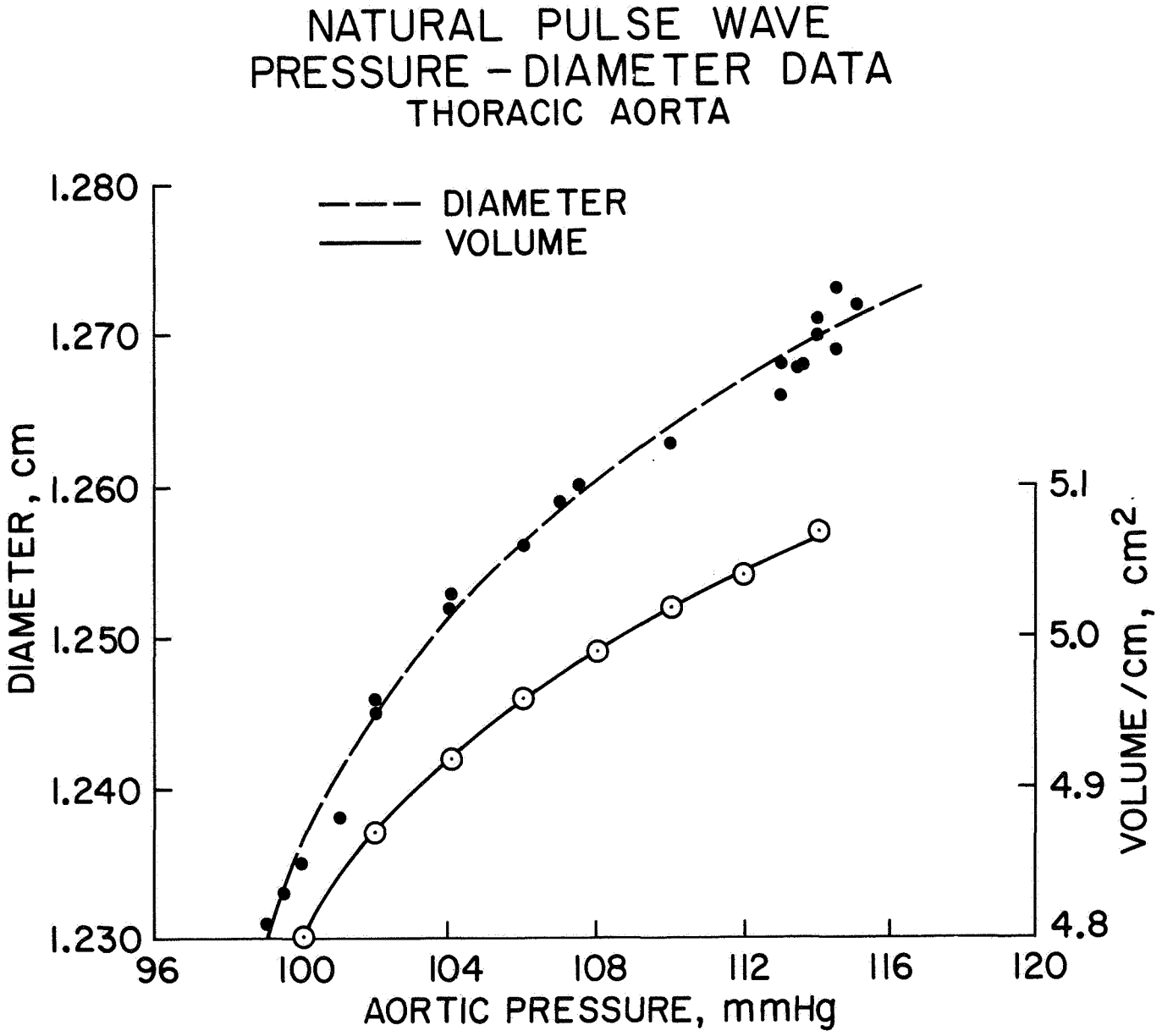

Figure 45. Pressure - diameter and pressure - volume data for the naturally occurring pressure fluctuations in the thoracic aorta.

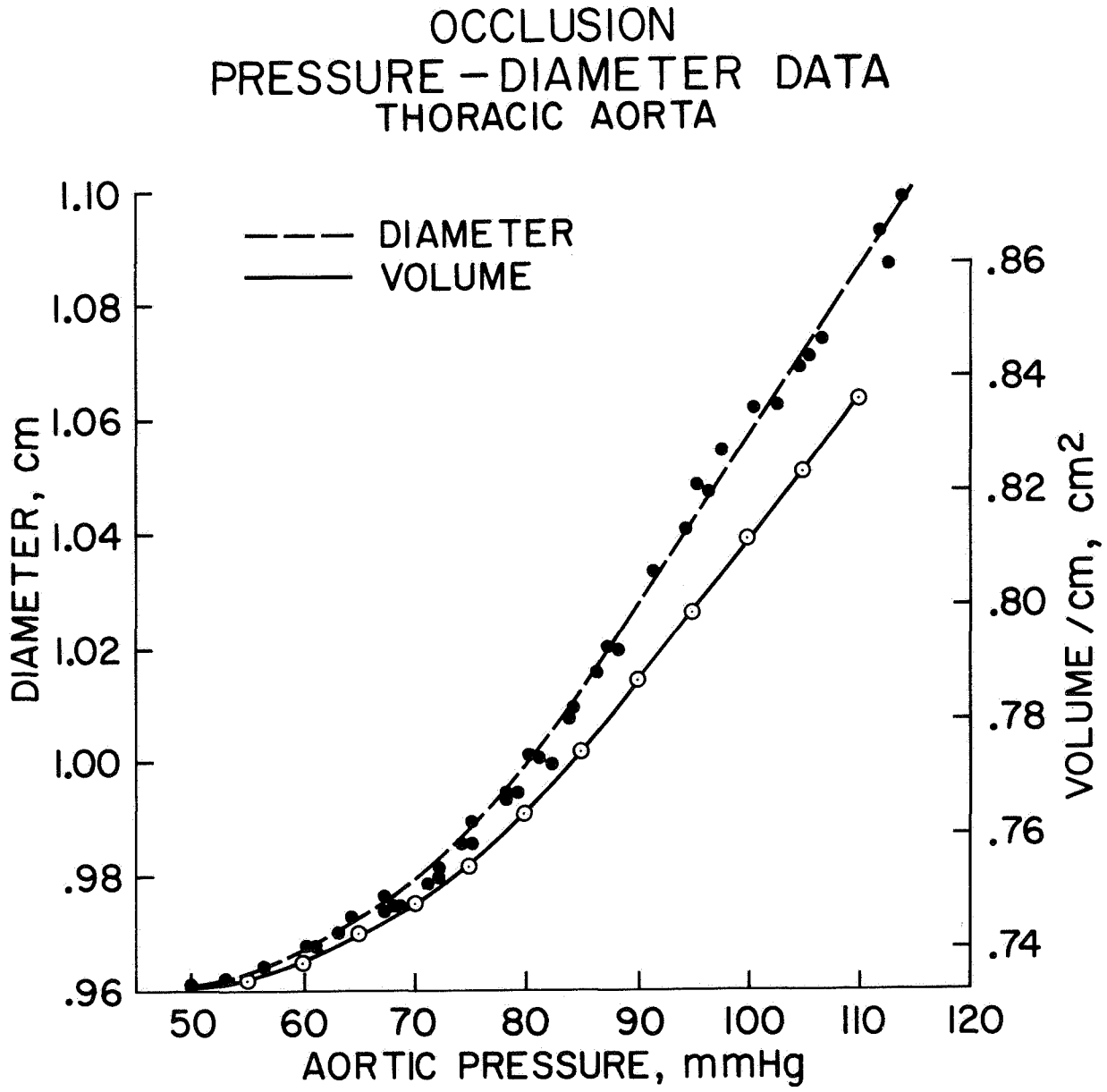

Figure 46. Pressure - diameter and pressure - volume data for the occluded thoracic aorta.

the vessel wall calculated at various pressure levels by the two different methods. The wave speeds and the dD/dp data were measured for the same wave trains, and the corresponding Young's moduli calculated with both equations shown as a function of pressure are given in Figures 47 and 48. For naturally occurring pressure fluctuations both methods yield Young's moduli which increase with pressure, but the values obtained from the distensibility measurements are consistently higher by as much as 50 percent. This disparity can possibly be attributed in part to experimental uncertainties regarding the response characteristics of the Pieper gauge at high frequencies when placed in the aorta and to over simplified mathematical models used in the derivation of the distensibility expression and the Moens-Kortweg equation. The values of E are of the same order as the Young's moduli measured on excised vessels and other in-vivo preparations (19).

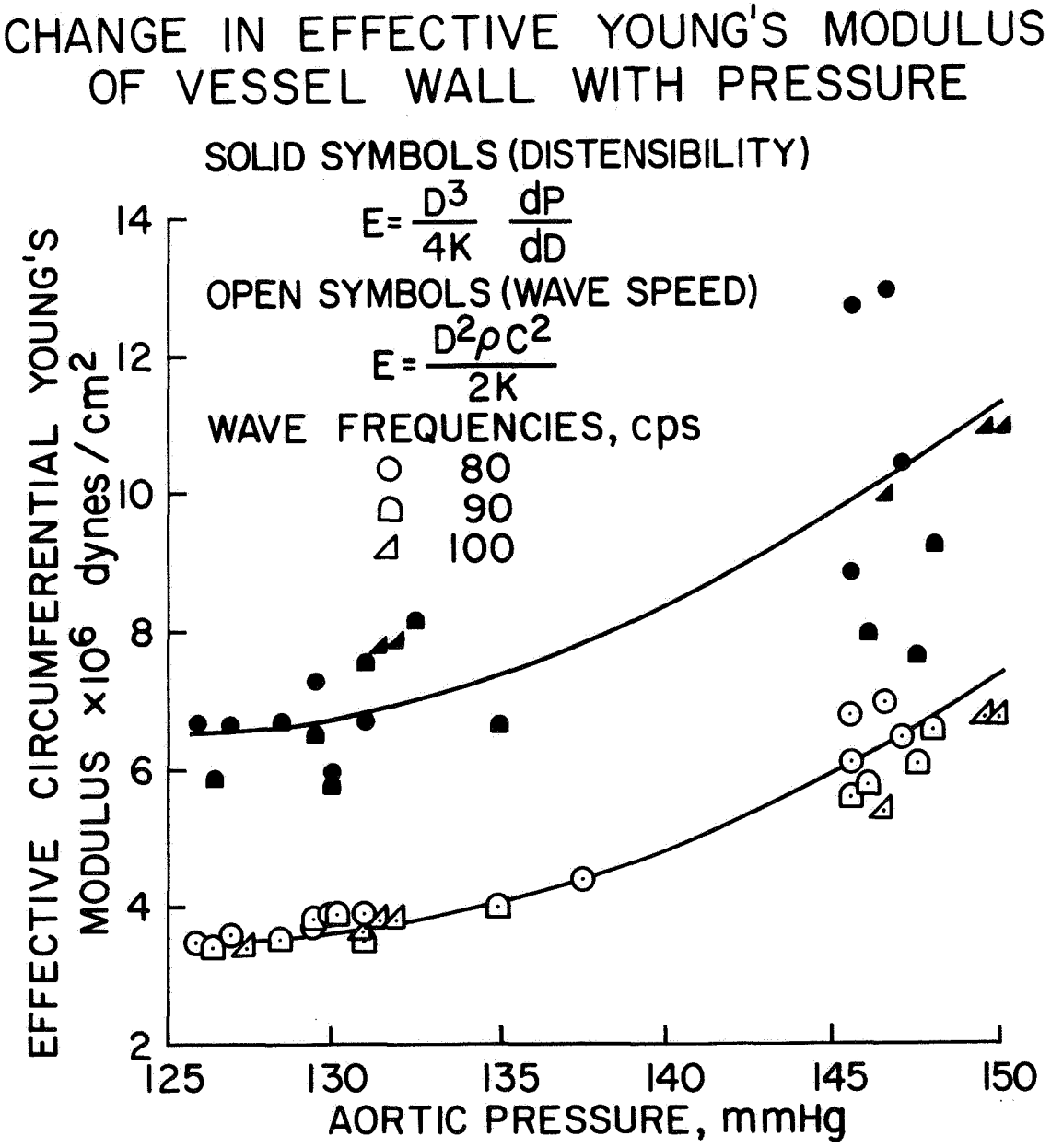

Figure 47. Change in the effective circumferential Young' s moduli for the vessel wall for naturally occurring pressure fluctuations in the aorta. Data points are calculated from distensibility and wave speed measurements.

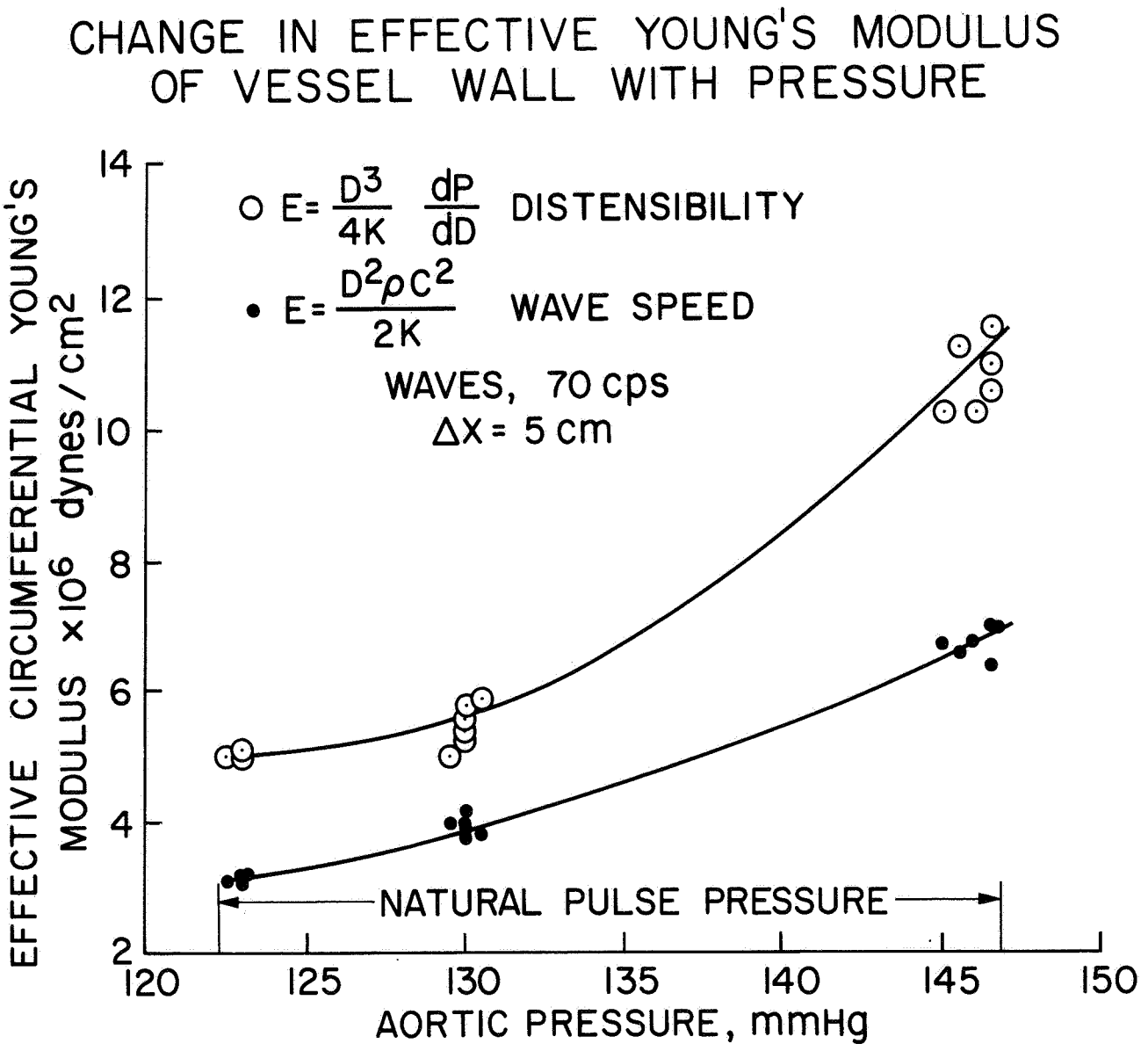

Figure 48. Change in the effective circumferential Young' s moduli for the vessel wall for naturally occurring pressure fluctuations in the aorta.

CHAPTER 5

GENERAL CONCLUSIONS AND DISCUSSION

The superposition of small amplitude sine wave trains on the natural pressure fluctuations in blood vessels appears to be a convenient method for determining the wave transmission characteristics of large arteries and veins. A direct in-vivo measurement of the dispersion and attenuation of pressure waves has long been considered essential for the formulation of valid mathematical models of the cardiovascular system. Previously investigators had relied upon the Fourier analysis of the natural pulse wave to obtain data on dispersion and attenuation. However, the results given in this dissertation indicate that the aorta behaves in a nonlinear fashion with respect to large amplitude pressure waves such as those generated by the heart. This precludes in a strict sense the resolution of the natural pressure pulse into harmonic components for the purpose of analyzing its wave propagation characteristics.

By measuring the speeds of trains of sine waves for frequencies between 40 and 200 cps dispersion data were obtained indicating in general that there is little change in wave speed with frequency for any given pressure level. Hence, the speed of a finite train of waves is indeed a good approximation to the phase velocity corresponding to the frequency of the sine waves. The observed absence of strong dispersion of pressure waves is in agreement with theoretical predictions (1, 2). For different dogs the wave speed in the thoracic aorta ranged in value between 4 and 6 m/sec.

The amplitude ratio A/A_o measured between two points in the aorta exhibits exponential decay of the form $A = A_o e^{\frac{-k\Delta x}{\lambda}}$, independent of the frequency and pressure. For the frequency range 40 to 200 cps the logarithmic decrement k ranged between 0.7 and 1.0 for downstream waves and 1.2 to 1.6 for upstream waves. This discrepancy in k for the two directions appears to be due to the taper of the vessel, and the true value of the attenuation coefficient for an idealized aorta with a uniform crossection would be approximately k = 1.0 to 1.2. The attenuation can be attributed primarily to dissipative mechanisms in the vessel wall, since the viscosity of the blood and radiation of energy into the surrounding medium are shown to be small. Therefore, the vessel wall clearly must have viscoelastic properties.

The dual impactor studies have demonstrated that pressure and blood flow can significantly affect the speed of waves. For the range of the natural pressure pulse the change in wave speed with pressure $\partial c/\partial p$ was found to be between $3 \frac{\text{cm/sec}}{\text{mm Hg}}$ and $6 \frac{\text{cm/sec}}{\text{mm Hg}}$ implying a stiffening of the vessel wall with pressure. This increase in wave speed with pressure constitutes a nonlinear behavior of the blood vessel.

Measurable mean flow appears to be present in the thoracic aorta during the entire cardiac cycle. It generally increases from less than 0.1 m/sec at diastole to approximately 0.6 to 1.0 m/sec during early systole. Pressure waves are convected by this flow and have an increased speed which becomes noticeable especially during early systole as a result of the combined effects of pressure and flow. The mean flow was determined with surprising accuracy

from the wave speed difference between downstream and upstream waves, and it was shown that $\bar{U} = 1/2(c^{D}(p) - c^{U}(p))$.

The discrepancy between the effective circumferential Young's moduli determined from preliminary measurements of the distensibility with a Pieper diameter gauge and from wave speed measurements may in part be attributed to experimental uncertainties regarding the response characteristics of the Pieper gauge at high frequencies in the aorta and to over simplified mathematical models used in the derivation of the distensibility expression and the Moens-Kortweg equation. It suggests that a more incisive experimental study should be undertaken and that more accurate mathematical models must be devised for the description of the mechanical behavior of blood vessels. Such models should take into account the viscoelastic nature of the wall material. Moreover, recent experiments on the carotid artery in which pressure and axial waves were generated simultaneously (43) have shown that the vessels may also exhibit noticeable anisotropy.

REFERENCES

1. Anliker, M., and Maxwell, J.: The dispersion of waves in blood vessels. In Biomechanics Symposium, edited by Y. C. Fung. New York, ASME, 1966, pp. 47-67.

2. Maxwell, J., and Anliker, M.: The dissipation and dispersion of small waves in arteries and veins with viscoelastic wall properties. Biophysical J. 8: 920, 1968.

3. Fung, Y. C. B.: Elasticity of soft tissues in simple elongation. Am. J. Physiol. 213: 1532, 1967.

4. Prager, W.: On the formulation of constitutive equations for living soft tissues. AFOSR Sci. Rpt. 67-2599, 1967. Defense Documentation Center, Alexandria, Virginia 22314.

5. Witzig, K.: Über erzwungene Wellenbewegungen zäher, inkompressibler Flüssigkeiten in elastischen Röhren. Inaugural Dissertation, Universität Bern, Wyss 1914.

6. Iberall, A. S.: Attenuation of oscillatory pressures in instrument lines. J. of Res. - Nat. Bureau of Stds. 45: 85, 1950.

7. Morgan, G. W., and Kiely, J. P.: Wave propagation in a viscous liquid contained in a flexible tube. J. Acoust. Soc. Am. 26: 326, 1954.

8. Womersley, J. R.: An elastic tube theory of pulse transmission and oscillatory flow in mammalian arteries. WADC Tech. Report TR 56-614. Defense Documentation Center. 1957.

9. Hardung, V.: Propagation of pulse waves in viscoelastic tubings. In Handbook of Physiology, Vol. I, Circulation, edited by W. F. Hamilton. Washington, D.C., Am. Physiol. Soc., 1962, pp. 107-135.

10. Klip, W.: Velocity and Damping of the Pulse Wave. The Hague, Martinus Nijhoff, 1962.

11. McDonald, D. A.: Blood Flow in Arteries. London, Edward Arnold, Ltd., 1960.

12. Fox, E. A., and Saibel, E.: Attempts in the mathematical analysis of blood flow. Trans. Soc. Rheol. 7: 25, 1963.

13. Rudinger, G.: Review of current mathematical methods for the analysis of blood flow. In Biomedical Fluid Mechanics Symposium. New York, ASME, 1966, pp. 1-33.

14. Skalak, R.: Wave propagation in blood flow. In Biomechanics, edited by Y. C. Fung. New York, Applied Mechanics Division ASME, 1966, pp. 20-46.

15. Fung, Y. C.: Biomechanics, its scope, history and some problems of continuum mechanics in physiology. J. Appl. Mech. Reviews, 21: 1, 1968.

16. Fenn, W. O.: Changes in length of blood vessels on inflation. In Tissue Elasticity, edited by J. W. Remington. Washington, D.C., Am. Physiol. Soc., 1957, pp. 154-160.

17. Bergel, D. C.: The dynamic elastic properties of the arterial wall. J. Physiol. 156: 458, 1961.

18. Apter, J. T., and Marquey, E.: Correlation of visco-elastic properties of large arteries with microscopic structure: V. Effects of sinusoidal forcings at low and at resonance frequencies. Cir. Res. 22: 393, 1968.

19. Patel, D. J., Greenfield, J. C., and Fry, D. L.: In vivo pressure-length-radius relationship of certain blood vessels in man and dog. In Pulsatile Blood Flow, edited by E. O. Attinger. New York, 1964, pp. 293-306.

20. Lee, J. S., Frasher, W. G., and Fung, Y. C.: Two dimensional finite deformation experiments on dog's arteries and veins. AFOSR Sci. Rpt. 67-1980, 1967. Defense Documentation Center.

21. McDonald, D. A., and Taylor, M. G.: The hydrodynamics of the arterial circulation. Prog. Biophys. Chem. 9: 107, 1959.

22. McDonald, D. A.: Regional pulse-wave velocity in the arterial tree. J. Appl. Physiol. 24: 73, 1968.

23. Landowne, M.: A method using induced waves to study pressure propagation in human arteries. Cir. Res. 5: 594, 1957.

24. Landowne, M.: Characteristics of impact and pulse wave propagation in brachial and radial arteries. J. Appl. Physiol. 112: 91, 1958.

25. Landowne, M.: Wave propagation in intact human arteries. Fed. Proc. 13: 83, 1954.

26. Peterson, Lysle H., The dynamics of pulsatile blood flow, Cir. Res. 2: 127, 1954.

27. King, A. L.: Some studies in tissue elasticity. In Tissue Elasticity, edited by J. W. Remington. Washington, D. C., Amer. Physiol. Soc., 1957, p. 123.

28. Dick, D., Kendrick, J., Matson, G., and Rideout, V. C.: Measurement of nonlinearity in the arterial system of the dog by a new method. Cir. Res. 22: 101, 1968.

29. Atabek, H. B., and Lew, H. S.: Wave propagation through a viscous incompressible fluid contained in an initially stressed elastic tube. Biophysical J. 6: 481, 1966.

30. Jones, E., Chang, I-Dee, and Anliker, M.: Effects of viscosity and external constraints on wave transmission in blood vessels, SUDAAR Report No. 344, Dept. of Aeronautics and Astronautics, Stanford University, Stanford, Calif., 1968.

31. Klip, W., Van Loon, P., and Klip, D.: Formulas for phase velocity and damping of longitudinal waves in thick-walled viscoelastic tubes. J. Appl. Physics 38: 3745, 1967.

32. Lindsay, R. B.: Mechanical Radiation. New York, McGraw-Hill Book Company, Inc., 1960.

33. Coon, G.: Diaphragm type capacitance transducer. U. S. Pat. Off. No. 3,027,769. 1962.

34. Brillouin, L.: Wave Propagation and Group Velocity. New York and London, Academic Press, 1960.

35. Morgan, G. W., and Ferrante, W. R.: Wave propagation in elastic tubes filled with streaming liquid. J. Acoust. Soc. Am. 27: 715, 1955.

36. Faber, J. J., and Purvis, J. H.: Conduction of cardiovascular sound along arteries. Cir. Res. 12: 308, 1963.

37. Muller, A., Helv. Physiol. et Pharmacol. Acta, 8:288, 1950.

38. Anliker, M., Wells, M., Ogden, E.: The transmission characteristics of large and small pressure waves in the abdominal vena cava, SUDAAR Report No. 362, Department of Aeronautics and Astronautics, Stanford University, Calif., 1968.

39. Learoyd, B. M., and Taylor, M. G.: Alterations with age in the visco-elastic properties of human arterial walls. Cir. Res. 18: 278, 1966.

40. Roach, M. R., and Burton, A. C.: The effect of age on the elasticity of human iliac arteries. Can. J. Biochem. 35: 181, 1957.

41. Pieper, H., and Paul, L.: Catheter-tip gauge for measuring blood flow velocity and vessel diameter in dogs. J. Appl. Physiol. 24: 259, 1968.

42. Remington, J.: The physiology of the aorta and its major branches, In Handbook of Physiology, Circulation, Vol. II, p. 799, 1963.

43. Anliker, M., Moritz, W., and Ogden, E.: Transmission characteristics of axial waves in blood vessels, SUDAAR Report No. 343, 1968.